

## ESO: An enhanced snake optimizer for real-world engineering problems

Liguo Yao <sup>a,b</sup>, Panliang Yuan <sup>a</sup>, Chieh-Yuan Tsai <sup>c</sup>, Taihua Zhang <sup>a,b,\*</sup>, Yao Lu <sup>a,b</sup>, Shilin Ding <sup>a</sup>

<sup>a</sup> School of Mechanical and Electrical Engineering, Guizhou Normal University, Guiyang, Guizhou 550025, China

<sup>b</sup> Technical Engineering Center of Manufacturing Service and Knowledge Engineering, Guizhou Normal University, Guiyang, Guizhou 550025, China

<sup>c</sup> Department of Industrial Engineering and Management, Yuan Ze University, Taoyuan 32003, Taiwan



### ARTICLE INFO

**Keywords:**

Snake optimizer

Novel opposition-based learning

Dynamic update mechanisms

Real-world engineering problems

### ABSTRACT

Meta-heuristic algorithms are an essential way to solve realistic optimization problems. Developing effective, accurate, and stable meta-heuristic algorithms has become the goal of optimization research. Snake Optimizer (SO) is a novel algorithm with good optimization results. However, due to the limitations of natural laws, the parameters are more fixed values in the exploration and exploitation phase, so the SO algorithm quickly falls into local optimization and slowly converges. This paper proposes an Enhanced Snake Optimizer (ESO) by introducing a novel opposition-based learning strategy and new dynamic update mechanisms (parameter dynamic update strategy, sine–cosine composite perturbation factors, Tent-chaos & Cauchy mutation) to achieve better performance. The effectiveness of ESO has been tested on 23 classic benchmark functions and the CEC 2019 function set. 13 functions of 23 classic benchmark functions have variants that belong to multiple dimensions (Dim = 30, 100, 500, 1000, and 2000). In addition, ESO is also used to solve four real-world engineering design problems. Experimental results and two statistical tests show that the proposed ESO performs better than the other 13 state-of-the-art algorithms, including SO. The MATLAB code of ESO is available from: <https://www.mathworks.cn/matlabcentral/fileexchange/120173-eso-an-enhanced-snake-optimizer>.

### 1. Introduction

Optimization problems play a significant role in human's pursuit of a higher quality of life. Many problems in life can be regarded as an optimization-seeking model, and the optimal result is obtained by solving the model. Optimization has complete applications in the fields of economics (Gbadega & Sun, 2022; Liang et al., 2013; Mousavi-Aval et al., 2017; Tsai et al., 2017), physics (Kumar et al., 2022; Mollajan et al., 2018; Wardhana & Pranowo, 2022; Wu et al., 2021), mathematics (Çil et al., 2020; Dabiri et al., 2017; Jafari et al., 2022; Mortazavi, 2021), engineering (Fan et al., 2022; Houssein et al., 2022; Moraes et al., 2015; Talatahari & Azizi, 2020), etc. Since the problems in the above fields are usually high-dimensional (Li et al., 2023; Liu et al., 2022; Tay & Osorio, 2022), nonlinear (Esmaelian et al., 2018; Shokri-Ghaleh et al., 2020; Tawhid & Ibrahim, 2021), discontinuous (Pereira et al., 2022; Xiao et al., 2022), and multi-constrained (Qin et al., 2022; Wang et al., 2019; Xia & Dong, 2022), more and more scholars are studying heuristic algorithms to solve these problems better. Heuristic algorithms are used to search for the best solution that is as close as possible to the feasible and optimal solution within an acceptable computational cost. Heuristic

algorithms can be broadly classified into biological evolution-based, animal instinct-based, thinking cognition-based, physical phenomena-based, and strategy enhancement-based.

Biological evolution-based algorithms are methods to achieve randomized search by simulating the mechanisms of mating, genetic and mutational evolution that exists in biological evolution, based on the evolutionary laws of the biological world. The main biological evolution-based algorithms are genetic algorithm (Holland, 1992), evolutionary strategies (Tinkle et al., 1970), biogeography-based optimization (Simon, 2008), and geometric probabilistic evolutionary algorithm (Segovia-Domínguez et al., 2020).

Animal instinct-based algorithms are the main heuristic algorithms that implement randomized search methods by simulating animals' instinctive behaviors such as rounding up, foraging, returning home, and courtship. The main animal instinct-based algorithms are particle swarm optimization (Poli et al., 2007), ant colony optimization (Dorigo et al., 2006), grey wolf optimizer (Mirjalili et al., 2014), chimp optimization algorithm (Khishe & Mosavi, 2020), slap swarm algorithm (Mirjalili et al., 2017), whale optimization algorithm (Mirjalili & Lewis, 2016), bald eagle search optimization algorithm (Alsattar et al., 2019),

\* Corresponding author at: School of Mechanical and Electrical Engineering, Guizhou Normal University, Guiyang, Guizhou 550025, China.

E-mail addresses: lgyao@gznu.edu.cn (L. Yao), yuanpanl2020@163.com (P. Yuan), cytsai@saturn.yzu.edu.tw (C.-Y. Tsai), zhangth542@gznu.edu.cn (T. Zhang), yao.lu@gznu.edu.cn (Y. Lu), zbrsxk@163.com (S. Ding).

marine predators algorithm (Faramarzi et al., 2020), black widow optimization (Hayyolalam & Pourhaji Kazem, 2020) and coati optimization algorithm (Dehghani et al., 2022).

Thinking cognition-based algorithms are the main methods of randomized search by simulating the behavior of humans in nature and life as a result of thinking cognition. The thinking cognition-based algorithms mainly are teaching–learning-based optimization (Rao et al., 2011), school based optimization algorithm (Farshchin et al., 2018), political optimizer (Askari et al., 2020), student psychology based optimization algorithm (Das et al., 2020), and social group optimization (Satapathy & Naik, 2016).

Physical phenomena-based algorithms are the main randomized search methods that simulate physical phenomena and their laws. The mainly physical phenomena-based algorithms are simulated annealing (Bertsimas & Tsitsiklis, 1993), sine cosine algorithm (Mirjalili, 2016), golden sine algorithm (Tanyildizi & Demir, 2017), electrostatic discharge algorithm (Bouchekara, 2019), archimedean optimization algorithm (Hashim et al., 2020), and atomic search optimization algorithm (Zhao et al., 2019).

Strategy enhancement-based algorithms are mainly new algorithms based on the original heuristic algorithms. By adding new strategies or the advantages of other algorithms, these algorithms can effectively avoid the shortcomings of the original heuristic algorithms and obtain better optimization results. Because of this, strategy enhancement-based algorithms are the focus of researchers' attention. The mainly strategy enhancement-based algorithms are modified equilibrium optimizer (Fan et al., 2021), opposition learning and spiral modelling based arithmetic optimization algorithm (Yang et al., 2022), improved political optimizer (Askari & Younas, 2021), hybrid social whale optimization algorithm (Aala Kalananda & Komanapalli, 2021), improved continuous ant colony optimization algorithms (Omran & Al-Sharhan, 2019), enhanced salp swarm algorithms using opposition-based learning schemes (Si et al., 2022), hybrid grey wolf optimizer and artificial bee colony algorithm (Gaidhane & Nigam, 2018).

Snake Optimizer (SO) is a novel algorithm that simulates the mating behavior of snakes to perform various optimization tasks proposed by Hashim and Hussien in 2022. The SO algorithm can be easily realized, does not depend on gradient knowledge, and has strong local exploitation ability. Compared with LSHADE, MFO, HHO, TEO, GOA, WOA and LSHADE-EpSin, SO has been proven to exhibit excellent performance (Hashim & Hussien, 2022). Despite the promising results achieved by the SO algorithm, there are still some shortcomings, such as slow convergence, low solution accuracy and easy to fall into local optimum in the exploration phase when the problem is complex. These drawbacks are mainly caused by the fixed values of some parameters in the algorithm, the population diversity is not sufficient, unbalanced exploitation and exploration capabilities in the search space, and the low possibility of large spatial jumps during the process of iteratively updating the population. Moreover, according to the No Free Lunch Theorem (Adam et al., 2019; Ho & Pepyne, 2002), one algorithm does not exist to solve all problems. Motivating these considerations, this paper proposes an Enhanced Snake Optimizer (ESO) based on SO by adopting a novel opposition-based learning strategy, dynamic parameters, sine–cosine composite perturbation, and Tent-chaos & Cauchy mutation to improve the performance of SO. To verify the effectiveness of ESO, the results are compared with 13 SOTA algorithms on two sets of functions and four engineering design optimization problems. The ESO algorithm improves both algorithm performance and practical problem-solving ability significantly.

The main contributions of this paper as shown below.

- A novel opposition-based learning strategy is proposed, named mirror imaging strategy based on convex lens imaging. The strategy combines the lens imaging strategy with the mirror imaging principle to effectively expand the generation range of opposition solutions.

- Dynamic update mechanisms, which include parameters dynamic update strategy, sine–cosine composite perturbation factors, Tent-chaos & Cauchy mutation, were used to improve the performance of the ESO algorithm in the exploration phase and exploration phase.
- The twenty-three standard test functions and CEC 2019 functions commonly used for intelligent optimization algorithms were used to evaluate the proposed ESO and compare the results with the other thirteen SOTA optimization algorithms.
- Four engineering design problems were used to evaluate the performance of the proposed ESO algorithm on real-world problems and to compare the results with the other thirteen state-of-the-art optimization algorithms.

The remainder of the paper is organized as follows: Section 2 reviews and introduces snake optimizer, and Section 3 describes ESO and all the strategies to improve performance in detail separately. Section 4 describes the results of ESO and the other thirteen SOTA algorithms on two function sets and analyzes the results. Section 5 describes the performance of ESO and other 13 SOTA algorithms on four real-world engineering design problems. Finally, Section 6 summarizes paper's results and presents ideas for further development.

## 2. Snake optimizer

Snake Optimizer (SO) is an optimization algorithm inspired by the snake mating process by simulating the snake mating behavior and constructing a corresponding model for solving it. The mating process of snakes is mainly limited by temperature and food quantity. Snakes will only mate when the temperature is low, and the food quantity is sufficient. Therefore, in SO, when the food quantity is insufficient, the main task of the snakes is to find food, which is considered the exploration phase of the optimization algorithm. When the food quantity is sufficient, it is the exploration phase of the optimization algorithm. The exploration phase is divided into two cases. When the temperature is high, the snakes cannot mate and has to wait for the arrival of low temperature. When the temperature is low, snakes enter the mating session. Since there is a possibility of more males than females, the mating session has a fighting mode and a mating mode. Males compete with each other to obtain the right to mate with females. When mating behavior is complete, females lay eggs and hatch into new snakes, thus completing the population renewal.

Each optimization method has to have an initial population. The initial population for the SO is generated by a random uniform distribution with the generation rule described in the following Eq. (1).

$$S_i = S_{\min} + rand_i \times (S_{\max} - S_{\min}) \quad (1)$$

where  $S_i$  denotes the position of the population individuals at the  $i$ -th time,  $rand_i$  denotes the random value between  $(0, 1)$  at the  $i$ -th time,  $S_{\max}$  and  $S_{\min}$  denote the population's maximum bounds and minimum bounds.

After obtaining the initial population, the distribution of the number of female and male individuals according to gender begins. In general, the number of males and females is equal. Therefore, the number of female and male individuals can be calculated by Eq. (2).

$$N_m = N_f = \frac{N_{\text{all}}}{2} \quad (2)$$

where  $N_{\text{all}}$  is the total population size,  $N_m$  and  $N_f$  denote the number of male and female snakes, respectively.

In SO, temperature and food quantity are two critical factors that determine snake mating, and temperature and food quantity can be defined by Eq. (3) and Eq. (4).

$$Temp = e^{-t/T} \quad (3)$$

$$FQ = c_1 \times e^{(t-T)/T} \quad (4)$$

where  $t$  denotes the current number of iterations,  $T$  denotes the total number of iterations, and  $c_1$  is a fixed constant of 0.5.

In the exploration phase, when  $FQ < 0.25$ , the snakes search for food by randomly selecting a location and updating it. Therefore, Eq. (5) and Eq. (6) can simulate the exploration phase.

$$S_i^m(t+1) = S_{rand}^m(t) \oplus c_2 \times e^{-f_{rand}^m/f_i^m} \times S_i = \begin{cases} S_{rand}^m(t) + c_2 \times e^{-f_{rand}^m/f_i^m} \times S_i \\ S_{rand}^m(t) - c_2 \times e^{-f_{rand}^m/f_i^m} \times S_i \end{cases} \quad (5)$$

$$S_i^f(t+1) = S_{rand}^f(t) \oplus c_2 \times e^{-f_{rand}^f/f_i^f} \times S_i = \begin{cases} S_{rand}^f(t) + c_2 \times e^{-f_{rand}^f/f_i^f} \times S_i \\ S_{rand}^f(t) - c_2 \times e^{-f_{rand}^f/f_i^f} \times S_i \end{cases} \quad (6)$$

where  $S_i^m$  denotes the position of the male snake at the  $i$ -th time and  $S_{rand}^m$  denotes the position of the random male snake.  $f_{rand}^m$  is the fitness of the male snake  $S_{rand}^m$ , and  $f_i^m$  is the fitness of the individual male snake at the  $i$ -th time.  $S_i^f$  denotes the position of the female snake at the  $i$ -th time, and  $S_{rand}^f$  denotes the position of the random female snake.  $f_{rand}^f$  is the fitness of the  $i$ -th individual female snake  $S_{rand}^f$ ,  $c_2$  is a fixed constant of 0.05, and  $\oplus$  denotes the sign direction operator.

During the exploration phase, when  $FQ > 0.25$  and also  $Temp > 0.6$ , the snake only eats food and does not go into mating. The process can be represented by Eq. (7).

$$\begin{aligned} S_i^{m,f}(t+1) &= S_{food} \oplus c_3 \times Temp \times rand_i \times (S_{food} - S_i^{m,f}(t)) \\ &= \begin{cases} S_{food} + c_3 \times Temp \times rand_i \times (S_{food} - S_i^{m,f}(t)) \\ S_{food} - c_3 \times Temp \times rand_i \times (S_{food} - S_i^{m,f}(t)) \end{cases} \end{aligned} \quad (7)$$

where  $S_i^{m,f}$  is the position of the male or female individual,  $S_{food}$  is the position of the optimal individual, and  $c_3$  is a fixed constant of 2.

When  $FQ > 0.25$  and also  $Temp \leq 0.6$ , the snake will enter the mating part, and since both male/female individuals want to finish mating with the superior heterosexual, there is a possibility of competition between male and female individuals. The winning individual can choose the mating partner first, so there is a fighting mode and a mating mode in the mating part, and the fighting mode is represented by Eq. (8) and Eq. (9), respectively.

$$S_i^m(t+1) = S_i^m(t) + c_3 \times e^{-f_{best}^f/f_i} \times rand_i \times (FQ \times S_{best}^f - S_i^m(t)) \quad (8)$$

$$S_i^f(t+1) = S_i^f(t) + c_3 \times e^{-f_{best}^m/f_i} \times rand_i \times (FQ \times S_{best}^m - S_i^f(t)) \quad (9)$$

where  $S_i^m$  denotes the position of the male snake in the  $i$ -th generation,  $S_{best}^f$  denotes the position of the optimal individual in the female snake,  $S_i^f$  denotes the position of the female snake in the  $i$ -th generation,  $S_{best}^m$  denotes the position of the optimal individual in the male snake,  $f_{best}^f$  is the fitness of the optimal individual in the female snake in the fight mode,  $f_{best}^m$  is the fitness of the optimal individual in the male snake in the fight mode, and  $f_i$  is the fitness of the individual.

The mating pattern is represented by Eq. (10) and Eq. (11), respectively.

$$S_i^m(t+1) = S_i^m(t) + c_3 \times e^{-m_i^f/f_i^m} \times rand_i \times (FQ \times S_i^f(t) - S_i^m(t)) \quad (10)$$

$$S_i^f(t+1) = S_i^f(t) + c_3 \times e^{-m_i^m/f_i^f} \times rand_i \times (FQ \times S_i^m(t) - S_i^f(t)) \quad (11)$$

where  $S_i^m$  is the position of the  $i$ -th individual in the male snake and  $S_i^f$  is the position of the  $i$ -th individual in the female snake.  $m_i^m$  denotes the fitness of the  $i$ -th individual male snake in the mating pattern, and  $m_i^f$  denotes the fitness of the  $i$ -th individual female snake in the mating pattern.

After completing the mating behavior, the female snakes will lay and

incubate eggs to obtain new snakes and come to replace the worst male/female individuals in the original population, depending on the gender of the new snake, respectively. The replacement process is represented by Eq. (12) and Eq. (13).

$$S_{worst}^m = S_{min} + rand_i \times (S_{max} - S_{min}) \quad (12)$$

$$S_{worst}^f = S_{min} + rand_i \times (S_{max} - S_{min}) \quad (13)$$

where  $S_{worst}^m$  is the worst individual among males and  $S_{worst}^f$  is the worst individual among females.

The pseudocode of the Snake Optimizer algorithm is shown in Algorithm 1.

#### Algorithm 1. Snake Optimizer (SO)

```

1. Define Dim, UB, LB, and Pop_Size(Nall), Max_Iter(T), Curr_Iter(t)
2. Initialize the population randomly Si(i = 1, 2, ..., Nall)
3. while (t < T) do
4.   Evaluate the fitness of each group Nm and Nf
5.   find fbestm and fbestf
6.   Define Temp using Eq. (3).
7.   Define food Quantity FQ using Eq. (4).
8.   if (Q < 0.25) then
9.     Perform exploration using Eqs. (5) and (6)
10.    else
11.      if (Temp > 0.6) then
12.        Perform exploitation Eq. (7)
13.      else
14.        if (rand > 0.6) then
15.          Snakes in Fight Mode Eqs. (8) and (9)
16.        else
17.          Snakes in Mating Mode Eqs. (10) and (11)
18.          Replace the worst male and female Eqs. (12) and (13)
19.        end if
20.      end if
21.    end if
22.  end while
23. Return the best solution.

```

### 3. Proposed ESO

As a heuristic algorithm, the SO algorithm has achieved good results in solving optimization problems due to its novel imitation idea. However, the limitations of biological behavior in nature make it still suffer from the drawbacks of quickly falling into local optimum and insufficient precision. This section proposed the ESO algorithm, which with four enhancement strategies based on the shortcomings of SO.

#### 3.1. Novel dynamic update mechanisms

In the SO algorithm, the food quantity is essential in deciding whether the algorithm is in the exploration or exploitation phase. In Eq. (4), the value of  $c_1$  is set as a fixed constant to 0.5, which makes the algorithm lack the ability to wander randomly in the exploration phase and exploration phase, so this paper adds perturbation factors to the original one to get a new dynamic update of  $c_1$ . The new  $c_1^{new}$  is calculated according to Eq. (14).

$$c_1^{new} = c_1 + \frac{1}{10} \times \cos\left(r_1^4 \times \frac{\pi}{2}\right) \quad (14)$$

where  $r_1$  is a random number between (0, 1).

In the exploration phase, the position updates are calculated by Eq. (5) and Eq. (6) for both male and female snakes searching for food. However, in the above equations,  $c_2$  sets the value of the fixed constant to 0.05, which is not conducive to updating the snake's position due to the fixed value setting and cannot jump out of the local optimum, thus quickly making the algorithm fall into the local optimum. In this paper, based on the original Eq. (5) and Eq. (6), perturbation factors are added to obtain a new dynamic update of  $c_2$ . The new  $c_2^{new}$  calculated according to Eq. (15).

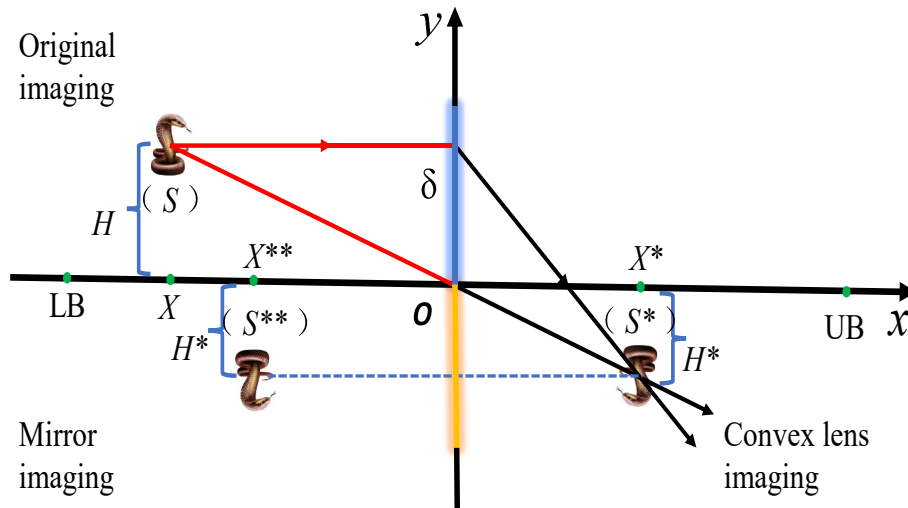


**Fig. 1.** Mirror imaging strategy based on convex lens imaging.

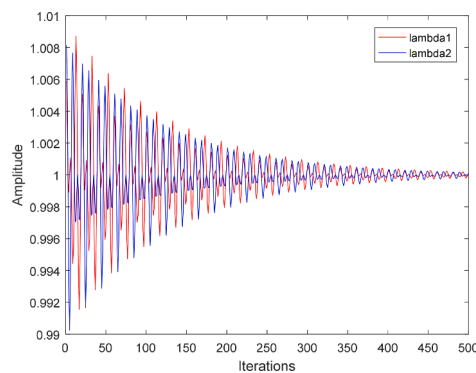


**Fig. 2.** Sine-cosine composite perturbation factors.

$$c_2^{new} = c_2 + \frac{1}{1000} \times \cos\left(r_2^4 \times \frac{\pi}{2}\right) \quad (15)$$

where  $r_2$  is a random number between (0, 1).

In the exploitation phase, the positions of male and female snakes are calculated by Eqs. (7)–(11), respectively. However, the value of  $c_3$  in the above equations is set as a fixed constant of 2. Due to the fixed value set, the snake position is updated slowly, reducing the algorithm's convergence speed and increasing the convergence time. In this paper, we add the sinusoidal factor that drives the curve down to accelerate the convergence speed of the algorithm based on the original one. The new dynamic update of  $c_3$  is obtained. The new  $c_3^{new}$  is calculated according to Eq. (16).

$$c_3^{new} = c_3 - 2 \times \sin\left(\left(\frac{t}{T}\right)^4 \times \frac{\pi}{2}\right) \quad (16)$$

### 3.2. Mirror imaging strategy based on convex lens imaging

Opposition-based learning (Tizhoosh, 2005) is an effective optimization strategy that aims to expand the search scope by computing the opposition solutions at the current positions, thus finding a more optimal solution to the optimization problem. As a kind of opposition-based learning, the Lens imaging learning strategy (Long et al., 2022) originates from the convex lens imaging in the law of optics, which refracts the object on one side of the convex lens to the other side of the

convex lens through the convex lens to obtain more optimal solutions. Inspired by the convex lens imaging mechanism and combined with the principle of mirror imaging (Xu et al., 2014), this paper proposes a novel opposition-based learning strategy, that is mirror imaging strategy based on convex lens imaging. The strategy obtains new opposition solutions symmetric to the inverse solution based on the principle of mirror imaging to obtain the opposition solutions. This strategy can expand the range of the opposition solutions of convex lens imaging, thus making it easier for the optimization process to jump out of the local optimum.

The mirror imaging strategy based on convex lens imaging is shown in Fig. 1. In two-dimensional space, the search range of the solution on the x-axis is  $[LB, UB]$ , the mirror region on the y-axis, and the positive half-axis of the y-axis is the convex mirror region (Blue). The negative half-axis is the plane mirror region (Yellow). Suppose a snake's individual ( $s$ ) is in the original mirror region with projection ( $X$ ) on the x-axis and height  $H$ . A real image ( $s^*$ ) can be obtained by convex lens imaging, which has a projection ( $X^*$ ) on the x-axis and height  $H^*$ , from which the opposition individual ( $s^*$ ) of the individual ( $s$ ) is obtained, and then by the principle of plane mirror image, the opposition individual ( $s^*$ ) is mirrored to obtain a new opposition individual ( $s^{**}$ ), which has with the projection of ( $X^{**}$ ) and the height of  $H^{**}$ , where  $|X^{**}| = |X^*|$ . Finally, the opposition individual ( $s^*$ ) and ( $s^{**}$ ) are obtained by the original individual ( $s$ ).

According to the principle of convex lens imaging, the individual ( $s$ ) takes the origin of coordinates ( $O$ ) as the base point to obtain the opposition point ( $s^*$ ), and the coordinates of the point can be calculated by Eq. (17).

$$\frac{(UB + LB)/2 - X}{X^* - (UB + LB)/2} = \frac{H}{H^*} \quad (17)$$

where  $UB$  is the upper limit and  $LB$  is the lower limit, let  $\delta = \frac{H}{H^*}$ .

$$X^* = \frac{UB + LB}{2} + \frac{UB + LB - X}{2\delta} \quad (18)$$

In lens imaging, the individual convex lens-imaging projection points on the x-axis are obtained differently for different lens thicknesses. The thickness of the convex lens can be defined as a dynamically adjusted value (scaling factor  $\delta$ ) to obtain more convex lens imaging solutions. Thus, more mirror imaging solutions are obtained. The scaling factor can increase the local exploitation capability of the optimization algorithm. A nonlinear dynamic scaling factor strategy is adopted in this paper. In

**Table 1**

Details of 23 benchmark functions.

Type	Functions	Dim	Range	$f_{\min}$
Unimodal	$F_1(x) = \sum_{i=1}^n x_i^2$	30,100,500,1000,2000	[-100,100]	0
	$F_2(x) = \sum_{i=1}^n  x_i  + \prod_{i=1}^n  x_i $	30,100,500,1000,2000	[-1.28,1.28]	0
	$F_3(x) = \sum_{i=1}^n \left( \sum_{j=1}^i x_j \right)^2$	30,100,500,1000,2000	[-100,100]	0
	$F_4(x) = \max_i \{  x_i , 1 \leq i \leq n \}$	30,100,500,1000,2000	[-100,100]	0
	$F_5(x) = \sum_{i=1}^{n-1} \left[ 100(x_{i+1} - x_i^2)^2 + (x_i - 1)^2 \right]$	30,100,500,1000,2000	[-30,30]	0
	$F_6(x) = \sum_{i=1}^n ([x_i + 0.5])^2$	30,100,500,1000,2000	[-100,100]	0
	$F_7(x) = \sum_{i=1}^n i x_i^4 + \text{random}[0, 1]$	30,100,500,1000,2000	[-1.28,1.28]	0
	$F_8(x) = \sum_{i=1}^n -x_i \sin(\sqrt{ x_i })$	30,100,500,1000,2000	[-500,500]	-418.9829 × n
	$F_9(x) = \sum_{i=1}^n [x_i^2 - 10 \cos(2\pi x_i) + 10]$	30,100,500,1000,2000	[-5.12,5.12]	0
	$F_{10}(x) = -20 \exp(-0.2 \sqrt{\frac{1}{n} \sum_{i=1}^n x_i^2}) - \exp\left(\frac{1}{n} \sum_{i=1}^n \cos(2\pi x_i)\right)$	30,100,500,1000,2000	[-32,32]	0
Multimodal	$F_{11}(x) = \frac{1}{4000} \sum_{i=1}^n x_i^2 - \prod_{i=1}^n \cos\left(\frac{x_i}{\sqrt{i}}\right) + 1$	30,100,500,1000,2000	[-600,600]	0
	$F_{12}(x) = \frac{\pi}{n} \left\{ 10 \sin(\pi y_i) + \sum_{i=1}^{n-1} (y_i - 1)^2 [1 + 10 \sin^2(\pi y_{i+1})] \right\} + (y_n - 1)^2$	30,100,500,1000,2000	[-50,50]	0
	$\sum_{i=1}^n u(x_i, 10, 100, 4)$			
	$y_i = 1 + \frac{x_i + 1}{4}$			
	$u(xi, a, k, m) = \begin{cases} k(x_i - a)^m, & x_i > a \\ 0, & -a < x_i < a \\ k(-x_i - a)^m, & x_i < -a \end{cases}$			
	$F_{13}(x) = 0.1 \left\{ \sin^2(3\pi x_1) + \sum_{i=1}^n (x_i - 1)^2 [1 + \sin^2(3\pi x_i + 1)] \right\} + \sum_{i=1}^n u(x_i, 5, 100, 4)$	30,100,500,1000,2000	[-50,50]	0
	$F_{14}(x) = \left( \frac{1}{500} + \sum_{j=1}^{25} \frac{1}{j + \sum_{i=1}^2 (x_i - a_{ij})^6} \right)^{-1}$	2		
	$F_{15}(x) = \sum_{i=1}^{11} \left( a_i - \frac{x_1 (b_i^2 + b_i x_2)}{b_i^2 + b_i x_3 + x_4} \right)^2$	4	[-5,5]	0.0003
	$F_{16}(x) = 4x_1^2 - 2.1x_1^4 + \frac{1}{3}x_1^6 + x_1 x_2 - 4x_2^2 + 4x_2^4$	2	[-5,5]	-1.0316
	$F_{17}(x) = \left\{ x_2 - \frac{5.1}{4\pi^2} x_1^2 + \frac{5}{\pi} x_1 - 6 \right\}^2 + 10 \left( 1 - \frac{1}{8\pi} \right) \cos x_1 + 10$	2	[-5, 5]	0.398
	$F_{18}(x) = [1 + (x_1 + x_2 + 1)^2 (19 - 14x_1 + 3x_1^2 - 14x_2 + 6x_1 x_2 + 3x_2^2)] \times [30 + (2x_1 - 3x_2)^2 \times (18 - 32x_1 + 12x_1^2 + 48x_2 - 36x_1 x_2 + 27x_2^2)]$	2	[-2,2]	3
	$F_{19}(x) = -\sum_{i=1}^4 c_i \exp\left(-\sum_{j=1}^3 a_{ij} (x_j - p_{ij})^2\right)$	3	[-1,2]	-3.86
	$F_{20}(x) = -\sum_{i=1}^4 c_i \exp\left(-\sum_{j=1}^6 a_{ij} (x_j - p_{ij})^2\right)$	6	[0,1]	-3.32
Fixed-dimension Multimodal	$F_{21}(x) = -\sum_{i=1}^5 [(X - a_i)(X - a_i)^T + c_i]^{-1}$	4	[0,10]	-10.1532
	$F_{22}(x) = -\sum_{i=1}^7 [(X - a_i)(X - a_i)^T + c_i]^{-1}$	4	[0,10]	-10.4028
	$F_{23}(x) = -\sum_{i=1}^{10} [(X - a_i)(X - a_i)^T + c_i]^{-1}$	4	[0,10]	-10.5364

**Table 2**

Details of CEC2019 benchmark functions.

No.	Functions	Dim	Range	$F_i^* = F_i(X^*)$
F1	Storn's Chebyshev Polynomial Fitting Problem	9	[-8192, 8192]	1
F2	Inverse Hilbert Matrix Problem	16	[-16384,16384]	1
F3	Lennard-Jones Minimum Energy Cluster	18	[-4,4]	1
F4	Rastrigin's Function	10	[-100,100]	1
F5	Griewangk's Function	10	[-100,100]	1
F6	Weierstrass Function	10	[-100,100]	1
F7	Modified Schwefel's Function	10	[-100,100]	1
F8	Expanded Schaffer's F6 Function	10	[-100,100]	1
F9	Happy Cat Function	10	[-100,100]	1
F10	Ackley Function	10	[-100,100]	1

**Table 3**

Parameters setting for algorithms.

Algorithms	Parameters and assignments
GWO	$a = 2$ (linearly decreases over iterations), $r_1 \in [0, 1], r_2 \in [0, 1]$
HHO	$J \in [0, 2]$
SCA	$a = 2$ (linearly decreases over iterations)
GJO	$a = 1.5$ (linearly decreases over iterations)
ALO	$w \in [2, 6]$
SOA	$F_C =$ decreases linearly from 2 to 0
AGWO	$B = 0.8, a = 2$ (linearly decreases over iterations)
MPSO	$c_1 = 2, c_2 = 2, W_{\min} = 0.2, W_{\max} = 0.9$
TACPSO	$c_1 = 2, c_2 = 2, W_{\min} = 0.2, W_{\max} = 0.9$
SHADE	$P_{best} = 0.1, Arc\ rate = 2$
LSHADE	$P_{best} = 0.1, Arc\ rate = 2$
LSHADE-EpSin	$P_{best} = 0.1, Arc\ rate = 2$
SO	$a = 2$ (linearly decreases over iterations)
ESO	$a = 2$ (linearly decreases over iterations)

**Table 4**

Comparison of results on benchmark functions (F1-F13) with 30 dimensions.

F(x)		GWO	HHO	SCA	GJO	ALO	SOA	AGWO	MPSO	TACPSO	SO	SHADE	LSHADE	LSHADE-EpSin	ESO
F1	Mean	1.2107E-27	4.4170E-96	1.0092E+01	3.4617E-54	1.3469E-03	8.1617E-12	3.9379E-146	6.8888E-01	2.1852E+01	7.8290E-93	1.4190E+04	6.0932E+03	4.4666E+03	<b>0.0000E+00</b>
	Std	2.0117E-27	1.4506E-95	1.6113E+01	8.4921E-54	1.1388E-03	1.8816E-11	2.0359E-145	1.2164E+00	4.1493E-01	3.5992E-92	2.4169E+03	1.9909E+03	1.4570E+03	<b>0.0000E+00</b>
	P	1.2118E-12	1.2118E-12	1.2118E-12	1.2118E-12	1.2118E-12	1.2118E-12	1.2118E-12	1.2118E-12	1.2118E-12	1.2118E-12	1.2118E-12	1.2118E-12	1.2118E-12	—
	Wr	(+)	(+)	(+)	(+)	(+)	(+)	(+)	(+)	(+)	(+)	(+)	(+)	(+)	—
F2	T	8.8967E-02	1.1557E-01	7.0800E-02	1.8707E-01	1.0391E+01	7.5967E-02	1.1093E+00	6.0433E-02	5.9467E-02	7.4333E-02	9.1333E-03	3.4733E-02	1.2067E-02	1.6367E-01
	Mean	1.0406E-16	9.4101E-51	1.6019E-02	2.1266E-32	4.5696E+01	1.6772E-08	3.9643E-82	2.6653E+01	6.6486E-01	2.8768E-43	2.0132E+02	4.5229E+01	4.0052E+01	<b>0.0000E+00</b>
	Std	8.3032E-17	3.2866E-50	2.8201E-02	3.7061E-32	4.7947E+01	1.5619E-08	1.0734E-81	1.6131E+01	9.6650E-01	5.2752E-43	3.0349E+02	7.8671E+00	8.4546E+00	<b>0.0000E+00</b>
	P	5.2190E-12	5.2190E-12	5.2190E-12	5.2190E-12	5.2190E-12	5.2190E-12	5.2190E-12	5.2190E-12	5.2190E-12	5.2190E-12	5.2190E-12	5.2190E-12	5.2190E-12	—
F3	Wr	(+)	(+)	(+)	(+)	(+)	(+)	(+)	(+)	(+)	(+)	(+)	(+)	(+)	—
	T	6.9967E-02	8.9267E-02	5.7567E-02	1.3827E-01	7.3762E+00	5.8433E-02	7.2480E-01	4.8333E-02	4.7467E-02	6.4500E-02	5.6000E-03	1.2933E-02	2.5733E-02	1.2470E-01
	Mean	1.8716E-04	1.5142E-63	9.3318E+03	5.2843E-17	4.4617E+03	6.4574E-04	1.4090E-77	1.3048E+04	1.0613E+03	4.2069E-53	4.0325E+04	2.8246E+04	1.2634E+04	<b>0.0000E+00</b>
	Std	9.7111E-04	8.2935E-63	6.5091E+03	1.9342E-16	2.0932E+03	3.1696E-03	7.6700E-77	6.3573E+03	1.1563E+03	2.2709E-52	6.0004E+03	7.0780E+03	3.4665E+03	<b>0.0000E+00</b>
F4	P	1.2118E-12	1.2118E-12	1.2118E-12	1.2118E-12	1.2118E-12	1.2118E-12	1.2118E-12	1.2118E-12	1.2118E-12	1.2118E-12	1.2118E-12	1.2118E-12	1.2118E-12	—
	Wr	(+)	(+)	(+)	(+)	(+)	(+)	(+)	(+)	(+)	(+)	(+)	(+)	(+)	—
	3.8683E-01	8.6240E-01	3.7720E-01	5.3620E-01	1.0092E+01	3.7843E-01	1.6831E+00	3.6200E-01	3.6080E-01	3.9853E-01	1.8200E-02	2.1333E-02	5.2433E-02	7.7920E-01	
	T	7.8667E-02	1.4037E-01	7.5133E-02	1.7670E-01	1.0427E+01	7.5767E-02	1.1339E+00	5.8267E-02	5.7733E-02	7.5867E-02	8.5000E-03	1.2400E-02	3.8167E-02	1.6267E-01
F5	Mean	5.8276E-07	2.7508E-48	3.4212E+01	7.6201E-15	1.6691E+01	5.5612E-03	8.1155E-61	1.8922E+01	1.0549E+01	2.4516E-40	6.0068E+01	4.5595E+01	3.4571E+01	<b>0.0000E+00</b>
	Std	4.5675E-07	1.0465E-47	1.3329E+01	3.5316E-14	3.7267E+00	9.3031E-03	1.7647E-60	5.0342E+00	4.1739E+00	6.0608E-40	6.2601E+00	7.7090E+00	4.7205E+00	<b>0.0000E+00</b>
	P	5.2190E-12	5.2190E-12	5.2190E-12	5.2190E-12	5.2190E-12	5.2190E-12	5.2190E-12	5.2190E-12	5.2190E-12	5.2190E-12	5.2190E-12	5.2190E-12	5.2190E-12	—
	Wr	(+)	(+)	(+)	(+)	(+)	(+)	(+)	(+)	(+)	(+)	(+)	(+)	(+)	—
F6	T	9.4933E-02	2.0390E-01	8.8833E-02	1.9190E-01	1.0192E+01	8.3300E-02	1.0253E+00	6.9333E-02	7.1867E-02	8.7433E-02	8.7333E-03	1.2667E-02	3.2533E-02	2.0190E-01
	Mean	8.5983E-01	<b>1.2063E-04</b>	3.4564E+01	2.6118E+00	1.1288E-03	3.2173E+00	3.3283E+00	2.6507E-01	2.4244E-01	9.4211E-01	1.4714E+04	6.0049E+03	4.9090E+03	1.6781E-02
	Std	3.9698E-01	<b>1.3465E-04</b>	5.5776E+01	6.2189E-01	8.6214E-04	4.3367E-01	3.3591E-01	3.3678E-01	7.2688E-01	5.9754E-01	2.1816E+03	1.7126E+03	1.8438E+03	3.0664E-02
	P	3.0199E-11	1.0035E-03	3.0199E-11	3.0199E-11	3.0199E-11	3.0199E-11	3.0199E-11	5.5329E-08	1.0315E-02	4.9752E-11	3.0199E-11	3.0199E-11	3.0199E-11	—
F7	Wr	(+)	(=)	(+)	(+)	(+)	(+)	(+)	(+)	(+)	(+)	(+)	(+)	(+)	—
	T	7.9500E-02	1.6057E-01	7.4067E-02	1.6987E-01	1.0462E+01	7.4967E-02	1.0746E+00	5.8933E-02	5.7567E-02	8.1800E-02	8.4667E-03	1.2733E-02	3.9300E-02	1.6953E-01
	Mean	2.0202E-03	<b>1.6257E-04</b>	1.2867E-01	5.4313E-04	2.3536E-01	2.3533E-03	2.0629E-04	2.2150E-01	7.8358E-02	2.3118E-04	8.4109E+00	2.2941E+00	1.4410E+00	1.8186E-04
	Std	1.0611E-03	<b>1.1652E-04</b>	1.2686E-01	5.4929E-04	8.5117E-02	1.4119E-03	1.8162E-04	5.0563E-01	3.7331E-02	2.0789E-04	2.5931E+00	1.2301E+00	5.7948E-01	1.1748E-04
F8	P	3.0199E-11	4.2039E-01	3.0199E-11	1.4067E-04	3.0199E-11	4.5043E-11	9.2344E-01	3.0199E-11	6.5204E-01	3.0199E-11	3.0199E-11	3.0199E-11	3.0199E-11	—
	Wr	(+)	(=)	(+)	(+)	(+)	(+)	(=)	(+)	(+)	(+)	(+)	(+)	(+)	—
	T	1.3600E-01	2.6587E-01	1.3080E-01	2.2723E-01	9.8949E+00	1.2543E-01	1.1503E+00	1.0887E-01	1.3017E-01	1.0133E-02	1.4200E-02	3.8100E-02	2.7560E-01	
	Mean	-5.8649E+03	-1.2539E+04	-3.7250E+03	-4.3201E+03	-5.6142E+03	-5.2742E+03	-3.1837E+03	-8.7724E+03	-8.7042E+03	-1.2488E+04	-3.7894E+03	-4.5706E+03	-4.2798E+03	<b>-1.2569E+05</b>
F9	Std	6.0892E+02	1.6215E+02	2.7521E+02	1.1281E+03	6.4662E+02	7.9286E+02	5.3681E+02	6.9092E+02	6.0809E+02	1.2175E+02	3.8913E+02	6.4771E+02	5.6008E+02	<b>1.5719E+00</b>
	P	3.0199E-11	3.8481E-03	3.0199E-11	3.0199E-11	2.6286E-11	3.0199E-11	3.0199E-11	3.0198E-11	3.0199E-11	5.5727E-10	3.0199E-11	3.0199E-11	3.0199E-11	—
	Wr	(+)	(+)	(+)	(+)	(+)	(+)	(+)	(+)	(+)	(+)	(+)	(+)	(+)	—
	T	1.0527E-01	2.1947E-01	9.6100E-02	1.9503E-01	9.7288E+00	9.1167E-02	1.0450E+00	7.4467E-02	7.5567E-02	1.0297E-01	1.0167E-02	1.4200E-02	6.1200E-02	2.0973E-01
F10	Mean	3.0136E+00	<b>0.0000E+00</b>	4.6111E+01	<b>0.0000E+00</b>	8.4307E+01	1.8680E+00	<b>0.0000E+00</b>	1.3194E+02	7.3431E+01	2.7043E+00	2.8379E+02	2.5366E+02	2.4312E+02	<b>0.0000E+00</b>
	Std	5.4427E+00	<b>0.0000E+00</b>	3.2188E+01	<b>0.0000E+00</b>	2.9608E+01	3.9048E+00	<b>0.0000E+00</b>	3.8349E+01	2.6104E+01	6.6149E+00	1.8745E+01	2.3012E+01	1.9276E+01	<b>0.0000E+00</b>
	P	4.2433E-12	NaN	1.2118E-12	NaN	1.2118E-12	1.2108E-12	NaN	1.2118E-12	1.2118E-12	4.7856E-08	1.2118E-12	1.2118E-12	1.2118E-12	—
	Wr	(+)	(=)	(+)	(=)	(+)	(+)	(=)	(+)	(+)	(+)	(+)	(+)	(+)	—
F11	T	7.9000E-02	1.9733E-01	7.4933E-02	1.7020E-01	9.8001E+00	7.4800E-02	9.8293E-01	6.3200E-02	6.1500E-02	8.2467E-02	8.8000E-03	1.1667E-02	3.2633E-02	1.6627E-01
	Mean	1.0001E-13	<b>8.8818E-16</b>	1.2991E+01	6.5725E-15	4.5401E+00	1.9961E+01	4.4409E-15	3.2357E+00	2.3123E+00	8.0846E-02	1.6973E+01	1.3658E+01	1.2807E+01	<b>8.8818E-16</b>
	Std	1.9444E-14	<b>0.0000E+00</b>	9.0777E+00	1.7702E-15	2.9522E+00	1.8306E-03	<b>0.0000E+00</b>	1.7945E+00	1.0237E+00	4.4281E-01	6.1197E-01	9.2323E-01	1.2643E+00	<b>0.0000E+00</b>
	P	1.1368E-12	NaN	1.2118E-12	4.1697E-13	1.2118E-12	1.2019E-12	1.6853E-14	1.2118E-12	1.2118E-12	4.1617E-14	1.2118E-12	1.2118E-12	1.2118E-12	—
F12	T	1.1637E-01	1.9537E-01	1.1400E-01	1.8833E-01	1.0082E+01	9.2133E-02	1.1240E+00	7.6900E-02	7.4533E-02	9.1933E-02	8.2000E-03	1.2833E-02	3.7067E-02	1.9410E-01
	Mean	5.8204E-03	<b>0.0000E+00</b>	1.0658E+00	<b>0.0000E+00</b>	6.5775E-02	2.0958E-02	<b>0.0000E+00</b>	3.3523E+00	1.0686E-01	4.7890E-02	1.3143E+02	5.1555E+01	4.3357E+01	<b>0.0000E+00</b>
	Std	1.1020E-02	<b>0.0000E+00</b>	5.4822E-01	<b>0.0000E+00</b>	2.8677E-02	3.9191E-02	<b>0.0000E+00</b>	1.6464E+01	1.3103E-01	1.5327E-01	3.0494E+01	1.6451E+01	1.2537E+01	<b>0.0000E+00</b>
	P	6.6167E-04	NaN	1.2118E-12	NaN	1.2118E-12	1.2118E-12	NaN	1.2118E-12	1.2118E-12	4.1926E-02	1.2118E-12	1.2118E-12	1.2118E-12	—

(continued on next page)

Table 4 (continued)

F(x)	GWO	HHO	SCA	GIO	ALO	SOA	AGWO	MPSO	TACPSO	SO	SHADE	L SHADE	LSHADE-EpsIn	ESO
Wr (+)	(=)	(+)	(=)	(+)	(+)	(=)	(+)	(+)	(+)	(+)	(+)	(+)	(+)	—
T 1.0243E-01	2.0840E-01	9.3633E-02	2.0197E-01	9.7046E+00	9.7367E-02	1.0269E+00	7.7800E-02	8.3116E-02	9.6600E-02	9.0667E-03	1.2200E-02	3.2367E-02	2.0570E-01	—
F12 Mean 6.1991E-02	1.0251E-05	4.8694E+04	2.0038E-01	1.1958E+01	3.5392E-01	2.8784E-01	3.6953E+00	1.7745E+00	6.5040E-02	1.2373E+07	8.1136E+05	1.9653E+05	3.7785E-04	—
Std 9.6010E-02	1.3681E-05	1.6268E+05	8.3705E-02	5.0315E+00	1.6749E-01	1.1157E-01	1.9735E+00	1.1428E+00	1.9078E-01	7.6620E-06	1.1171E+06	2.8470E+05	4.2895E-04	—
P 3.0199E-11	3.5201E-07	3.0199E-11	3.0199E-11	3.0199E-11	3.0199E-11	3.0199E-11	—							
Wr (+)	(-)	(+)	(+)	(+)	(+)	(+)	(+)	(+)	(+)	(+)	(+)	(+)	(+)	—
T 2.8473E-01	6.1513E-01	2.5773E-01	4.0033E-01	1.0326E+01	2.8373E-01	1.4826E+00	2.9440E-01	2.6513E-01	4.1507E+00	5.2347E+07	1.4467E-02	4.1267E-02	5.5817E-01	—
F13 Mean 6.0277E-01	7.1070E-05	7.7132E-05	1.7097E+00	2.5767E+01	2.0669E+00	2.1946E-00	9.3253E+00	4.1507E+00	2.66117E-01	5.25541E-01	7.5824E+06	2.6460E+06	1.6083E-03	—
Std 2.2617E-01	1.1639E-04	2.2879E+06	2.3434E-01	1.8077E+01	2.0806E-01	1.4917E-01	6.7860E+00	4.6291E+00	4.5664E-01	2.4113E-07	7.4390E+06	1.8347E+06	2.6224E-03	—
P 3.3384E-11	6.5183E-09	3.0199E-11	3.0199E-11	3.0199E-11	3.0199E-11	3.0199E-11	—							
Wr (+)	(-)	(+)	(+)	(+)	(+)	(+)	(+)	(+)	(+)	(+)	(+)	(+)	(+)	—
T 2.6027E-01	5.9603E-01	2.5683E-01	3.6573E-01	1.0085E+01	2.5190E-01	1.3513E+00	2.4327E-01	2.5190E-01	2.5670E-01	1.4133E-02	1.7900E-02	3.9633E-02	5.3730E-01	—
Wilcoxon's rank sum test	5/4/4	13/0/0	13/0/0	13/0/0	13/0/0	13/0/0	13/0/0	13/0/0	13/0/0	13/0/0	13/0/0	13/0/0	13/0/0	—
Friedman value	5.5769	2.0192	10.5390	5.2692	9.0385	6.9615	3.9231	9.9231	8.3077	5.1154	12.8850	12.2690	11.2690	1.6923
Friedman rank	6	2	11	5	9	7	3	10	8	4	14	13	12	1

the early stage of algorithm iteration, a considerable value can be obtained, which enables the algorithm to search more significantly in different dimension areas and improve the diversity of the population. Smaller values are obtained later in the algorithm iteration, and a refined search is performed near the optimal individual to improve the local search capability. The nonlinear dynamic scaling factor is calculated in Eq. (19).

$$\delta = \delta_{\max} \times \left[ (\delta_{\max} - \delta_{\min}) - 2 \times \left( \frac{t}{T} \right)^2 \right] \quad (19)$$

where  $\delta_{\max}$  is the maximum scaling factor,  $\delta_{\min}$  is the minimum scaling factor, and  $T$  is the maximum number of iterations. Here  $\delta_{\max} = 10$ , and  $\delta_{\min} = 9$ .

Extending Eq. (18) to k-dimensional space yields the expression.

$$X_k^* = \frac{UB_k + LB_k}{2} + \frac{UB_k + LB_k - X_k}{2\delta} - \frac{X_k}{\delta} \quad (20)$$

Since male and female snakes are equally crucial in snake optimizer, a specular imaging strategy based on convex lens imaging was used for both individuals.

### 3.3. Sine-cosine composite perturbation factors

In the standard SO algorithm, the snake will enter the mating part when the food is sufficient, and the temperature is low. Since both male/female individuals want to finish mating with the superior heterosexual, there is a possibility of competition between male and female individuals. Furthermore, the winning individual can choose the mating partner first, so there is a fight mode and a mating mode in the mating part. It can be seen that the fight mode is more important in the mating part, and this mode helps to select the best individual. However, this mode also has certain disadvantages. That is, the optimal individual position update directly determines the efficiency and accuracy of the overall algorithm finding the best. Therefore, the strong dependence on the optimal individual is not conducive to the algorithm to find the best, easy to make the algorithm into a local optimum, and not easy to jump out of the local. In order to solve this drawback, the paper proposes new perturbation factors, which utilize the compound perturbation of sine and cosine. The introduction of the perturbation factors can make the algorithm jump out of the local range and improve its optimality-seeking ability to avoid falling into the local optimum. Considering that the perturbation factors are different between male and female snakes, the definitions as shown in Eq. (21) and Eq. (22). The perturbation factors graph for 500 iterations is shown in Fig. 2.

$$\lambda_1 = 1 + \frac{1}{10000} \times (\sin(a \times 4\pi \times t) + \cos(a \times 6\pi \times t)) \times e^{\left( \frac{\pi}{100} \times \frac{T-t}{4} \right)} \quad (21)$$

$$\lambda_2 = 1 + \frac{1}{10000} \times (\cos(a \times 4\pi \times t) + \sin(a \times 6\pi \times t)) \times e^{\left( \frac{\pi}{100} \times \frac{T-t}{4} \right)} \quad (22)$$

The uncertainty of the dynamic change of sine and cosine disturbance factors was used to disturb the position update of male and female snakes in battle mode to different degrees, so that male and female snakes have a more comprehensive area searchability. The search scale of the algorithm can be expanded to improve the ability of the algorithm to jump out of the local extreme value. After the disturbance factor is added, the position update rules of male and female snakes in combat mode are shown in Eqs. (23) and (24).

$$S_i^m(t+1) = \lambda_1 \times S_i^m(t) + c_3 \times e^{-f_{best}^i/f_i} \times rand_i \times (FQ \times S_{best}^f - S_i^m(t)) \quad (23)$$

$$S_i^f(t+1) = \lambda_2 \times S_i^f(t) + c_3 \times e^{-f_{best}^m/f_i} \times rand_i \times (FQ \times S_{best}^m - S_i^f(t)) \quad (24)$$

**Table 5**

Comparison of results on benchmark functions (F1-F13) with 100 dimensions.

F(x)		GWO	HHO	SCA	GJO	ALO	SOA	AGWO	MPSO	TACPSO	SO	SHADE	LSHADE	LSHADE-EpSin	ESO
F1	Mean	1.4681E-12	5.4863E-94	1.1278E+04	1.3975E-27	3.9859E+03	2.3279E-05	6.1986E-106	2.7145E+04	6.2021E+03	3.4171E-81	8.8102E+04	5.6397E+04	4.3988E+04	<b>0.0000E+00</b>
	Std	1.7239E-12	2.1224E-93	6.6893E+03	3.5346E-27	1.3440E+03	2.1482E-05	3.3901E-105	9.3654E+03	1.7840E+03	1.1490E-80	1.2058E+04	8.1959E+03	7.6652E+03	<b>0.0000E+00</b>
	P	1.2118E-12	1.2118E-12	1.2118E-12	1.2118E-12	1.2118E-12	1.2118E-12	1.2118E-12	1.2118E-12	1.2118E-12	1.2118E-12	1.2118E-12	1.2118E-12	1.2118E-12	—
	Wr	(+)	(+)	(+)	(+)	(+)	(+)	(+)	(+)	(+)	(+)	(+)	(+)	(+)	—
	T	1.6000E-01	1.3030E-01	1.1247E-01	2.0127E-01	2.6519E+01	1.2457E-01	2.4518E+00	7.7267E-02	7.9700E-02	1.2877E-01	8.3667E-03	1.3967E-02	3.5900E-02	2.0283E-01
F2	Mean	3.8796E-08	1.0756E-48	8.6481E+00	1.2389E-17	2.5377E+04	8.2982E-05	8.3517E-59	2.6650E+02	1.0487E+02	6.6538E-36	1.5855E+22	4.0708E+14	6.2870E+10	<b>0.0000E+00</b>
	Std	1.0920E-08	4.5096E-48	6.2976E+00	7.6451E-18	1.3717E+05	4.3807E-05	2.3548E-58	4.3739E+01	2.7344E+01	4.3285E-36	7.0194E+22	1.8281E+15	3.3889E+11	<b>0.0000E+00</b>
	P	1.2118E-12	1.2118E-12	1.2118E-12	1.2118E-12	1.2118E-12	1.2118E-12	1.2118E-12	1.2118E-12	1.2118E-12	1.2118E-12	1.2118E-12	1.2118E-12	1.2118E-12	—
	Wr	(+)	(+)	(+)	(+)	(+)	(+)	(+)	(+)	(+)	(+)	(+)	(+)	(+)	—
	T	1.7420E-01	1.3223E-01	1.1653E-01	2.1343E-01	2.5994E+01	1.2793E-01	2.4427E+00	8.4667E-02	8.5900E-02	1.4257E-01	9.3667E-03	1.3700E-02	3.6933E-02	2.2463E-01
F3	Mean	6.7022E+02	6.7711E-42	2.4062E+05	2.5364E+00	7.7678E+04	9.2401E+01	7.4766E-48	2.2972E+05	7.7916E+04	1.3980E-35	4.4074E+05	3.1523E+05	1.5312E+05	<b>0.0000E+00</b>
	Std	5.3845E+02	3.7087E-41	5.0927E+04	8.9636E+00	3.3409E+04	1.9568E+02	4.0941E-47	4.6379E+04	2.0757E+04	7.5272E-35	6.6282E+04	6.0342E+04	4.3397E+04	<b>0.0000E+00</b>
	P	1.2118E-12	1.2118E-12	1.2118E-12	1.2118E-12	1.2118E-12	1.2118E-12	1.2118E-12	1.2118E-12	1.2118E-12	1.2118E-12	1.2118E-12	1.2118E-12	1.2118E-12	—
	Wr	(+)	(+)	(+)	(+)	(+)	(+)	(+)	(+)	(+)	(+)	(+)	(+)	(+)	—
	T	1.1467E+00	2.3486E+00	1.0499E+00	1.1478E+00	2.8261E+01	1.0485E+00	4.5520E+00	1.0167E+00	1.0370E+00	1.0950E+00	4.0367E-02	2.8900E-02	7.8700E-02	2.1676E+00
F4	Mean	8.1040E-01	6.0517E-48	9.0412E+01	5.1790E+00	3.4202E+01	7.2405E+01	6.2084E-50	6.6242E+01	4.5933E+01	8.5413E-37	8.4124E+01	7.4964E+01	5.6506E+01	<b>1.5856E-300</b>
	Std	7.9405E-01	3.3124E-47	2.8334E+00	9.7496E+00	4.7072E+00	1.7763E+01	1.0251E-49	5.6322E+00	2.9085E+00	1.2192E-36	4.2706E+00	6.2201E+00	6.9458E+00	<b>0.0000E+00</b>
	P	9.4001E-12	9.4001E-12	9.3936E-12	9.4001E-12	9.3936E-12	9.4001E-12	9.3936E-12	9.3936E-12	9.4001E-12	9.4001E-12	9.4001E-12	9.4001E-12	9.4001E-12	—
	Wr	(+)	(+)	(+)	(+)	(+)	(+)	(+)	(+)	(+)	(+)	(+)	(+)	(+)	—
	T	1.3920E-01	1.4597E-01	1.1087E-01	2.0077E-01	2.6639E+01	1.2220E-01	2.4505E+00	7.7533E-02	7.5867E-02	1.3373E-01	8.5667E-03	1.4667E-02	5.8567E-02	2.0533E-01
F5	Mean	9.8042E+01	<b>2.7217E-02</b>	1.0984E+08	9.8281E+01	6.9738E+05	9.8709E+01	9.8262E+01	2.6381E+07	3.1482E+06	7.1889E+01	1.7896E+08	7.6913E+07	4.5549E+07	8.6794E+00
	Std	5.6678E-01	<b>3.7049E-02</b>	4.6158E+07	4.9516E-01	5.2157E+05	2.2949E-01	5.6543E-01	2.8566E+07	1.9736E+06	3.8585E+01	4.3830E+07	2.0431E+07	1.3235E+07	2.4501E+01
	P	8.9934E-11	2.1156E-01	3.0199E-11	6.6955E-11	3.0199E-11	3.3384E-11	9.9186E-11	3.0199E-11	3.0199E-11	1.1737E-09	3.0199E-11	3.0199E-11	3.0199E-11	—
	Wr	(+)	(=)	(+)	(+)	(+)	(+)	(+)	(+)	(+)	(+)	(+)	(+)	(+)	—
	T	1.7303E-01	2.2037E-01	1.2587E-01	2.3087E-01	2.6718E+01	1.2917E-01	2.5150E+00	8.7267E-02	8.5867E-02	1.5190E-01	9.7333E-03	1.4333E-02	3.8133E-02	2.5907E-01
F6	Mean	1.0083E+01	<b>2.7135E-04</b>	1.0586E+04	1.6638E+01	4.7169E+03	-2.3369E+04	1.9152E+01	3.2276E+04	6.4213E+03	1.0833E+01	8.7502E+04	5.6795E+04	4.2921E+04	3.8198E-01
	Std	1.0140E+00	<b>3.0141E-04</b>	8.2643E+03	7.2716E-01	2.1362E+03	3.9967E+03	3.55510E-01	1.1923E+04	1.9953E+03	1.1022E+01	9.5482E+03	7.8983E+03	8.0824E+03	6.8703E-01
	P	3.0199E-11	3.3520E-08	3.0199E-11	3.0199E-11	3.0199E-11	3.0199E-11	3.0199E-11	3.0199E-11	3.0199E-11	3.0199E-11	3.0199E-11	3.0199E-11	3.0199E-11	—
	Wr	(+)	(-)	(+)	(+)	(+)	(+)	(+)	(+)	(+)	(+)	(+)	(+)	(+)	—
	T	1.4597E-01	1.7360E-01	1.1040E-01	1.9230E-01	2.5850E+01	1.1937E-01	2.3619E+00	7.4667E-02	7.4800E-02	1.3603E-01	8.6667E-03	1.4733E-02	3.8033E-02	2.2213E-01
F7	Mean	6.8976E-03	<b>1.4818E-04</b>	1.2897E+02	1.1891E-03	5.0922E+00	7.6273E-03	4.0693E-04	1.0183E+02	1.5688E+01	2.4156E-04	2.7913E+02	1.1604E+02	7.2243E+01	2.1941E-04
	Std	2.5533E-03	1.3842E-04	7.2456E+01	7.5301E-04	1.6781E+00	4.5998E-03	2.6623E-04	5.2228E+01	1.8569E+01	2.0768E-04	4.4781E+01	3.6555E+01	1.9927E+01	<b>1.3246E-04</b>
	P	3.0199E-11	7.9590E-03	3.0199E-11	1.4643E-10	1.4643E-10	3.0199E-11	2.0523E-03	3.0199E-11	3.0199E-11	8.8830E-01	3.0199E-11	3.0199E-11	3.0199E-11	—
	Wr	(+)	(-)	(+)	(+)	(+)	(+)	(+)	(+)	(+)	(=)	(+)	(+)	(+)	—
	T	3.0037E-01	5.0157E-01	2.7178E-01	3.7677E-01	2.7001E+01	2.8017E-01	2.8166E+00	2.3457E-01	2.3610E-01	2.9820E-01	1.4200E-02	2.0467E-02	4.4300E-02	5.5287E-01
F8	Mean	-1.5967E+04	-4.1894E+04	-6.7842E+03	-1.0235E+04	-1.8062E+04	-9.8571E+03	-5.6413E+03	-2.3083E+04	-2.2861E+04	-4.1676E+04	-7.1222E+03	-7.8361E+03	-8.1323E+03	<b>-4.1898E+04</b>
	Std	3.0494E+03	7.4476E+00	5.2252E+02	4.3400E+03	1.7303E+01	1.1019E+03	7.2270E+02	1.7772E+03	1.4318E+03	4.0855E+02	7.7454E+02	7.6376E+02	9.7888E+02	<b>1.3378E+00</b>
	P	3.0199E-11	1.9527E-03	3.0199E-11	3.0199E-11	1.7203E-12	3.0199E-11	3.0199E-11	3.0199E-11	3.8202E-10	3.0199E-11	3.0199E-11	3.0199E-11	3.0199E-11	—
	Wr	(+)	(+)	(+)	(+)	(+)	(+)	(+)	(+)	(+)	(+)	(+)	(+)	(+)	—
	T	1.7940E-01	2.6163E-01	1.5320E-01	2.6203E-01	2.6625E+01	1.6057E-01	2.4984E+00	1.1037E-01	1.1167E-01	1.7947E-01	1.0467E-02	1.5700E-02	6.5833E-02	3.0937E-01
F9	Mean	8.9016E+00	<b>0.0000E+00</b>	2.8216E+02	<b>0.0000E+00</b>	3.6351E+02	4.2707E+00	<b>0.0000E+00</b>	7.3418E+02	4.5957E+02	5.4751E+00	1.1675E+03	1.0822E+03	1.0020E+03	<b>0.0000E+00</b>
	Std	6.5225E+00	<b>0.0000E+00</b>	1.4038E+02	<b>0.0000E+00</b>	6.9116E+01	5.7224E+00	<b>0.0000E+00</b>	7.1627E+01	6.7165E+01	1.9232E+01	3.9666E+01	5.1240E+01	3.3924E+01	<b>0.0000E+00</b>
	P	1.2118E-12	NaN	1.2118E-12	NaN	1.2118E-12	1.2118E-12	NaN	1.2118E-12	5.3750E-06	1.2118E-12	1.2118E-12	1.2118E-12	1.2118E-12	—
	Wr	(+)	(=)	(+)	(=)	(+)	(+)	(=)	(+)	(+)	(+)	(+)	(+)	(+)	—
	T	1.6780E-01	2.4697E-01	1.5433E-01	2.6717E-01	3.1043E+01	1.5823E-01	2.9798E+00	1.1413E-01	1.1327E-01	1.8390E-01	1.2067E-02	1.5467E-02	5.4467E-02	2.8457E-01
F10	Mean	1.2653E-07	<b>8.8818E-16</b>	1.8439E+01	5.0271E-14	1.4164E+01	1.9966E+01	7.7568E-15	1.8558E+01	1.2531E+01	4.4409E-15	1.8941E+01	1.7450E+01	1.6577E+01	<b>8.8818E-16</b>
	Std	4.2329E-08	<b>0.0000E+00</b>	5.0564E+00	8.1523E-15	1.3261E+00	4.4829E-04	9.0135E-16	7.2462E-01	1.2384E+00	0.0000E+00	2.4150E-01	4.8800E-01	4.7089E-01	<b>0.0000E+00</b>
	P	1.2118E-12	NaN	1.2118E-12	1.0071E-12	1.2118E-12	1.1313E-12	4.1574E-14	1.2118E-12	1.2118E-12	5.3750E-06	1.2118E-12	1.2118E-12	1.2118E-12	—
	Wr	(+)	(=)	(+)	(+)	(+)	(+)	(+)	(+)	(+)	(+)	(+)	(+)	(+)	—
	T	1.9037E-01	2.5893E-01	1.7373E-01	2.7424E-01	3.0551E+01	1.6800E-01	2.8802E+00	1.2310E-01	1.2047E-01	1.8247E-01	1.3500E-02	1.5900E-02	5.0733E-02	2.8660E-01
F11	Mean	1.5738E-03	<b>0.0000E+00</b>	1.0594E+02	<b>0.0000E+00</b>	4.0579E+01	2.0249E-02	<b>0.0000E+00</b>	2.5630E+02	5.8680E+01	<b>0.0000E+00</b>	8.1655E+02	5.2858E+02	4.0810E+02	<b>0.0000E+00</b>
	Std	6.7995E-03	<b>0.0000E+00</b>	8.8020E+01	<b>0.0000E+00</b>	1.6344E+01	3.0942E-02	<b>0.0000E+00</b>	9.8671E+01	1.8504E+01	<b>0.0000E+00</b>	9.3160E+01	6.4692E+01	6.7061E+01	<b>0.0000E+00</b>
	P	1.2118E-12	NaN	1.2118E-12	NaN	1.2118E-12	1.2118E-12	NaN	1.2118E-12	1.2118E-12	NaN	1.2118E-12	1.2118E-12	1.2118E-12	—

(continued on next page)

Table 5 (continued)

F(x)	GWO	HHO	SCA	GIO	ALO	SOA	AGWO	MPSO	TACPSO	SO	SHADE	L SHADE	LSHADE-EpsIn	ESO
Wr (+)	(=)	(+)	(=)	(+)	(+)	(+)	(=)	(+)	(+)	(=)	(+)	(+)	(+)	—
T 2.2060E-01	3.0867E-01	1.8723E-01	3.2243E-01	3.1021E+01	1.9020E-01	3.0971E+00	1.5217E-01	1.4533E-01	1.9153E-01	1.3867E-02	1.6167E-02	1.6167E-02	3.5493E-01	
F12 Mean 3.1077E-01	4.3871E-06	3.2848E+08	5.8353E-01	1.2324E+03	7.7374E-01	7.4823E-01	6.7386E+06	9.5267E+04	8.9169E-02	2.9105E+08	6.2647E+07	3.1612E+07	4.5250E-04	
Std 7.0187E-02	4.1144E-05	1.5763E-08	7.3235E-02	3.4297E+03	8.7282E-02	4.4192E-02	7.9952E+06	1.9887E+05	2.3966E-01	1.0127E+08	1.8807E+07	2.0196E+07	9.3168E-04	
P 3.0199E-11	4.6390E-05	3.0199E-11	—											
Wr (+)	(-)	(+)	(+)	(+)	(+)	(+)	(+)	(+)	(+)	(+)	(+)	(+)	(+)	—
T 5.7893E-01	1.2120E+00	5.5963E-01	6.9500E-01	2.9789E+01	5.6413E-01	3.6466E+00	5.1200E-01	5.0797E-01	5.7543E-01	2.5867E-02	3.1400E-02	6.2267E-02	1.1293E+00	
F13 Mean 6.7959E+00	1.3703E-04	5.5297E-08	8.4172E+00	1.4519E+05	9.3520E+00	9.2488E-00	6.2439E+07	3.0355E+06	1.4189E+00	6.8146E-08	2.2718E+08	1.0222E+08	1.2661E-02	
Std 4.5582E-01	2.8554E-04	2.0905E-08	3.1864E-01	1.4688E+05	2.8906E-01	1.6550E-01	1.0540E+08	3.1511E+06	3.0191E+00	3.8878E-08	6.6482E+07	2.0401E-02	—	
P 3.0199E-11	5.0922E-08	3.0199E-11	—											
Wr (+)	(-)	(+)	(+)	(+)	(+)	(+)	(+)	(+)	(+)	(+)	(+)	(+)	—	—
T 5.4343E-01	1.1264E+00	5.3407E-01	6.3690E-01	2.6841E+01	5.2727E-01	3.2137E+00	4.8067E-01	5.3803E-01	5.8063E-01	2.2633E-02	3.1500E-02	5.3400E-02	1.0553E+00	
Wilcoxon's rank sum test	5/4/4	13/0/0	13/0/0	11/2/0	13/0/0	11/2/0	13/0/0	13/0/0	13/0/0	13/0/0	13/0/0	13/0/0	—	—
Friedman value	5.8846	2.0962	11.4615	5.4231	8.3846	7.1538	3.8077	11.0385	8.8462	4.2308	12.6538	11.5000	10.6154	1.9038
Friedman rank	6	2	12	5	8	7	3	11	9	4	14	13	10	1

### 3.4. Tent-chaos and Cauchy mutation

In the snake optimizer, after the mating behavior of male and female snakes, the female snake will lay and hatch eggs to obtain new baby snakes. The new snakes will replace the inferior individuals to replenish the population and start a new cycle iteration. In the new iteration, to prevent the algorithm from falling into the local optimum and speed up the convergence speed as much as possible, this paper introduces Tent-chaos (Bharti & Singh, 2016; Ibrahim et al., 2018; Xu et al., 2014) and Cauchy mutation strategies (Li et al., 2017; Wang et al., 2020; Zhao, Fang, Liu, et al., 2022) to improve the ability of the algorithm to jump out of local. By comparing individual fitness with the population's average fitness, the individuals with lower-than-average fitness use the Cauchy mutation, and those with higher-than-average fitness use the Tent-chaos perturbation. Finally, the new and old individuals before and after the mutation were compared, and the optimal individuals were selected to remain in the population.

Chaos (Vieira & Mosna, 2022) is a common nonlinear phenomenon in nature. Due to the randomness, ergodicity, and regularity of chaos variables, it can not only effectively maintain the diversity of the population but also help the algorithm to jump out of the local optimal and improve the global search ability. Many scholars have applied it to the optimization of search problems. Chaotic perturbation generates chaotic variables  $Z_T$  through Tent chaotic mapping, carries the chaotic variables to the solution space of the problem to be solved, and finally perturbs the individuals chaotically. The Tent chaotic mapping is shown in Eq. (25), the solution space is shown in Eq. (26), and the chaotic perturbation rules are according to Eq. (27).

$$z_{i+1} = (2z_i) \bmod 1 + rand \times \frac{1}{N_T} \quad (25)$$

where  $N_T$  is the number of particles in the chaotic sequence, and  $rand$  is a random number between (0, 1).

$$Y_{new}^d = d_{\min} + (d_{\max} - d_{\min}) \times Z_d \quad (26)$$

where  $d_{\min}$  and  $d_{\max}$  are the minimum and maximum values of the  $d$ -th dimensional variable  $Y_{new}^d$ , respectively.

$$Y_{new}^* = \frac{Y^* + Y_{new}}{2} \quad (27)$$

where  $Y^*$  is the individual to be chaotically perturbed,  $Y_{new}$  is the amount of chaotic perturbation generated, and  $Y_{new}^*$  is the individual after the chaotic perturbation.

The Cauchy mutation is derived from the Cauchy distribution, characterized by a small peak at zero and a slow decline from the peak to the zero value, which can make the mutation range more uniform. By introducing the Cauchy operator into the target position update, the adjustment ability of the Cauchy operator is brought into play to enhance the ability of the algorithm to jump out of the local optimum, and the Cauchy mutation is shown in Eq. (28).

$$\text{mutation}(m) = m \times (1 + \tan(\pi \times (rand - 0.5))) \quad (28)$$

where  $m$  is the position of the original individual,  $\text{mutation}(m)$  is the position of the individual after the Cauchy mutation, and  $rand$  is a random number in the interval (0, 1).

By combining the above-proposed strategy with the original SO algorithm and replacing the unreasonable parts and links in the SO algorithm, the optimization capability and efficiency of the original SO can be effectively enhanced. The pseudocode of the Enhanced Snake Optimizer algorithm is shown in Algorithm 2.

**Table 6**

Comparison of results on benchmark functions (F1-F13) with 500 dimensions.

F(x)		GWO	HHO	SCA	GJO	ALO	SOA	AGWO	MPSO	TACPSO	SO	SHADE	LSHADE	LSHADE-EpSin	ESO
F1	Mean	1.5673E-03	2.1910E-93	2.1274E+05	6.0945E-13	2.1315E+05	1.2182E-01	9.5541E-16	7.7000E+05	2.9855E+05	4.2991E-71	5.8583E+05	4.3381E+05	3.9832E+05	<b>0.0000E+00</b>
	Std	6.0411E-04	1.1557E-92	8.2117E+04	4.6912E-13	3.9230E+04	1.1361E-01	5.2235E-15	3.1590E+04	1.9069E+04	5.7155E-71	3.5030E+04	3.6737E+04	1.1053E+05	<b>0.0000E+00</b>
P		1.2118E-12	1.2118E-12	1.2118E-12	1.2118E-12	1.2118E-12	1.2118E-12	1.2118E-12	1.2118E-12	1.2118E-12	1.2118E-12	1.2118E-12	1.2118E-12	—	
Wr	(+)	(+)	(+)	(+)	(+)	(+)	(+)	(+)	(+)	(+)	(+)	(+)	(+)	(+)	—
T	5.9330E-01	3.1107E-01	4.8640E-01	6.3213E-01	1.7563E+02	5.4843E-01	1.4966E+01	2.9920E-01	2.9330E-01	9.0380E-01	2.7000E-02	6.3500E-02	3.5997E-01	1.0491E+00	
F2	Mean	1.0586E-02	3.0924E-49	9.6785E+01	6.6797E-09	3.7536E+230	6.0352E-03	5.2738E-13	3.7505E+116	1.1448E+37	1.3796E-31	1.0000E+30	1.0000E+30	9.0000E+29	<b>0.0000E+00</b>
	Std	1.6966E-03	1.5745E-48	2.3657E-12	3.4264E-09	Inf	3.6774E-03	2.8467E-12	2.3657E-12	6.2701E+37	1.5802E-31	1.4314E+14	1.4314E+14	3.0513E+29	<b>0.0000E+00</b>
P		2.3657E-12	2.3657E-12	2.3657E-12	2.3657E-12	2.3657E-12	2.3657E-12	2.3657E-12	2.3657E-12	2.3657E-12	4.1617E-14	4.1617E-14	1.4070E-13	—	
Wr	(+)	(+)	(+)	(+)	(+)	(+)	(+)	(+)	(+)	(+)	(+)	(+)	(+)	(+)	—
T	6.3900E-01	3.3613E-01	5.2670E-01	6.7030E-01	1.8145E+02	5.8900E-01	1.5017E+01	3.1920E-01	3.1447E-01	9.6480E-01	2.7767E-02	3.2000E-02	4.0970E-01	1.1173E+00	
F3	Mean	3.2619E+05	6.2871E-36	6.9187E+06	4.6597E+04	1.9856E+06	1.7762E+05	9.6810E+01	4.5218E+06	1.8993E+06	4.5829E-25	1.0789E+07	8.5598E+06	8.4658E+06	<b>0.0000E+00</b>
	Std	9.4743E+04	3.4151E-35	1.5817E+06	2.9461E+04	5.8814E+05	1.0911E+05	4.9501E+02	7.7027E+05	3.8624E+05	2.5101E-24	1.7222E+06	1.6866E+06	3.3832E+06	<b>0.0000E+00</b>
P		1.2118E-12	1.2118E-12	1.2118E-12	1.2118E-12	1.2118E-12	1.2118E-12	1.2118E-12	1.2118E-12	1.2118E-12	1.2118E-12	1.2118E-12	1.2118E-12	—	
Wr	(+)	(+)	(+)	(+)	(+)	(+)	(+)	(+)	(+)	(+)	(+)	(+)	(+)	(+)	—
T	8.7700E+00	1.9939E+01	8.6771E+00	8.8899E+00	1.9636E+02	8.8876E+00	3.1332E+01	8.2180E+00	8.1707E+00	9.0271E+00	3.1117E-01	3.1980E-01	7.0900E-01	1.7471E+01	
F4	Mean	6.4647E+01	2.4373E-49	9.9095E+01	8.3494E+01	4.7441E+01	9.8796E+01	3.5759E-04	9.9244E+01	6.9904E+01	7.4089E-34	9.6394E+01	9.3118E+01	9.2373E+01	<b>0.0000E+00</b>
	Std	4.9681E+00	6.8735E-49	2.5875E-01	4.2479E+00	3.3588E+00	5.5431E-01	1.2241E-03	1.9860E-01	2.6243E+00	1.1538E-33	8.6253E-01	2.2841E+00	6.6474E+00	<b>0.0000E+00</b>
P		7.8787E-12	7.8787E-12	7.8787E-12	7.8787E-12	7.8787E-12	7.8787E-12	7.8787E-12	7.8787E-12	7.8787E-12	7.8787E-12	7.8787E-12	7.8787E-12	—	
Wr	(+)	(+)	(+)	(+)	(+)	(+)	(+)	(+)	(+)	(+)	(+)	(+)	(+)	(+)	—
T	6.0003E-01	4.2067E-01	4.9503E-01	6.4153E-01	1.7951E+02	5.5640E-01	1.4725E+01	2.9240E-01	2.8830E-01	9.4527E-01	2.6900E-02	3.0267E-02	3.7653E-01	1.0533E+00	
F5	Mean	4.9802E+02	<b>1.1836E-01</b>	1.9073E+09	4.9829E+02	1.5627E+08	8.9277E+02	4.9881E+02	2.5698E+09	4.2859E+08	3.5481E+02	1.5307E+09	8.0021E+08	8.6086E+08	1.4590E+01
	Std	3.8374E-01	<b>1.7458E-01</b>	4.2843E+08	1.2795E-01	4.7175E+07	5.6025E+02	5.4034E-02	2.3162E+08	4.6288E+07	2.1745E+02	1.8311E+08	1.4329E+08	5.3414E+08	4.7969E+01
P		3.0199E-11	1.2732E-02	3.0199E-11	3.0199E-11	3.0199E-11	3.0199E-11	3.0199E-11	3.0199E-11	3.0199E-11	4.5726E-09	3.0199E-11	3.0199E-11	3.0199E-11	—
Wr	(+)	(-)	(+)	(+)	(+)	(+)	(+)	(+)	(+)	(+)	(+)	(+)	(+)	(+)	—
T	6.2953E-01	6.2760E-01	5.0367E-01	6.5253E-01	1.7684E+02	5.7410E-01	1.4599E+01	3.1100E-01	3.0930E-01	9.7947E-01	2.7500E-02	3.2267E-02	3.7600E-01	1.2089E+00	
F6	Mean	9.1633E+01	<b>1.8515E-03</b>	2.1053E+05	1.0920E+02	2.2560E+05	1.1622E+02	1.1961E+02	7.6885E+05	2.9562E+05	8.7993E+01	5.9316E+05	4.2942E+05	3.5781E+05	4.0957E-02
	Std	1.6480E+00	<b>2.2293E-03</b>	6.6764E+04	1.2126E+00	4.2916E+04	7.6280E-01	6.1939E-01	2.7135E+04	1.9908E+04	5.1543E+01	4.8458E+04	3.4760E+04	7.4532E+04	7.3793E-02
P		3.0199E-11	1.4110E-09	3.0199E-11	3.0199E-11	3.0199E-11	3.0199E-11	3.0199E-11	3.0199E-11	3.0199E-11	5.4617E-09	3.0199E-11	3.0199E-11	3.0199E-11	—
Wr	(+)	(-)	(+)	(+)	(+)	(+)	(+)	(+)	(+)	(+)	(+)	(+)	(+)	(+)	—
T	5.8367E-01	5.2300E-01	4.7453E-01	5.8913E-01	1.6955E+02	5.3363E-01	1.3698E+01	2.7907E-01	2.8063E-01	9.3043E-01	2.5233E-02	2.9000E-02	3.6580E-01	1.1004E+00	
F7	Mean	5.1264E-02	<b>1.8549E-04</b>	1.4093E+04	6.0873E-03	9.4344E+02	1.0270E-01	3.9055E-03	1.8511E+04	6.2906E+03	2.5254E-04	1.2605E+04	6.6818E+03	6.6670E+03	1.9791E-04
	Std	1.5468E-02	1.7263E-04	3.6549E+03	3.3156E-03	3.0810E+02	3.6580E-02	2.3848E-03	1.4584E+03	1.8211E+03	2.0640E-04	1.9451E+03	1.3105E+03	3.7814E+03	<b>1.2912E-04</b>
P		3.0199E-11	4.2896E-01	3.0199E-11	3.0199E-11	3.0199E-11	3.0199E-11	3.0199E-11	3.0199E-11	3.0199E-11	4.8252E-01	3.0199E-11	3.0199E-11	3.0199E-11	—
Wr	(+)	(=)	(+)	(+)	(+)	(+)	(+)	(+)	(+)	(=)	(+)	(+)	(+)	(+)	—
T	1.4240E+00	2.2478E+00	1.3196E+00	1.4764E+00	1.7539E+02	1.3752E+00	1.5902E+01	1.1137E+00	1.1156E+00	1.7730E+00	5.7200E-02	5.9500E-02	4.1197E-01	2.8214E+00	
F8	Mean	-5.7892E+04	-2.0948E+05	-1.5550E+04	-2.4535E+04	-9.2867E+04	-2.3369E+04	-1.1842E+04	-6.1072E+04	-6.4866E+04	-2.0807E+05	-1.5960E+04	-1.8761E+04	-1.7538E+04	<b>-2.0949E+05</b>
	Std	3.6020E+03	1.7266E+01	7.2846E+02	1.3130E+04	1.1038E+04	3.9967E+03	1.4014E+03	4.2044E+03	2.6701E+03	2.5254E+03	1.7079E+03	1.6331E+03	2.8856E+03	<b>4.0425E+00</b>
P		3.0199E-11	5.9428E-02	3.0199E-11	3.0199E-11	3.0199E-11	3.0199E-11	3.0199E-11	3.0199E-11	3.0199E-11	3.0199E-11	3.0199E-11	3.0199E-11	3.0199E-11	—
Wr	(+)	(=)	(+)	(+)	(+)	(+)	(+)	(+)	(+)	(+)	(+)	(+)	(+)	(+)	—
T	1.0062E+00	8.8150E-01	7.4190E-01	8.4203E-01	1.3681E+02	9.1980E-01	1.0503E+01	4.8873E-01	4.7117E-01	1.4213E+00	2.5133E-02	3.6667E-02	4.6637E-01	1.7910E+00	
F9	Mean	7.6069E+01	<b>0.0000E+00</b>	1.1070E+03	4.5172E-12	3.7396E+03	1.1229E+01	<b>0.0000E+00</b>	5.9219E+03	4.4750E+03	4.0550E+00	6.4155E+03	6.0235E+03	5.8464E+03	<b>0.0000E+00</b>
	Std	2.6248E+01	<b>0.0000E+00</b>	4.3740E+02	2.0335E-12	8.3786E+02	1.3520E+01	<b>0.0000E+00</b>	1.4342E+02	1.1028E+02	2.0783E+01	1.0696E+02	1.0936E+02	2.4898E+02	<b>0.0000E+00</b>
P		1.2118E-12	NaN	1.2118E-12	9.7910E-13	1.2118E-12	1.2118E-12	NaN	1.2118E-12	1.2118E-12	8.1523E-02	1.2118E-12	1.2118E-12	1.2118E-12	—
Wr	(+)	(=)	(+)	(+)	(+)	(+)	(+)	(=)	(+)	(+)	(+)	(+)	(+)	(+)	—
T	7.8250E-01	8.5910E-01	8.5080E-01	7.4090E-01	1.7994E+02	7.7713E-01	1.5787E+01	4.9213E-01	4.7807E-01	1.1529E+00	3.2167E-02	3.5533E-02	3.8213E-01	1.4557E+00	
F10	Mean	1.8888E-03	<b>8.8818E-16</b>	1.7673E+01	3.2739E-08	1.5786E+01	1.9967E+01	1.3323E-14	2.0266E+01	1.8187E+01	4.9146E-15	1.9481E+01	1.8684E+01	1.8334E+01	<b>8.8818E-16</b>
	Std	2.7410E-04	<b>0.0000E+00</b>	4.9406E+00	1.2835E-08	8.3858E-01	4.0867E-05	2.6549E-14	6.4321E-02	1.8996E-01	1.2283E-15	1.6687E-01	1.9729E-01	6.4907E-01	<b>0.0000E+00</b>
P		1.2118E-12	NaN	1.2118E-12	1.2118E-12	1.2118E-12	1.2118E-12	NaN	1.2118E-12	1.2118E-12	1.2118E-12	1.2118E-12	1.2118E-12	1.2118E-12	—
Wr	(+)	(=)	(+)	(+)	(+)	(+)	(+)	(+)	(+)	(+)	(+)	(+)	(+)	(+)	—
T	8.0170E-01	8.8593E-01	7.7413E-01	7.8500E-01	1.9236E+02	8.3377E-01	1.6310E+01	5.2707E-01	5.1930E-01	1.2052E+00	3.3000E-02	3.7700E-02	4.2467E-01	1.5232E+00	
F11	Mean	1.0568E-02	<b>0.0000E+00</b>	1.9382E+03	3.5285E-13	1.9845E+03	4.3823E-02	<b>0.0000E+00</b>	6.9349E+03	2.6544E+03	<b>0.0000E+00</b>	5.2482E+03	3.9985E+03	3.3908E+03	<b>0.0000E+00</b>
	Std	2.7883E-02	<b>0.0000E+00</b>	5.5039E+02	1.3782E-12	4.1814E+02	6.2816E-02	<b>0.0000E+00</b>	6.6552E+02	1.3459E+02	<b>0.0000E+00</b>	3.7622E+02	3.8562E+02	6.5152E+02	<b>0.0000E+00</b>
P		1.2118E-12	NaN	1.2118E-12	1.2118E-12	1.2118E-12	1.2118E-12	NaN	1.2118E-12	1.2118E-12	1.2118E-12	1.2118E-12	1.2118E-12	1.2118E-12	—

(continued on next page)

**Table 6 (continued)**

F(x)	GWO	HHO	SCA	GIO	ALO	SOA	AGWO	MPSO	TACPSO	SO	SHADE	L SHADE-EpSIN	ESO
Wr (+)	(=)	(+)	(+)	(+)	(+)	(=)	(+)	(+)	(+)	(=)	(+)	(+)	—
T 8.0547E-01	9.6077E-01	7.5917E-01	7.9160E-01	1.7842E+02	8.3653E-01	1.5582E+01	5.5623E-01	5.4487E-01	1.1326E+00	3.4233E-02	4.8920E-01	1.4907E-00	
F12 Mean 7.4357E-01	1.8916E-06	5.7306E+09	9.2209E-01	3.9137E+07	1.9342E+00	1.0974E+00	5.0862E+09	3.4784E+08	1.3071E-01	2.8387E+09	1.1453E+09	1.0391E+09	
Std 5.2899E-02	2.8962E-06	1.1594E-09	2.6655E-02	2.9511E+07	1.0013E+00	1.4746E-02	6.6337E+08	5.8517E+07	3.5046E-01	4.7911E+08	1.8009E+08	2.0142E-05	
P 3.0199E-11	1.3595E-07	3.0199E-11	1.3889E-04										
Wr (+)	(-)	(+)	(+)	(+)	(+)	(+)	(+)	(+)	(+)	(+)	(+)	(+)	—
T 2.6363E+00	5.4428E+00	2.5745E+00	2.7267E+00	1.7799E+02	2.5801E+00	1.8969E+01	2.3169E+00	2.3222E+00	2.9969E+00	9.9033E-02	1.0193E-01	5.4039E+00	
F13 Mean 5.0912E+01	4.8916E-04	9.7990E-09	4.8062E+01	3.2328E+08	7.6578E+01	4.9532E+01	1.0267E+10	1.2032E+09	9.5488E+00	6.0125E+09	2.8393E+09	9.7579E-03	
Std 1.4836E+00	1.9345E-03	1.9276E-09	3.4418E-01	2.0699E+08	1.9562E+01	1.1266E-01	8.7342E+08	1.5159E+08	1.5200E+01	1.0017E+09	6.6081E+08	3.1158E-02	
P 3.0199E-11	3.1573E-05	3.0199E-11	—										
Wr (+)	(-)	(+)	(+)	(+)	(+)	(+)	(+)	(+)	(+)	(+)	(+)	(+)	—
T 2.7207E+00	5.5694E+00	2.6451E+00	2.7249E+00	1.9028E+02	2.6912E+00	2.1205E+01	2.4383E+00	2.4370E+00	3.1385E+00	1.0163E-01	1.0623E-01	5.6351E+00	
Wilcoxon's rank sum test	13/0/0	5/4/4	13/0/0	13/0/0	13/0/0	13/0/0	13/0/0	11/2/0	13/0/0	13/0/0	13/0/0	13/0/0	—
Friedman value	6.3462	1.7308	10.9038	5.6154	9.5385	7.3462	4.2692	11.0962	9.0769	3.8077	11.2692	10.5385	11.7692
Friedman rank	6	2	11	5	9	7	4	12	8	3	13	10	14

**Algorithm 2.** Enhanced Snake Optimizer (ESO)

---

1. Define  $Dim$ ,  $UB$ ,  $LB$ , and  $\text{Pop\_Size}(N_{all})$ ,  $\text{Max\_Iter}(T)$ ,  $\text{Curr\_Iter}(t)$ ,
2. Initialize the population randomly  $S_i (i = 1, 2, \dots, N_{all})$
3. **while** ( $t < T$ ) **do**
4. Define  $c_1^{\text{new}}$ ,  $c_2^{\text{new}}$ , and  $c_3^{\text{new}}$  using Eqs. (14), (15), and (16).
5. Evaluate the fitness of each group  $N_m$  and  $N_t$
6. Find  $f_{best}^m$  and  $f_{best}^f$
7. Get the opposite position  $X_{best}^{m*}$ ,  $X_{best}^{f*}$  of  $X_{best}^m$  and  $X_{best}^f$  using Eq. (20)
8. Calculate the fitness function values of  $X_{best}^{m*}$  and  $X_{best}^m$  set the better one as  $X_{best}^m$
9. Calculate the fitness function values of  $X_{best}^{f*}$  and  $X_{best}^f$  set the better one as  $X_{best}^f$
10. Define Temp using Eq. (3).
11. Define Food Quantity FQ using Eq. (4).
12. **if** ( $Q < 0.25$ ) **then**
13. Perform exploration using Eqs. (5) and (6)
14. **else**
15. **if** ( $\text{Temp} > 0.6$ ) **then**
16. Perform exploitation Eq. (7)
17. **else**
18. **if** ( $\text{rand} > 0.6$ ) **then**
19. Snakes in Fight Mode Eqs. (8) and (9)
20. **else**
21. Snakes in Mating Mode Eqs. (23) and (24)
22. Replace the worst male and female Eqs. (12) and (13)
23. **end if**
24. **end if**
25. **end if**
26. Calculate the average fitness of all snakes  $f_{avg}$
27. For 1:  $N_{all}$
28. **if**  $f_{snake} < f_{avg}$
29. Get  $X_{snake}$  using Eq. (28)
30. Calculate the fitness function values of  $X_{snake}^*$  and  $X_{snake}$ , set the better one as  $X_{snake}$
31. **else**
32. Get  $X_{snake}^*$  using Eq. (27)
33. Calculate the fitness function values of  $X_{snake}^*$  and  $X_{snake}$ , set the better one as  $X_{snake}$
34. **end if**
35. **end while**
36. Return the best solution.

**3.5. Computational time complexity of ESO**

Designing the algorithm with the lowest time complexity for any given problem is one of the essential goals in designing algorithms. When there are multiple algorithms for solving a given problem, choosing the algorithm with the lowest time complexity among them is an important criterion to follow when choosing an algorithm. Therefore, this paper uses the Big O notion (Huang et al., 2021) to analyze the algorithm's time complexity between the proposed method and the original algorithm.

The SO initializes population needs time  $O(n \times d)$ , where  $n$  represents population size and  $d$  represents the dimensions of the problem. The fitness evaluation of each population requires time  $O(n)$ . The selection of the strongest individual requires time  $O(n)$ . The update of the individual requires time  $O(n \times d)$ . Therefore, the SO algorithm time complexity is  $O(n \times d \times T)$ .

Compared to SO, ESO has added several parts. The calculation of each individual with the opposite requires time  $O(2 \times d)$ . The Tent-chaos and Cauchy mutation requires time  $O(n)$ , parameters dynamic update strategy and sine–cosine composite perturbation factors without increasing the time of the algorithm. According to the Big O notion, only the highest order items are retained, so the time complexity of ESO is  $O(n \times d \times T)$ . Therefore, the time complexity of SO and ESO are equal. That is, although several strategies are added, they do not increase the complexity of the ESO algorithm.

**Table 7**

Comparison of results on benchmark functions (F1-F13) with 1000 dimensions.

F(x)		GWO	HHO	SCA	GJO	ALO	SOA	AGWO	MPSO	TACPSO	SO	SHADE	LSHADE	LSHADE-EpSin	ESO	
F1	Mean	2.4146E-01	2.7219E-92	4.6272E+05	2.7063E-09	5.7062E+05	9.9543E-01	1.4236E-02	1.9050E+06	7.8439E+05	5.5380E-68	1.2074E+06	9.3444E+05	7.7803E+04	<b>0.0000E+00</b>	
	Std	7.9814E-02	1.4790E-91	1.6968E+05	2.5709E-09	8.4847E+04	6.3175E-01	4.5840E-02	5.1467E+04	2.0113E+04	1.9185E-67	6.5748E+04	7.7803E+04	1.3308E+05	<b>0.0000E+00</b>	
	P	1.2118E-12	1.2118E-12	1.2118E-12	1.2118E-12	1.2118E-12	1.2118E-12	1.2118E-12	1.2118E-12	1.2118E-12	1.2118E-12	1.2118E-12	1.2118E-12	1.2118E-12	—	
	Wr	(+)	(+)	(+)	(+)	(+)	(+)	(+)	(+)	(+)	(+)	(+)	(+)	(+)	—	
F2	T	3.3986E-02	1.3368E-02	2.6622E-02	2.9989E-02	9.9664E+00	2.9917E-02	7.4067E-01	1.5224E-02	1.5134E-02	8.6131E-02	1.2267E-03	1.3244E-03	4.2398E-02	8.4578E-02	—
	Mean	6.1080E-01	4.9851E-48	Inf	4.3450E-07	Inf	1.8885E-02	4.2024E-03	1.0893E+190	3.1916E+149	5.6892E-25	1.0000E+30	1.0000E+30	1.0000E+30	<b>0.0000E+00</b>	
	Std	3.3928E-01	1.9678E-47	NaN	1.5769E-07	NaN	9.2245E-03	2.0320E-02	Inf	1.7481E+150	3.1087E-24	1.4314E+14	1.4314E+14	1.4314E+14	<b>0.0000E+00</b>	
	P	1.2118E-12	1.2118E-12	1.6853E-14	1.2118E-12	1.6853E-14	1.2118E-12	1.2118E-12	1.2118E-12	1.2118E-12	1.6853E-14	1.6853E-14	1.6853E-14	1.6853E-14	—	
F3	Wr	(+)	(+)	(+)	(+)	(+)	(+)	(+)	(+)	(+)	(+)	(+)	(+)	(+)	—	
	T	4.1101E-02	1.8578E-02	3.4709E-02	4.2002E-02	1.2569E+01	3.7333E-02	1.0767E+00	2.0328E-02	2.0162E-02	1.0499E-01	1.2700E-03	1.3644E-03	5.6348E-02	1.0462E-01	—
	Mean	1.5570E+06	2.3406E-26	2.8191E+07	3.3788E+05	7.5624E+06	1.0693E+06	6.0255E+05	1.6143E+07	7.5297E+06	1.2418E-07	4.2876E+07	3.2858E+07	3.0253E+07	<b>0.0000E+00</b>	
	Std	3.4449E+05	1.2820E-25	7.8685E+06	1.5536E+05	2.0199E+06	5.7795E+05	5.9967E+05	2.2801E+06	1.3998E+06	6.8014E-07	7.9653E+06	6.1025E+06	1.1431E+07	<b>0.0000E+00</b>	
F4	P	1.2118E-12	1.2118E-12	1.2118E-12	1.2118E-12	1.2118E-12	1.2118E-12	1.2118E-12	1.2118E-12	1.2118E-12	1.2118E-12	1.2118E-12	1.2118E-12	1.2118E-12	—	
	Wr	(+)	(+)	(+)	(+)	(+)	(+)	(+)	(+)	(+)	(+)	(+)	(+)	(+)	—	
	T	7.3342E-01	1.6561E+00	7.3034E-01	7.4176E-01	1.3077E+01	7.2934E-01	2.3730E+00	7.2083E-01	7.1270E-01	7.9131E-01	2.5311E-02	2.5141E-02	7.9201E-02	1.5536E+00	—
	Mean	7.7086E+01	2.2396E-49	9.9628E+01	9.0720E+01	5.3431E+01	9.9601E+01	8.6657E+01	9.9613E+01	7.6834E+01	5.7223E-33	9.7927E+01	9.6681E+01	9.5504E+01	<b>0.0000E+00</b>	
F5	Std	3.4059E+00	8.6968E-49	9.1398E-02	2.3091E+00	4.5375E+00	1.2489E-01	3.0697E+01	1.3367E-01	2.6645E+00	8.5159E-33	6.8251E-01	1.3342E+00	4.6895E+00	<b>0.0000E+00</b>	—
	P	1.2118E-12	1.2118E-12	1.2118E-12	1.2118E-12	1.2118E-12	1.2118E-12	1.2118E-12	1.2118E-12	1.2118E-12	1.2118E-12	1.2118E-12	1.2118E-12	1.2118E-12	—	
	Wr	(+)	(+)	(+)	(+)	(+)	(+)	(+)	(+)	(+)	(+)	(+)	(+)	(+)	—	
	T	3.8296E-02	1.9724E-02	3.1168E-02	3.6841E-02	1.2033E+01	3.4668E-02	9.6504E-01	1.8394E-02	1.8163E-02	1.0018E-01	1.5056E-03	1.6678E-03	6.3418E-02	1.0657E-01	—
F6	Mean	1.0590E+03	<b>8.5781E-01</b>	3.9408E+09	9.9812E+02	5.5934E+08	1.0300E+04	9.9895E+02	7.1144E+09	1.3346E+09	7.6528E+02	3.2584E+09	1.8112E+09	1.5560E+09	4.8274E+01	—
	Std	2.6248E+01	8.0367E-02	6.2381E+08	7.8366E-02	1.7754E+08	6.8790E+03	<b>8.8511E-02</b>	2.0654E+08	7.2625E+07	3.7204E+02	4.1397E+08	2.6490E+08	6.5606E+08	1.8223E-01	—
	P	3.0199E-11	1.3703E-03	3.0199E-11	3.0199E-11	3.0199E-11	3.0199E-11	3.0199E-11	3.0199E-11	3.0199E-11	3.0199E-11	3.0199E-11	3.0199E-11	3.0199E-11	3.0199E-11	—
	Wr	(+)	(=)	(+)	(+)	(+)	(+)	(+)	(+)	(+)	(+)	(+)	(+)	(+)	—	
F7	T	1.2069E+00	8.8477E-01	9.7103E-01	1.1969E+00	3.6299E+02	1.1198E+00	2.9859E+01	5.8400E-01	5.8178E-01	3.2742E+00	5.1167E-02	6.0967E-02	1.4707E+00	3.3641E+00	—
	Mean	2.0332E+02	<b>5.8807E-03</b>	4.2497E+05	2.3102E+02	5.8197E+05	2.4131E+02	2.4670E+02	1.9131E+06	7.7900E+05	1.4325E+02	1.2487E+06	9.0343E+05	7.7992E+05	1.6604E+00	—
	Std	3.2480E+00	<b>9.7101E-03</b>	1.6649E+05	1.2576E+00	8.2054E+04	2.1268E+00	1.0470E+00	4.9870E+04	1.9306E+04	1.0303E+02	7.6157E+04	6.8253E+04	1.6642E+05	5.1323E-01	—
	P	3.0199E-11	1.8608E-06	3.0199E-11	3.0199E-11	3.0199E-11	3.0199E-11	3.0199E-11	3.0199E-11	3.0199E-11	3.0199E-11	3.0199E-11	3.0199E-11	3.0199E-11	3.0199E-11	—
F8	Wr	(+)	(-)	(+)	(+)	(+)	(+)	(+)	(+)	(+)	(+)	(+)	(+)	(+)	—	
	T	3.5428E-02	2.1492E-02	2.8198E-02	3.2798E-02	1.0863E+01	3.2153E-02	8.2375E-01	1.6146E-02	1.6110E-02	9.5424E-02	1.3211E-03	1.5111E-03	4.5803E-02	9.6439E-02	—
	Mean	1.4715E-01	<b>1.4414E-04</b>	6.9120E+04	1.5130E-02	8.0985E+03	3.9321E-01	2.0447E-02	1.0948E+05	4.1647E+04	2.2807E-04	5.1274E+04	2.7220E+04	2.5775E+04	1.8212E-04	—
	Std	3.6486E-02	<b>1.7096E-04</b>	1.5098E+04	6.8092E-03	3.1320E+03	1.7057E-01	1.3955E-02	4.7616E+03	8.4493E+03	2.0781E-04	6.9439E+03	2.6014E+03	1.2684E+04	9.3989E-05	—
F9	Wr	(+)	(=)	(+)	(+)	(+)	(+)	(+)	(+)	(+)	(=)	(+)	(+)	(+)	—	
	T	9.5966E-02	1.4583E-01	9.2923E-02	9.7973E-02	1.2705E+01	9.9184E-02	1.1956E+00	7.6040E-02	7.5986E-02	1.6833E-01	3.6389E-03	3.6767E-03	5.7793E-02	2.2936E-01	—
	Mean	-8.5586E+04	-4.1895E+05	-2.1403E+04	-3.7880E+04	-1.8059E+05	-3.2846E+04	-1.6856E+04	-9.1929E+04	-9.1710E+04	-4.1594E+05	-2.1744E+04	-2.5161E+04	-2.4550E+04	<b>-4.1898E+05</b>	—
	Std	2.3477E+04	5.9065E+01	1.5780E+03	2.2560E+04	<b>0.0000E+00</b>	3.5379E+03	1.8451E+03	4.6358E+03	6.2520E+03	6.0434E+03	2.3823E+03	2.4833E+03	2.9289E+03	1.1737E+01	—
F10	P	3.0199E-11	1.5638E-02	3.0199E-11	3.0199E-11	1.2118E-12	3.0199E-11	3.0199E-11	3.0199E-11	3.0199E-11	2.1544E-10	3.0199E-11	3.0199E-11	3.0199E-11	3.0199E-11	—
	Wr	(+)	(+)	(+)	(+)	(+)	(+)	(+)	(+)	(+)	(+)	(+)	(+)	(+)	—	
	T	5.3744E-02	4.8048E-02	4.7081E-02	5.0357E-02	1.2634E+01	5.0777E-02	1.0903E+00	3.1589E-02	3.1436E-02	1.2241E-01	1.8778E-03	1.9622E-03	5.5404E-02	1.3913E-01	—
	Mean	1.8961E+02	<b>0.0000E+00</b>	1.8813E+03	2.2513E-10	8.7252E+03	1.3316E+01	8.5193E-02	1.3264E+04	1.0218E+04	7.5353E-02	1.3052E+04	1.2159E+04	1.1874E+04	<b>0.0000E+00</b>	—
F11	Std	4.1205E+01	<b>0.0000E+00</b>	9.2363E+02	1.9271E-10	3.9511E+02	1.3596E+01	3.8857E-01	2.2392E+02	2.6991E+02	4.1273E-01	2.5370E+02	2.6838E+02	4.2433E+02	<b>0.0000E+00</b>	—
	P	1.2118E-12	NaN	1.2118E-12	1.2098E-12	1.2118E-12	1.2118E-12	1.9346E-10	1.2118E-12	1.2118E-12	3.3371E-01	1.2118E-12	1.2118E-12	1.2118E-12	1.2118E-12	—
	Wr	(+)	(=)	(+)	(+)	(+)	(+)	(+)	(+)	(+)	(+)	(+)	(+)	(+)	—	
	T	4.9386E-02	3.6873E-02	4.2392E-02	4.4278E-02	1.2649E+01	4.7431E-02	1.0905E+00	2.8746E-02	2.8273E-02	1.1467E-01	1.8011E-03	1.9111E-03	5.7718E-02	1.2697E-01	—
F12	Mean	1.7998E-02	<b>8.8818E-16</b>	1.7729E+01	1.3175E-06	1.6034E+01	1.9967E+01	9.5379E-04	2.0493E+01	1.8724E+01	5.2699E-15	1.9616E+01	1.8752E+01	1.8244E+01	<b>8.8818E-16</b>	—
	Std	2.7593E-03	<b>0.0000E+00</b>	4.5192E+00	6.4948E-07	2.4723E+00	2.4975E-05	1.3892E-03	3.7240E-02	9.7881E-02	1.5283E-15	1.3254E-01	2.0232E-01	6.2081E-01	<b>0.0000E+00</b>	—
	P	1.2118E-12	NaN	1.2118E-12	1.2118E-12	1.2118E-12	1.2118E-12	1.2118E-12	1.2118E-12	1.2118E-12	1.9687E-13	1.2118E-12	1.2118E-12	1.2118E-12	1.2118E-12	—
	Wr	(+)	(=)	(+)	(+)	(+)	(+)	(+)	(+)	(+)	(+)	(+)	(+)	(+)	—	
F13	T	5.0484E-02	3.8568E-02	4.5219E-02	4.5630E-02	1.2708E+01	4.9949E-02	1.0992E+00	2.9983E-02	2.9897E-02	1.1986E-01	1.8711E-03	1.9456E-03	6.2704E-02	1.2978E-01	—
	Mean	5.7117E-02	<b>0.0000E+00</b>	4.3170E+03	2.7585E-09	5.3448E+03	1.3520E-01	1.4906E-03	1.7137E+04	7.0053E+03	<b>0.0000E+00</b>	1.0883E+04	8.3529E+03	6.9318E+03	<b>0.0000E+00</b>	—
	Std	8.5580E-02	<b>0.0000E+00</b>	1.7153E+03	1.3975E-08	1.0539E+03	1.2842E-01	7.8879E-03	3.6627E+02	2.4372E+02	<b>0.0000E+00</b>	7.7645E+02	6.5535E+02	1.0048E+03	<b>0.0000E+00</b>	—
	P	1.2118E-12	NaN	1.2118E-12	1.2118E-12	1.2118E-12	1.2118E-12</td									

**Table 7 (continued)**

F(x)	GWO	HHO	SCA	GIO	ALO	SOA	AGWO	MPSO	TACPSO	SO	SHADE	L SHADE	LSHADE-EpSin	ESO
Wr (+)	(=)	(+)	(+)	(+)	(+)	(+)	(+)	(+)	(+)	(=)	(+)	(+)	(+)	—
T 5.3508E-02	4.6092E-02	4.9160E-02	4.9384E-02	1.3076E+01	5.3874E-02	1.3076E+00	1.30739E-02	3.3203E-02	1.2014E-01	5.9789E-03	2.0978E-03	6.0779E-02	1.3428E-01	—
F12 Mean 1.2030E+00	1.4002E-06	1.2641E+10	1.0195E+00	2.2087E+08	3.7213E+01	1.1580E+00	1.5425E+10	1.4004E+09	9.2853E-02	5.9784E+09	2.5473E+09	2.3133E+09	2.1443E-05	—
Std 2.1279E-01	1.7230E-06	2.8106E-09	4.6174E-02	1.0346E+08	1.7140E+02	1.0281E-02	9.5565E+08	1.7358E+08	2.2276E-01	9.4154E+08	6.7566E+08	1.5409E+09	3.4666E-05	—
P (+)	9.0632E-08	3.0199E-11	3.0199E-11	3.0199E-11	3.0199E-11	3.0199E-11	3.0199E-11	3.0199E-11	3.0199E-11	3.0199E-11	3.0199E-11	3.0199E-11	3.0199E-11	—
Wr (+)	(=)	(+)	(+)	(+)	(+)	(+)	(+)	(+)	(+)	(+)	(+)	(+)	(+)	—
T 9.8523E-02	1.5666E-01	9.3256E-02	9.7433E-02	1.2833E+01	9.9018E-02	1.3097E+00	7.8312E-02	7.6391E-02	1.6904E-01	3.4656E-03	3.5956E-03	5.5666E-02	2.3059E-01	—
F13 Mean 1.2039E+02	1.0238E-03	2.0968E+10	9.8729E+01	1.2215E+09	4.5806E+02	9.9807E-01	3.0199E-11	4.1780E+09	1.5508E+01	1.1790E+10	6.2645E+09	5.5447E+09	3.7674E-02	—
Std 6.9977E+00	1.3421E-03	4.7455E-09	1.3605E+00	4.7689E+08	1.2106E+03	1.5193E-01	1.4643E+09	3.0358E+08	1.5908E+01	1.2290E+09	2.5591E+09	7.2789E-02	—	—
P (+)	3.0199E-11	3.5638E-04	3.0199E-11	3.0199E-11	3.0199E-11	3.0199E-11	3.0199E-11	3.0199E-11	3.0199E-11	3.0199E-11	3.0199E-11	3.0199E-11	3.0199E-11	—
Wr (+)	(=)	(+)	(+)	(+)	(+)	(+)	(+)	(+)	(+)	(+)	(+)	(+)	(+)	—
T 9.9547E-02	1.5855E-01	9.5066E-02	9.7363E-02	1.2904E+01	9.6252E-02	1.2329E+00	7.8673E-02	7.8532E-02	1.6965E-01	3.4778E-03	3.5944E-03	5.7960E-02	2.3405E-01	—
Wilcoxon's rank sum test	5/4/4	13/0/0	13/0/0	13/0/0	13/0/0	13/0/0	13/0/0	13/0/0	13/0/0	13/0/0	13/0/0	13/0/0	13/0/0	—
Friedman value	6.5769	1.6923	11.6731	4.7308	9.2115	7.0769	5.6923	10.6538	9.3462	3.8846	11.2308	10.4231	11.1538	1.6538
Friedman rank	6	2	14	4	8	7	5	11	9	3	13	10	12	1

## 4. Experiments and results analysis

### 4.1. Baseline algorithms and benchmark function sets

In order to verify the validity of the proposed ESO, thirteen well-known algorithms and two function sets are used in this paper. The thirteen algorithms used in this paper are GWO (Mirjalili et al., 2014), HHO (Heidari et al., 2019), SCA (Mirjalili, 2016), GJO (Chopra & Mohsin Ansari, 2022), ALO (Mirjalili, 2015), SOA (Dhiman & Kumar, 2019), AGWO (Ma et al., 2022), MPSO (Tian & Shi, 2018), TACPSO (Tang & Zhang, 2009), SO (Hashim & Hussien, 2022), SHADE (Tanabe & Fukunaga, 2013), L-SHADE (Tanabe & Fukunaga, 2014) and LSHADE-EpSin (Awad et al., 2016). In these algorithms, HHO, GJO, SOA, and SO are the relatively new *meta-heuristic* methods, GWO, SCA, and ALO are classic *meta-heuristic* methods. At the same time, AGWO, MPSO, and TACPSO are the well-performing *meta-heuristic* optimization techniques on the classical benchmark problems in Table 1. SHADE, L-SHADE, and LSHADE-EpSin are classical evolutionary algorithms and have achieved excellent results in CEC problems in Table 2. Therefore, this paper selects the above 13 algorithms as the baseline algorithms. The two function sets of well-known optimization problems have different characteristics. The first function set contains 23 functions, including seven unimodal functions, six multimodal functions, and ten fixed-dimension multimodal functions. In the optimization problem, the unimodal function is used to test the exploitation capability of the optimization algorithm. Because the unimodal function only has one extreme value, which is used to test the exploration capability of the optimization algorithm because there are multiple extreme values. The details of the first function set are shown in Table 1. The second function set (CEC 2019) contains ten functions, all in fixed dimensions, which are often used to test improved optimization algorithms due to their particular design. The details of the second function set are shown in Table 2.

Run ESO and thirteen algorithms on two function sets and compare the results. The parameters and values involved in the 14 algorithms are shown in Table 3. In order to exclude the influence of other factors, all algorithms adopt uniform parameter settings. The number of independent continuous runs of the algorithm is 30, the number of populations is 50, and the number of iterations is 500. The comparison indicators include mean, standard deviation, p-value, Wilcoxon's rank sum test, Friedman test, and run time per iteration. The best results of the test are shown in bold format. The simulation software is MATLAB 2016b.

### 4.2. Results comparison and analysis

For the first function set, according to whether the dimensions are fixed values or not, they are divided into non-fixed dimensional functions (F1-F13) and fixed dimensional functions (F14-F23). Among them, for the non-fixed dimensional functions, this paper adopts five dimensions of 30, 100, 500, 1000, and 2000. The fixed dimensions are according to the values listed in Table 1. The robustness and generalizability of the proposed ESO is demonstrated by solving the functions in different dimensions. Tables 4-8 show the results for the non-fixed dimensions in different dimensions. Table 9 shows the results of the fixed dimensional functions in fixed dimension, including the mean value (Mean), standard deviation (Std), p-value, Wilcoxon's rank sum test (Rosner et al., 2003), and Friedman test (López-Vázquez & Hochstain, 2017) for 14 algorithms. For Wilcoxon's rank sum test, the significance level is set to 0.05, and the symbol “+/-” is used to indicate that the performance of ESO is better than, similar to, or worse than the corresponding algorithm. Thus, it is possible to judge the adopted algorithms from multiple perspectives. Figs. 3-7 show a box plot of 14 algorithms for solving 13 functions with non-fixed dimensions, and Fig. 8 shows a box plot of 14 algorithms for solving ten functions with fixed dimensions. As one of the tools for describing statistics, the box plot can visually identify outliers in the data batch. The five lines from bottom to

**Table 8**

Comparison of results on benchmark functions (F1-F13) with 2000 dimensions.

F(x)		GWO	HHO	SCA	GJO	ALO	SOA	AGWO	MPSO	TACPSO	SO	SHADE	LSHADE	LSHADE-EpSin	ESO		
F1	Mean	1.1611E+01	2.1360E-91	9.5571E+05	1.4697E-06	1.3990E+06	9.6387E+00	6.1002E+02	4.2988E+06	1.8116E+06	3.0931E-66	2.4483E+06	1.8429E+06	1.4679E+06	<b>0.0000E+00</b>		
	Std	2.2437E+00	1.1567E-90	2.9468E+05	1.2500E-06	2.4039E+05	6.2833E+00	1.0371E+03	6.0234E+04	3.9715E+04	5.8908E-66	1.5266E+05	1.4107E+05	2.7560E+05	<b>0.0000E+00</b>		
	P	1.2118E-12	1.2118E-12	1.2118E-12	1.2118E-12	1.2118E-12	1.2118E-12	1.2118E-12	1.2118E-12	1.2118E-12	1.2118E-12	1.2118E-12	1.2118E-12	1.2118E-12	—		
	Wr	(+)	(+)	(+)	(+)	(+)	(+)	(+)	(+)	(+)	(+)	(+)	(+)	(+)	—		
F2	T	2.2627E+00	8.1367E-01	1.7911E+00	9.7118E+00	7.2624E+02	2.1601E+00	5.8670E+01	1.0883E+00	1.0776E+00	1.0954E+01	1.1307E-01	8.8933E-02	1.4525E+01	9.7118E+00	—	
	Mean	1.1720E+01	3.5513E-48	Inf	1.3943E-05	Inf	5.5906E-02	4.4985E+00	4.9957E+211	1.0308E+163	5.6301E-21	1.0000E+30	1.0000E+30	1.0000E+30	<b>0.0000E+00</b>	—	
	Std	5.6936E+00	1.2530E-47	NaN	5.3654E-06	NaN	1.6097E-02	4.5822E+00	Inf	Inf	3.0502E-20	1.4314E+14	1.4314E+14	1.4314E+14	<b>0.0000E+00</b>	—	
	P	1.2118E-12	1.2118E-12	1.6853E-14	5.2190E-12	1.6853E-14	1.2118E-12	1.2118E-12	1.2118E-12	1.2118E-12	1.6853E-14	1.6853E-14	1.6853E-14	1.6853E-14	—	—	
F3	Wr	(+)	(+)	(+)	(+)	(+)	(+)	(+)	(+)	(+)	(+)	(+)	(+)	(+)	—	—	
	T	2.2511E+00	9.2770E-01	1.8071E+00	2.3229E+00	6.9735E+02	2.0000E+00	5.8315E+01	1.1461E+00	1.1427E+00	9.9693E+00	6.5233E-02	6.8833E-02	1.1464E+01	1.0683E+01	—	—
	Mean	6.6907E+06	2.7388E-13	1.1286E+08	1.9839E+06	2.9714E+07	4.8811E+06	1.0448E+07	6.5761E+07	3.0717E+07	3.1084E-04	1.7232E+08	1.2344E+08	1.2990E+08	<b>0.0000E+00</b>	—	
	Std	1.2645E+06	1.5001E-12	2.2379E+07	8.7706E+05	8.8071E+06	2.0170E+06	5.2961E+06	1.1492E+07	6.5637E+06	1.7025E-03	3.6155E+07	1.9583E+07	5.7350E+07	<b>0.0000E+00</b>	—	
F4	P	1.2118E-12	1.2118E-12	1.2118E-12	1.2118E-12	1.2118E-12	1.2118E-12	1.2118E-12	1.2118E-12	1.2118E-12	1.2118E-12	1.2118E-12	1.2118E-12	1.2118E-12	—	—	
	Wr	(+)	(+)	(+)	(+)	(+)	(+)	(+)	(+)	(+)	(+)	(+)	(+)	(+)	—	—	
	T	6.0853E+01	1.4081E+02	6.0323E+01	6.1173E+01	7.3675E+02	6.0102E+01	1.7110E+02	5.9352E+01	5.9456E+01	6.9934E+01	2.0629E+00	2.0196E+00	1.3699E+01	1.2995E+02	—	—
	Mean	8.6539E+01	4.3776E-49	9.9790E+01	9.3546E+01	5.7142E+01	9.9786E+01	9.9793E+01	9.9801E+01	8.3345E+01	2.4910E-32	9.8941E+01	9.7966E+01	9.8705E+01	<b>0.0000E+00</b>	—	
F5	Std	2.8517E+00	1.8730E-48	8.3225E-02	1.7154E+00	4.5661E+00	6.2758E-02	6.0329E-02	6.8362E-02	1.9525E+00	2.7420E-32	3.7703E-01	1.0859E+00	1.3436E+00	<b>0.0000E+00</b>	—	
	P	1.2118E-12	1.2118E-12	1.2118E-12	1.2118E-12	1.2118E-12	1.2118E-12	1.2118E-12	1.2118E-12	1.2118E-12	1.2118E-12	1.2118E-12	1.2118E-12	1.2118E-12	—	—	
	Wr	(+)	(+)	(+)	(+)	(+)	(+)	(+)	(+)	(+)	(+)	(+)	(+)	(+)	—	—	
	T	2.2462E+00	1.0183E+00	1.8545E+00	2.3422E+00	6.9139E+02	1.8954E+00	5.8313E+01	1.0752E+00	1.0874E+00	1.0538E+01	9.3867E-02	8.4300E-02	1.3337E+01	9.6600E+00	—	—
F6	Mean	4.4413E+03	<b>5.5025E-01</b>	8.9482E+09	1.9987E+03	1.5408E+09	2.1573E+05	3.0947E+05	1.6876E+10	3.3744E+09	1.3078E+03	6.6148E+09	3.8112E+09	3.5107E+07	1.2527E+02	—	
	Std	8.7407E+02	<b>7.4115E-01</b>	1.3415E+09	2.7581E+00	4.8723E+08	1.5733E+05	6.3159E+05	4.0731E+08	1.3136E+08	8.6052E+02	7.3290E+08	5.2479E+08	1.6885E+09	4.1277E+02	—	
	P	3.0199E-11	3.2553E-01	3.0199E-11	3.0199E-11	3.0199E-11	3.0199E-11	3.0199E-11	3.0199E-11	3.0199E-11	3.0199E-11	3.0199E-11	3.0199E-11	3.0199E-11	3.0199E-11	—	
	Wr	(+)	(=)	(+)	(+)	(+)	(+)	(+)	(+)	(+)	(+)	(+)	(+)	(+)	—	—	
F7	T	2.2749E+00	1.4347E+00	1.9156E+00	2.5264E+00	6.9375E+02	1.9816E+00	5.3904E+01	1.0454E+00	1.0495E+00	9.9334E+00	1.0463E-01	8.9533E-02	1.1634E+01	9.9087E+00	—	—
	Mean	6.3533E-01	<b>2.5336E-04</b>	2.9888E+05	3.1114E-02	4.9872E+04	5.3130E+00	1.2758E+00	5.3747E+05	2.2667E+05	2.5365E-04	2.1047E+05	1.2738E+05	1.0730E+05	1.6347E-04	—	
	Std	1.2763E-01	<b>2.7943E-04</b>	6.0980E+04	1.1524E-02	1.5341E+04	3.0287E+00	1.5289E+00	1.7376E+04	3.0474E+04	2.1199E-04	2.6738E+04	2.1838E+04	5.7542E+04	1.1007E-04	—	
	P	3.0199E-11	6.4142E-01	3.0199E-11	3.0199E-11	3.0199E-11	3.0199E-11	3.0199E-11	3.0199E-11	3.0199E-11	3.0199E-11	3.0199E-11	3.0199E-11	3.0199E-11	3.0199E-11	—	
F8	Wr	(+)	(=)	(+)	(+)	(+)	(+)	(+)	(+)	(+)	(+)	(+)	(+)	(+)	—	—	
	T	5.4750E+00	8.3808E+00	5.0056E+00	5.2995E+00	6.9846E+02	5.2360E+00	6.0660E+01	4.3358E+00	4.3714E+00	1.3544E+01	2.1793E-01	2.0153E-01	1.4091E+01	1.6676E+01	—	—
	Mean	6.3533E-01	<b>2.5336E-04</b>	2.9888E+05	3.1114E-02	4.9872E+04	5.3130E+00	1.2758E+00	5.3747E+05	2.2667E+05	2.5365E-04	2.1047E+05	1.2738E+05	1.0730E+05	1.6347E-04	—	
	Std	1.2763E-01	<b>2.7943E-04</b>	6.0980E+04	1.1524E-02	1.5341E+04	3.0287E+00	1.5289E+00	1.7376E+04	3.0474E+04	2.1199E-04	2.6738E+04	2.1838E+04	5.7542E+04	1.1007E-04	—	
F9	Wr	(+)	(=)	(+)	(+)	(+)	(+)	(+)	(+)	(+)	(=)	(+)	(+)	(+)	—	—	
	T	5.4750E+00	8.3808E+00	5.0056E+00	5.2995E+00	6.9846E+02	5.2360E+00	6.0660E+01	4.3358E+00	4.3714E+00	1.3544E+01	2.1793E-01	2.0153E-01	1.4091E+01	1.6676E+01	—	—
	Mean	-1.2931E+05	-8.3310E+05	-3.0295E+04	-5.7635E+04	-3.6118E+05	-4.4333E+04	-2.2921E+04	-1.3354E+05	-1.2973E+05	-8.3315E+05	-3.1250E+04	-3.6406E+04	-3.5969E+04	<b>-8.3795E+05</b>	—	
	Std	2.8664E+04	2.6359E+04	2.0328E+03	3.1969E+04	<b>5.9203E-11</b>	4.6933E+03	3.4155E+03	8.9836E+03	6.5780E+03	6.0358E+03	3.8272E+03	4.6318E+03	4.3118E+03	2.8061E+01	—	
F10	P	3.0199E-11	1.6687E-01	3.0199E-11	3.0199E-11	1.2118E-12	3.0199E-11	3.0199E-11	3.0199E-11	3.0199E-11	9.7555E-10	3.0199E-11	3.0199E-11	3.0199E-11	—	—	
	Wr	(+)	(=)	(+)	(+)	(+)	(+)	(+)	(+)	(+)	(+)	(+)	(+)	(+)	—	—	
	T	2.7658E+00	2.2380E+00	2.3637E+00	2.8392E+00	6.9968E+02	2.5553E+00	5.5398E+01	1.6232E+00	1.6128E+00	1.1020E+01	1.0360E-01	9.3033E-02	1.3429E+01	1.1327E+01	—	—
	Mean	5.8762E+02	<b>0.0000E+00</b>	3.2506E+03	3.7950E-08	1.9570E+04	2.5368E+01	1.1240E+02	2.8740E+04	2.2458E+04	<b>0.0000E+00</b>	2.6412E+04	2.4645E+04	2.4018E+04	<b>0.0000E+00</b>	—	
F11	Std	1.0113E+02	<b>0.0000E+00</b>	1.4297E+03	2.4766E-08	8.4130E+02	1.5025E+01	1.0725E+02	2.8922E+02	3.1765E+02	<b>0.0000E+00</b>	4.9386E+02	4.8035E+02	8.6757E+02	<b>0.0000E+00</b>	—	
	P	1.2118E-12	NaN	1.2118E-12	1.2118E-12	1.2118E-12	1.2118E-12	1.2118E-12	1.2118E-12	1.2118E-12	NaN	1.2118E-12	1.2118E-12	1.2118E-12	—	—	
	Wr	(+)	(=)	(+)	(+)	(+)	(+)	(+)	(+)	(+)	(=)	(+)	(+)	(+)	—	—	
	T	2.7915E+00	1.6981E+00	2.4627E+00	2.4378E+00	7.3986E+02	2.7061E+00	5.9376E+01	1.5982E+00	1.5781E+00	1.1125E+01	1.1713E-01	1.0013E-01	1.2997E+01	1.0932E+01	—	—
F12	Mean	4.6728E-01	<b>0.0000E+00</b>	1.0090E+04	4.6919E-08	1.2795E+04	3.1250E-01	2.7688E+01	3.8711E+04	1.6300E+04	<b>0.0000E+00</b>	2.1970E+04	1.6745E+04	1.4755E+04	<b>0.0000E+00</b>	—	
	Std	1.2738E-01	<b>0.0000E+00</b>	2.4688E+03	4.9932E-08	2.2371E+03	1.8882E-01	3.3582E+01	6.1527E+02	4.1195E+02	<b>0.0000E+00</b>	2.0437E+03	1.3676E+03	2.9038E+03	<b>0.0000E+00</b>	—	
	P	1.2118E-12	NaN	1.2118E-12	1.2118E-12	1.2118E-12	1.2118E-12	1.2118E-12	1.2118E-12	1.2118E-12	NaN	1.2118E-12	1.2118E-12	1.2118E-12	—	—	

(continued on next page)

**Table 8 (continued)**

F(x)	GWO	HHO	SCA	GIO	ALO	SOA	AGWO	MPSO	TACPSO	SO	SHADE	L SHADE	LSHADE-EpsIn	ESO
Wr (+)	(=)	(+)	(+)	(+)	(+)	(+)	(+)	(+)	(+)	(=)	(+)	(+)	(+)	—
T 2.9906E+00	2.1704E+00	7.7036E+00	2.7273E+00	7.3679E+02	6.3607E+01	1.8423E+00	1.1439E+01	1.8043E+00	1.1439E+01	1.2880E-01	1.0907E-01	1.4572E+01	1.1387E+01	—
F12 Mean 3.1381E+00	2.0889E+00	2.7551E+10	1.1940E+00	1.0430E+09	1.7107E+06	8.7048E+05	3.8197E+10	4.3157E+09	3.0084E-02	1.2370E+10	5.2541E+09	5.1695E+09	1.2426E+04	—
Std 8.1568E-01	2.9203E+06	4.1360E+09	2.4345E+01	6.3654E+08	2.7827E+06	3.8506E+06	1.6779E+09	3.0022E+08	6.8788E-02	2.3278E+09	1.0225E+09	3.7390E+09	1.9897E+04	—
P 3.0199E-11	7.2208E-06	3.0199E-11	2.2273E-09	3.0199E-11	3.0199E-11	3.0199E-11	3.0199E-11	—						
Wr (+)	(-)	(+)	(+)	(+)	(+)	(+)	(+)	(+)	(+)	(+)	(+)	(+)	(+)	—
T 4.6859E+00	6.4460E+00	4.3285E+00	4.6490E+00	7.4334E+02	4.6287E+00	6.6587E+01	3.4946E+00	3.4816E+00	1.3542E+01	1.8897E+01	1.7137E-01	1.3301E+01	1.4683E+01	—
F13 Mean 4.0315E+02	2.5668E-03	4.4939E+10	2.2060E+02	3.7421E+09	4.7135E+05	1.4681E-06	7.3137E+10	1.1265E+10	2.6587E+10	2.6336E+01	1.3563E+10	1.1447E+10	1.4132E+01	—
Std 4.7763E+01	4.8426E-03	5.9968E-09	6.6237E+01	1.4022E+09	7.4990E+05	3.2291E-06	1.9869E+09	5.2144E+08	3.2893E-09	2.4477E+09	2.4347E+09	2.4937E+01	—	—
P 3.0199E-11	8.1975E-07	3.0199E-11	8.1014E-10	3.0199E-11	3.0199E-11	3.0199E-11	3.0199E-11	—						
Wr (+)	(-)	(+)	(+)	(+)	(+)	(+)	(+)	(+)	(+)	(+)	(+)	(+)	(+)	—
T 4.7598E+00	6.5115E+00	4.2714E+00	4.5432E+00	7.4095E+02	4.5167E+00	6.3326E+01	3.5326E+00	1.3510E+01	1.6390E-01	1.3549E+01	1.4830E+01	1.3549E+01	1.4830E+01	—
Wilcoxon's rank sum test	13/0/0	4/7/2	13/0/0	13/0/0	13/0/0	13/0/0	13/0/0	13/0/0	13/0/0	13/0/0	13/0/0	13/0/0	13/0/0	—
Friedman value	6.0769	2.2308	11.7692	4.8846	9.0000	6.5000	7.0769	11.0962	9.5962	3.0385	11.1538	10.2692	10.8077	1.5000
Friedman rank	5	2	14	4	8	6	7	12	9	3	13	10	11	1

top indicate the minimum, lower quartile, median, upper quartile, and maximum values, respectively. Therefore, it can be well used as a complement to the data in Tables 4–9 for a better and more comprehensive comparison of the results of all algorithms.

Table 4 shows the performance of 14 algorithms in non-fixed dimension functions in 30 dimensions. It can be seen that ESO achieves optimal values for 8 of the 13 non-fixed dimensional functions, and the highest number of the best value is obtained among all 14 algorithms. The result ranked in the top three among the five functions that failed to obtain the optimal value. In order to show the performances of ESO and other algorithms more objectively, the statistical methods of Wilcoxon's rank sum test and Friedman test are introduced in this paper. The Wilcoxon's rank sum test counts the results of ESO compared with other algorithms, and ESO achieves the result of 157/8/4. The Friedman value shows the overall results achieved by each algorithm in 13 functions. The result of 1.6923 is ranked first in the Friedman rank, which proves that ESO achieves more excellent results than other algorithms in 30 dimensions. Fig. 3 shows the results of 14 algorithms on 13 functions more comprehensively in the form of box plots, and it can be seen that ESO achieves excellent results.

Table 5 shows the performance of 14 algorithms in non-fixed dimension functions in 100 dimensions. It can be seen that ESO achieves optimal values for 8 of the 13 non-fixed dimensional functions, and the highest number of the best value is obtained among all 14 algorithms. Among the five functions that failed to obtain the optimal value ranked second. In order to show the performances of ESO and other algorithms more objectively, the statistical methods of Wilcoxon's rank sum test and Friedman test are introduced in this paper. The Wilcoxon's rank sum test counts the results of ESO compared with other algorithms, and ESO achieves the result of 153/12/4. The Friedman value shows the overall results achieved by each algorithm in 13 functions. The result of 1.9038 is ranked first in the Friedman rank, which proves that ESO achieves more excellent results than other algorithms in 100 dimensions. Fig. 4 shows the results of 14 algorithms on 13 functions more comprehensively in the form of box plots, and it can be seen that ESO achieves excellent results.

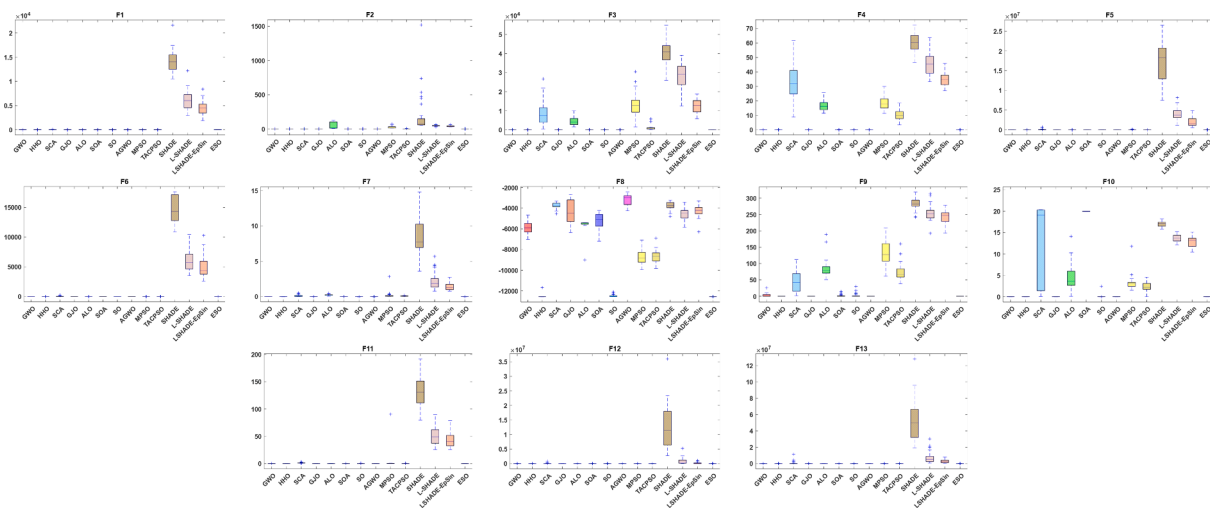
Table 6 shows the performance of 14 algorithms in non-fixed dimension functions in 500 dimensions. It can be seen that ESO achieves optimal values for 8 of the 13 non-fixed dimensional functions, and the highest number of the best value is obtained among all 14 algorithms. Among the five functions that failed to obtain the optimal value ranked second. In order to show the performances of ESO and other algorithms more objectively, the statistical methods of Wilcoxon's rank sum test and Friedman test are introduced in this paper. The Wilcoxon's rank sum test counts the results of ESO compared with other algorithms, and ESO achieves the result of 156/9/4. The Friedman value shows the overall results achieved by each algorithm in 13 functions. The result of 1.6923 is ranked first in the Friedman rank, which proves that ESO achieves more excellent results than other algorithms in 500 dimensions. Fig. 5 shows the results of 14 algorithms on 13 functions more comprehensively in the form of box plots, and it can be seen that ESO achieves excellent results.

Table 7 shows the performance of 14 algorithms in non-fixed dimension functions in 1000 dimensions. It can be seen that ESO achieves optimal values for 8 of the 13 non-fixed dimensional functions, and the highest number of the best value is obtained among all 14 algorithms. Among the five functions that failed to obtain the optimal value ranked second. In order to show the performances of ESO and other algorithms more objectively, the statistical methods of Wilcoxon's rank sum test and Friedman test are introduced in this paper. The Wilcoxon's rank sum test counts the results of ESO compared with other algorithms, and ESO achieves the result of 159/6/4. The Friedman value shows the overall results achieved by each algorithm in 13 functions. The result of 1.6538 is ranked first in the Friedman rank, which proves that ESO achieves more excellent results than other algorithms in 1000 dimensions. Fig. 6 shows the results of 14 algorithms on 13 functions more

**Table 9**

Comparison of results on benchmark functions (F14-F23) with fixed dimensions.

F(x)	GWO	HHO	SCA	GJO	ALO	SOA	AGWO	MPSO	TACPSO	SO	SHADE	LSHADE	LSHADE-EpSin	ESO		
F14	Mean	3.9378E+00	1.1305E+00	1.8550E+00	4.2584E+00	1.9230E+00	2.3157E+00	7.2532E+00	<b>9.9800E-01</b>	<b>9.9800E-01</b>	9.9805E-01	3.0914E+00	1.5506E+00	1.6480E+00	<b>9.9800E-01</b>	
	Std	3.9294E+00	3.4368E-01	1.9012E+00	4.3765E+00	1.2158E+00	1.8603E+00	4.4532E+00	1.5969E-16	<b>1.3675E-16</b>	2.6490E-04	2.7978E+00	1.2277E+00	1.0234E+00	1.1068E-10	
P	3.1657E-11	2.6788E-10	5.2152E-12	7.2043E-12	3.6006E-10	5.8096E-12	5.2114E-12	8.5217E-01	9.0927E-01	8.5187E-05	5.2152E-12	5.2152E-12	5.2152E-12	—	—	
Wr	(+)	(+)	(+)	(+)	(+)	(+)	(+)	(+)	(=)	(=)	(+)	(+)	(+)	(+)	—	
T	5.4373E-01	1.4050E+00	5.3603E-01	6.0870E-01	1.3115E+00	5.4067E-01	1.1574E+00	5.3327E-01	5.3583E-01	5.4627E-01	2.5300E-02	2.9533E-02	7.2100E-02	1.1705E+00	—	
F15	Mean	3.0751E-03	<b>3.3637E-04</b>	9.3642E-04	4.9314E-04	3.5686E-03	1.2061E-03	3.1461E-03	1.8425E-03	4.6009E-04	1.0973E-03	1.0234E-02	1.0234E-02	3.8050E-03	3.6649E-04	
	Std	6.8997E-03	<b>2.1401E-05</b>	3.2464E-04	1.7629E-04	6.7542E-03	1.6795E-04	6.9320E-03	3.7709E-03	3.2562E-04	3.6410E-03	8.4333E-03	8.4333E-03	4.8636E-03	9.0291E-05	
P	7.2884E-03	2.6433E-01	4.9752E-11	5.9706E-05	1.2057E-10	1.0937E-10	1.5178E-03	4.1640E-09	7.2939E-04	2.0523E-03	3.0199E-11	3.0199E-11	3.0199E-11	—	—	
Wr	(+)	(=)	(+)	(+)	(+)	(+)	(+)	(+)	(+)	(+)	(+)	(+)	(+)	(+)	—	
T	4.8233E-02	1.3990E-01	4.6933E-02	1.2087E-01	1.4623E+00	4.7967E-02	2.3073E-01	4.4333E-02	4.6567E-02	5.4433E-02	8.3333E-03	1.1867E-02	5.8467E-02	1.3510E-01	—	
F16	Mean	<b>-1.0316E+00</b>	<b>-1.0170E+00</b>	<b>-1.0305E+00</b>	<b>-1.0273E+00</b>	<b>-1.0316E+00</b>	—									
	Std	2.1612E-08	7.4197E-10	3.7505E-05	1.1180E-05	9.6671E-14	1.1191E-06	2.3145E-07	<b>6.1849E-16</b>	5.9752E-16	5.4546E-16	1.4750E-02	2.2593E-03	8.6307E-03	6.2939E-16	—
P	6.4328E-12	6.4328E-12	6.4328E-12	6.4328E-12	6.4328E-12	6.4328E-12	6.4328E-12	6.4328E-12	6.4328E-12	6.4328E-12	6.4328E-12	6.4328E-12	6.4328E-12	—	—	
Wr	(+)	(+)	(+)	(+)	(+)	(+)	(+)	(+)	(=)	(=)	(+)	(+)	(+)	(+)	—	
T	3.7000E-02	1.1520E-01	3.6000E-02	1.0087E-01	8.1817E-01	3.6267E-02	1.3570E-01	3.4733E-02	3.4567E-02	4.1333E-02	7.1000E-03	1.0767E-02	5.0967E-02	1.1593E-01	—	
F17	Mean	<b>3.9789E-01</b>	<b>3.9789E-01</b>	3.9956E-01	<b>3.9789E-01</b>	<b>3.9789E-01</b>	3.9796E-01	3.9790E-01	<b>3.9789E-01</b>	<b>3.9789E-01</b>	4.0140E-01	3.9790E-01	3.9808E-01	<b>3.9789E-01</b>	—	
	Std	6.3532E-07	5.1072E-06	1.4058E-03	7.4064E-06	3.8531E-14	6.0460E-05	9.7278E-06	<b>0.0000E+00</b>	<b>0.0000E+00</b>	<b>0.0000E+00</b>	4.2681E-03	2.2400E-05	2.0625E-04	<b>0.0000E+00</b>	—
P	1.2118E-12	1.2118E-12	1.2118E-12	1.2118E-12	1.2019E-12	1.2118E-12	1.2118E-12	NaN	NaN	NaN	1.2118E-12	1.2118E-12	1.2118E-12	—	—	
Wr	(+)	(+)	(+)	(+)	(+)	(+)	(+)	(+)	(=)	(=)	(+)	(+)	(+)	(+)	—	
T	3.6433E-02	1.2200E-01	3.5133E-02	1.1033E-01	9.2210E-01	3.5400E-02	1.4857E-01	3.3600E-02	3.3600E-02	4.1167E-02	7.8000E-03	1.2700E-02	6.7633E-02	1.2240E-01	—	
F18	Mean	5.7000E+00	<b>3.0000E+00</b>	<b>3.0001E+00</b>	<b>3.0000E+00</b>	<b>3.0000E+00</b>	3.0000E+00	<b>3.0000E+00</b>	<b>3.0000E+00</b>	<b>3.0000E+00</b>	6.6000E+00	3.2838E+00	3.0010E+00	3.0048E+00	<b>3.0000E+00</b>	
	Std	1.4789E+01	1.0624E-06	1.7555E-04	8.6928E-06	6.8970E-13	3.5999E-04	2.4321E-06	1.6012E-15	1.4566E-15	9.3351E+00	2.3377E-01	1.1894E-03	6.3446E-03	<b>9.8958E-16</b>	—
P	9.3352E-12	9.3352E-12	9.3352E-12	9.3352E-12	9.3352E-12	9.3352E-12	9.3352E-12	9.3352E-12	9.3352E-12	9.3352E-12	9.3352E-12	9.3352E-12	9.3352E-12	—	—	
Wr	(+)	(+)	(+)	(+)	(+)	(+)	(+)	(+)	(+)	(+)	(+)	(+)	(+)	(+)	—	
T	3.0833E-02	1.0507E-01	2.9733E-02	9.7400E-02	7.8787E-01	3.1567E-02	1.1877E-01	2.7767E-02	2.8400E-02	3.3833E-02	6.6000E-03	5.5400E-02	9.8333E-03	9.4533E-02	—	
F19	Mean	-3.8619E+00	-3.8592E+00	-3.8550E+00	-3.8591E+00	<b>-3.8628E+00</b>	-3.8568E+00	-3.8608E+00	<b>-3.8628E+00</b>	<b>-3.8628E+00</b>	-3.8582E+00	-3.8627E+00	-3.8624E+00	<b>-3.8628E+00</b>	—	
	Std	2.2373E-03	5.1476E-03	3.6820E-03	3.8148E-03	1.4267E-12	3.2703E-03	3.0192E-03	2.5973E-15	2.5391E-15	2.5270E-15	3.9962E-03	7.4513E-05	6.4273E-04	<b>2.4795E-15</b>	—
P	1.4488E-11	1.4488E-11	1.4488E-11	1.4488E-11	1.4488E-11	1.4488E-11	1.4488E-11	3.7358E-02	3.0873E-01	3.8163E-01	1.4488E-11	1.4488E-11	1.4488E-11	—	—	
Wr	(+)	(+)	(+)	(+)	(+)	(+)	(+)	(+)	(=)	(=)	(+)	(+)	(+)	(+)	—	
T	7.5500E-02	2.1587E-01	7.0633E-02	1.4400E-01	1.1932E+00	7.4400E-02	2.3763E-01	7.2400E-02	7.2967E-02	7.9600E-02	7.9000E-03	1.2200E-02	5.7967E-02	1.7993E-01	—	
F20	Mean	-3.2443E+00	-3.0972E+00	-2.8079E+00	-3.0844E+00	-3.2622E+00	-2.9367E+00	-3.2783E+00	-3.2959E+00	-3.2663E+00	-3.3101E+00	-3.1165E+00	-3.2544E+00	-3.1758E+00	<b>-3.3220E+00</b>	
	Std	7.7208E-02	9.9630E-02	5.2939E-01	2.3791E-01	6.0868E-02	3.9514E-01	7.4947E-02	5.4175E-02	6.0590E-02	3.6278E-02	1.2126E-01	7.0881E-02	9.4594E-02	<b>4.1381E-05</b>	—
P	1.5581E-08	3.0199E-11	3.0199E-11	8.1527E-11	6.3088E-01	3.0199E-11	6.0658E-11	3.8089E-05	6.6044E-01	2.2845E-06	3.0199E-11	3.0199E-11	3.0199E-11	—	—	
Wr	(+)	(+)	(+)	(+)	(=)	(+)	(+)	(-)	(=)	(=)	(+)	(+)	(+)	(+)	—	
T	7.5600E-02	2.0487E-01	7.1800E-02	1.4827E-01	2.1446E+00	7.3900E-02	3.2380E-01	7.1967E-02	7.2833E-02	7.8967E-02	8.0000E-03	1.1800E-02	5.5767E-02	1.9387E-01	—	
F21	Mean	-9.6457E+00	-5.1972E+00	-2.5371E+00	-8.5382E+00	-5.6167E+00	-3.0993E+00	-8.5446E+00	-7.3125E+00	-6.0528E+00	-1.0108E+01	-3.1799E+00	-5.8590E+00	-6.2445E+00	<b>-1.0153E+01</b>	
	Std	1.5415E+00	7.9168E-01	2.0682E+00	2.5193E+00	2.9711E+00	3.8082E+00	2.9744E+00	3.3962E+00	3.1154E+00	1.5362E-01	1.4701E+00	2.6858E+00	1.9575E+00	<b>1.8511E-11</b>	—
P	2.2204E-11	2.2204E-11	2.2204E-11	2.2204E-11	4.9757E-11	2.2204E-11	2.2204E-11	2.4558E-03	2.3179E-05	1.1012E-04	2.2204E-11	2.2204E-11	2.2204E-11	—	—	
Wr	(+)	(+)	(+)	(+)	(+)	(+)	(+)	(+)	(+)	(+)	(+)	(+)	(+)	(+)	—	
T	1.2473E-01	3.1643E-01	1.1957E-01	1.8770E-01	1.5341E+00	1.2363E-01	3.5570E-01	1.2017E-01	1.1917E-01	1.2520E-01	9.8333E-03	1.4167E-02	5.2067E-02	2.9087E-01	—	
F22	Mean	-1.0401E+01	-5.0370E+00	-3.6954E+00	-9.4332E+00	-7.1480E+00	-6.4238E+00	-9.3436E+00	-8.6972E+00	-8.2357E+00	-1.0376E+01	-3.1275E+00	-6.9908E+00	-6.0070E+00	<b>-1.0403E+01</b>	
	Std	1.3156E-03	2.5836E-01	2.0465E+00	2.2017E+00	3.4121E+00	4.0150E+00	2.4072E+00	2.9188E+00	3.1790E+00	6.8158E-02	1.2588E+00	2.9005E+00	2.4284E+00	<b>3.5570E-06</b>	—
P	1.9431E-11	1.9431E-11	1.9431E-11	1.9431E-11	3.2383E-09	1.9431E-11	1.9431E-11	8.4695E-01	1.8900E-01	9.7751E-04	1.9431E-11	1.9431E-11	1.9431E-11	—	—	
Wr	(+)	(+)	(+)	(+)	(+)	(+)	(+)	(=)	(=)	(+)	(+)	(+)	(+)	(+)	—	
T	1.6667E-01	4.3267E-01	1.6830E-01	2.4437E-01	1.6448E+00	1.6733E-01	4.5273E-01	1.6173E-01	1.6323E-01	1.6840E-01	1.1900E-02	1.5833E-02	5.4667E-02	3.9080E-01	—	
F23	Mean	-1.0264E+01	-5.2970E+00	-3.6086E+00	-1.0342E+01	-6.8246E+00	-6.7481E+00	-8.4692E+00	-8.8231E+00	-7.9226E+00	-1.0484E+01	-2.9569E+00	-7.0293E+00	-4.5060E+00	<b>-1.0536E+01</b>	
	Std	1.4812E+00	9.4473E-01	1.2516E+00	9.7898E-01	3.6245E+00	4.1960E+00	3.4686E+00	3.1942E+00	3.5573E+00	1.5359E-01	1.0899E+00	3.1230E+00	2.1676E+00	<b>6.4000E-13</b>	—
P	2.0924E-11	2.0924E-11	2.0924E-11	2.0924E-11	2.0924E-11	2.0924E-11	2.0924E-11	9.0027E-01	2.8890E-01	1.0826E-05	2.0924E-11	2.0924E-11	2.0924E-11	—	—	
Wr	(+)	(+)	(+)	(+)	(+)	(+)	(+)	(=)	(=)	(+)	(+)	(+)	(+)	(+)	—	
T	2.4507E-01	6.3340E-01	2.4613E-01	3.2303E-01	1.8372E+00	2.4267E-01	6.2563E-01	2.3983E-01	2.4527E-01	2.4957E-01	1.5267E-02	2.0233E-02	6.4067E-02	5.4397E-01	—	
Wilcoxon's rank sum test	10/0/0	10/0/0	10/0/0	10/0/0	10/0/0	10/0/0	9/1/0	2/7/1	2/7/1	6/3/1	10/0/0	10/0/0	2/6/2	—	—	
Friedman value	7.4750	6.6750	9.9500	7.5750	7.3750	10.4000	8.3250	5.3500	5.3000	4.2500	11.4500	9.1750	9.5500	<b>2.1500</b>	—	
Friedman rank	7	5	12	8	6	13	9	4	3	2	14	10	11	1	—	



**Fig. 3.** Boxplot analysis for benchmark functions (F1-F13) with 30 dimensions.

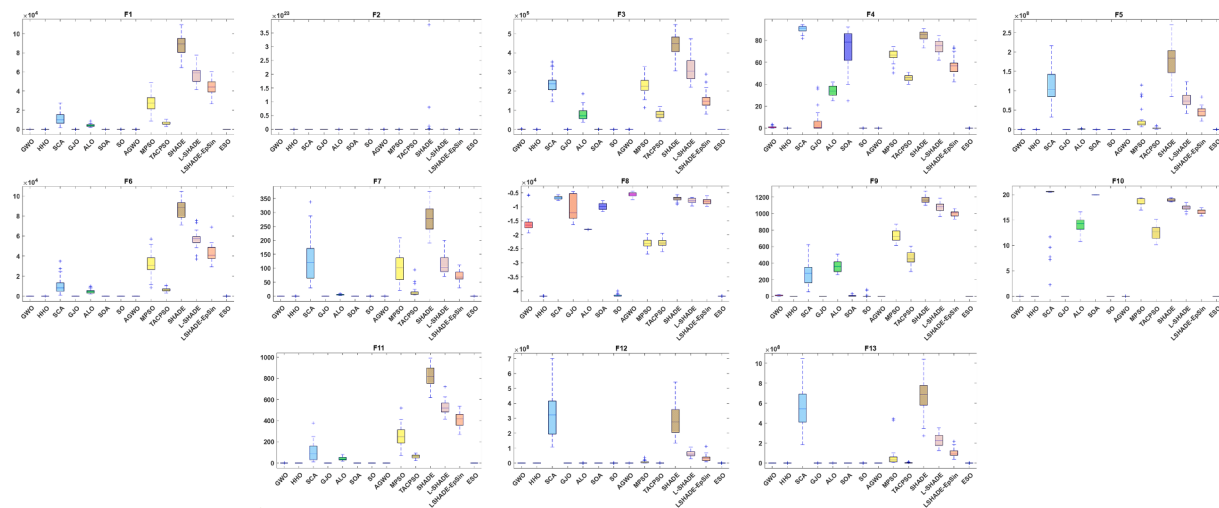


**Fig. 4.** Boxplot analysis for benchmark functions (F1-F13) with 100 dimensions.

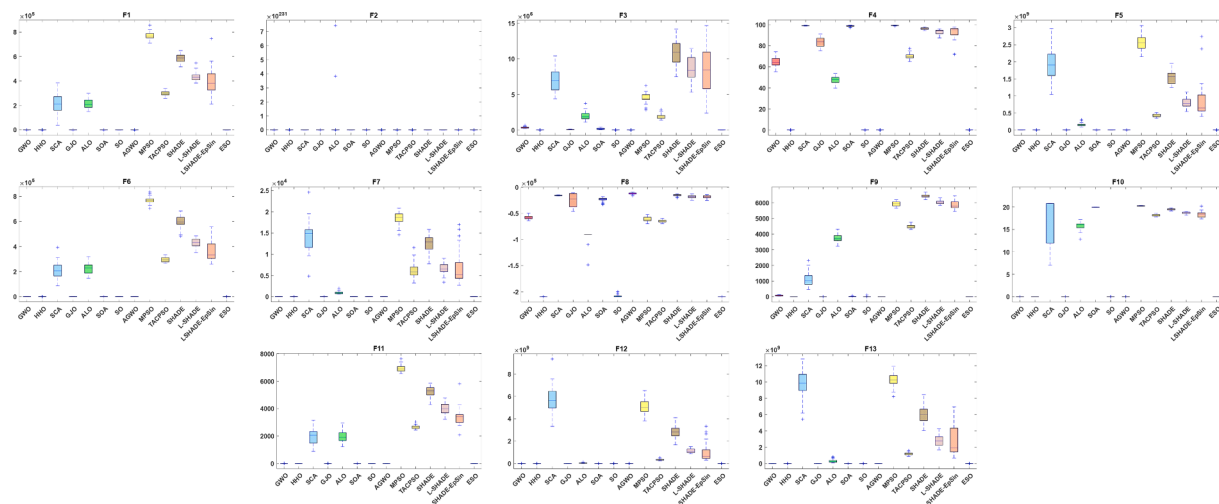


**Fig. 5.** Boxplot analysis for benchmark functions (F1-F13) with 500 dimensions.

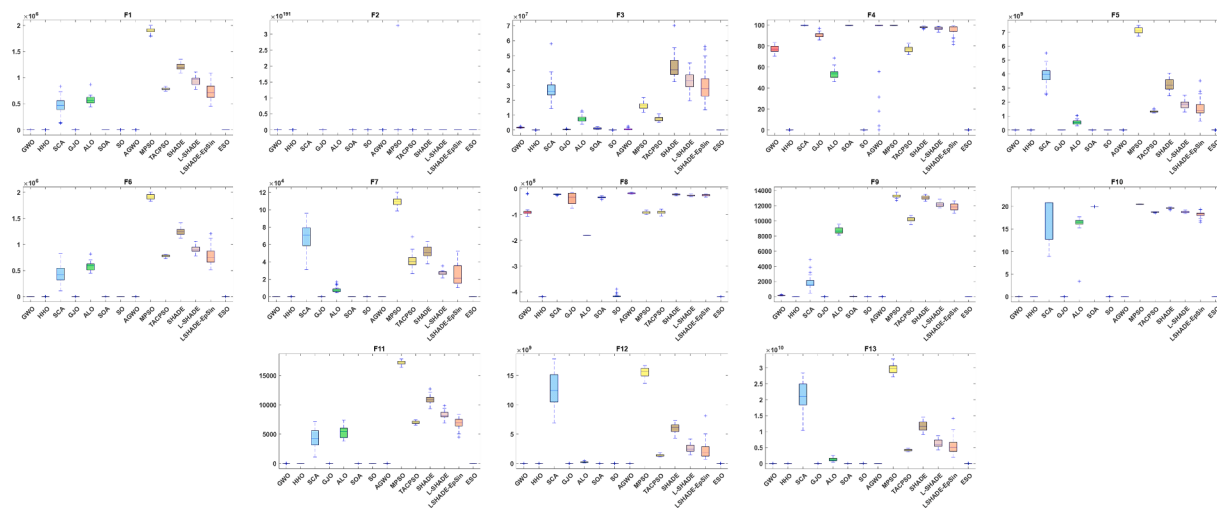


**Fig. 6.** Boxplot analysis for benchmark functions (F1-F13) with 1000 dimensions.

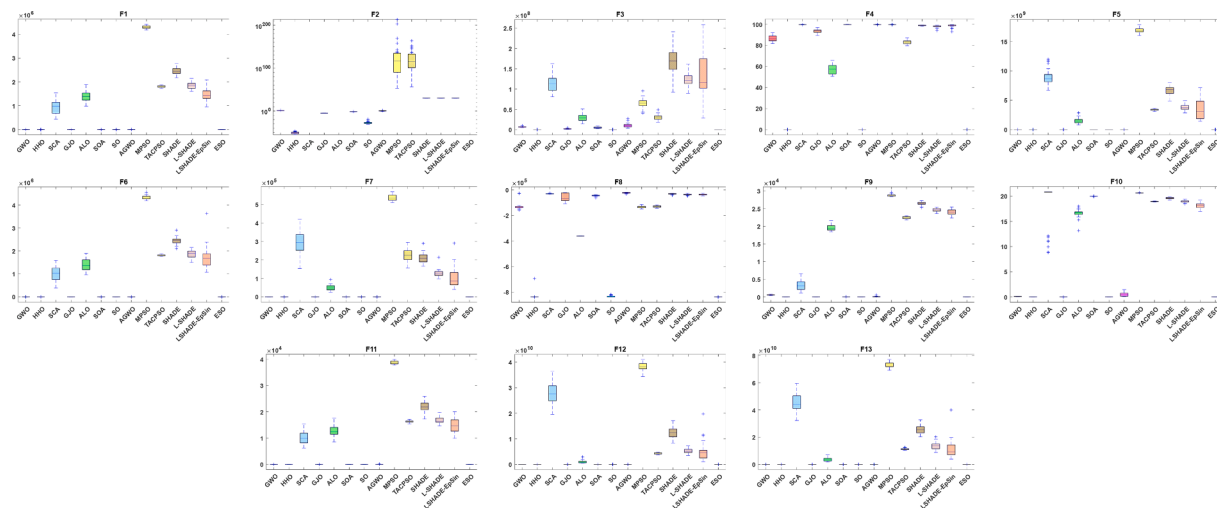


**Fig. 7.** Boxplot analysis for benchmark functions (F1-F13) with 2000 dimensions.

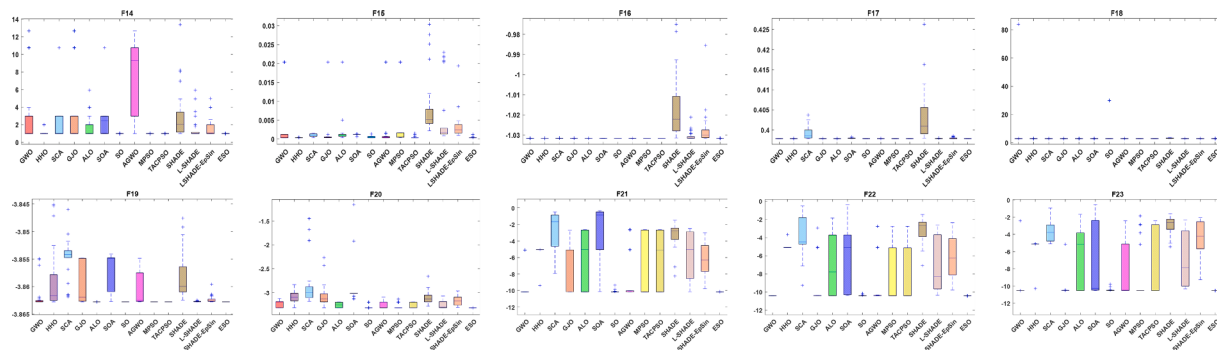


**Fig. 8.** Boxplot analysis for benchmark functions (F14-F23) with fixed dimensions.

comprehensively in the form of box plots, and it can be seen that ESO achieves excellent results.

Table 8 shows the performance of 14 algorithms in non-fixed dimension functions in 2000 dimensions. It can be seen that ESO achieves optimal values for 8 of the 13 non-fixed dimensional functions, and the highest number of the best value is obtained among all 14 algorithms. Among the five functions that failed to obtain the optimal value

ranked second. In order to show the performances of ESO and other algorithms more objectively, the statistical methods of Wilcoxon's rank sum test and Friedman test are introduced in this paper. The Wilcoxon's rank sum test counts the results of ESO compared with other algorithms, and ESO achieves the result of 157/10/2. The Friedman value shows the overall results achieved by each algorithm in 13 functions. The result of 1.5000 is ranked first in the Friedman rank, which proves that ESO

**Table 10**

Comparison of results on CEC2019 benchmark functions.

F(x)		GWO	HHO	SCA	GJO	ALO	SOA	AGWO	MPSO	TACPSO	SO	SHADE	LSHADE	LSHADE-EpSin	ESO
F1	Mean	5.6924E+04	<b>1.0000E+00</b>	2.6326E+06	1.3044E+04	4.0641E+06	5.0113E+02	5.9891E+02	7.5597E+06	2.3532E+05	2.8645E+04	1.1256E+08	2.9146E+07	5.1474E+07	<b>1.0000E+00</b>
	Std	1.2063E+05	<b>0.0000E+00</b>	3.7416E+06	6.4702E+04	3.9118E+06	1.3992E+03	3.2689E+03	9.6571E+06	3.8510E+05	3.4020E+04	5.9495E+07	1.7069E+07	3.7553E+07	<b>0.0000E+00</b>
	P	1.2118E-12	NaN	1.2118E-12	1.2118E-12	1.2118E-12	1.2118E-12	4.1926E-02	1.2118E-12	4.5736E-12	1.2118E-12	1.2118E-12	1.2118E-12	1.2118E-12	—
	Wr	(+)	(=)	(+)	(+)	(+)	(+)	(+)	(+)	(+)	(+)	(+)	(+)	(+)	—
F2	T	7.9767E-02	1.6890E-01	7.5100E-02	1.1763E-01	2.3105E+00	7.5767E-02	5.1413E+00	6.9833E-02	6.9833E-02	7.7100E-02	6.7667E-03	9.2000E-03	2.7067E-02	1.6503E-01
	Mean	4.9733E+02	5.0000E+00	4.1209E+03	1.2478E+02	3.0343E+03	2.0236E+02	2.5171E+02	9.8995E+02	4.3452E+02	2.2864E+02	1.0443E+04	6.5982E+03	8.3745E+03	<b>4.5258E+00</b>
	Std	2.8773E+02	0.0000E+00	2.0091E+03	1.4732E+02	1.5579E+03	3.1935E+02	2.8060E+02	1.4004E+03	2.3212E+02	1.4938E+02	1.5396E+03	1.8081E+03	2.3369E+03	<b>3.2030E-01</b>
	P	2.8003E-11	4.7884E-08	2.8003E-11	1.3250E-09	2.8003E-11	1.6573E-10	1.2082E-09	2.8003E-11	2.8003E-11	2.8003E-11	2.8003E-11	2.8003E-11	2.8003E-11	—
F3	Wr	(+)	(+)	(+)	(+)	(+)	(+)	(+)	(+)	(+)	(+)	(+)	(+)	(+)	—
	T	5.7100E-02	1.0883E-01	4.9767E-02	1.0653E-01	3.8217E+00	5.2667E-02	4.0273E-01	4.0733E-02	4.0267E-02	5.0067E-02	6.3000E-03	8.1667E-03	2.6600E-02	1.2760E-01
	Mean	5.9349E+00	6.5158E+00	1.0112E+01	6.4639E+00	6.3286E+00	8.5793E+00	5.9438E+00	7.7433E+00	5.8716E+00	6.1102E+00	1.1600E+01	1.1085E+01	1.1485E+01	<b>5.3656E+00</b>
	Std	1.5933E+00	9.0210E-01	1.2078E+00	1.5636E+00	1.4127E+00	1.4318E+00	9.1740E-01	1.6851E+00	1.7548E+00	1.3305E+00	5.0910E-01	4.3490E-01	4.6950E-01	<b>6.0250E-01</b>
F4	P	9.1171E-01	2.8790E-06	3.0199E-11	8.3146E-03	3.1466E-02	6.7220E-10	1.1711E-02	2.0023E-06	7.9522E-02	1.5367E-01	3.0199E-11	3.0199E-11	3.0199E-11	—
	Wr	(=)	(+)	(+)	(+)	(+)	(+)	(+)	(=)	(=)	(=)	(+)	(+)	(+)	—
	T	5.3900E-02	1.0610E-01	4.9333E-02	1.0480E-01	3.6296E+00	5.1033E-02	3.9597E-01	3.9067E-02	3.9067E-02	4.9400E-02	6.3333E-03	8.4000E-03	2.6967E-02	1.2633E-01
	Mean	1.9259E+01	5.0466E+01	5.1263E+01	3.1744E+01	2.5765E+01	2.8629E+01	4.1508E+01	2.4266E+01	1.7576E+01	2.0774E+01	6.5210E+01	5.5098E+01	5.3380E+01	<b>1.4708E+01</b>
F5	Std	7.3328E+00	1.6743E+01	7.5578E+00	1.1828E+01	9.0682E+00	8.1568E+00	8.1357E+00	6.9575E+00	6.9999E+00	8.2795E+00	1.1003E+01	8.6967E+00	8.9098E+00	<b>5.5812E+00</b>
	P	1.0763E-02	1.0937E-10	3.0199E-11	2.3897E-08	4.4205E-06	9.2603E-09	3.3384E-11	1.8608E-06	1.2235E-01	7.6171E-03	3.0199E-11	3.0199E-11	3.0199E-11	—
	Wr	(+)	(+)	(+)	(+)	(+)	(+)	(+)	(+)	(=)	(+)	(+)	(+)	(+)	—
	T	5.2533E-02	1.1793E-01	4.8867E-02	9.7333E-02	2.4860E+00	4.9833E-02	2.8430E-01	4.4467E-02	4.3233E-02	5.0933E-02	5.9667E-03	8.6667E-03	2.1000E-02	1.3847E-01
F6	Mean	2.0632E+00	2.0190E+00	1.1430E+01	6.7662E+00	1.1987E+00	4.9479E+00	4.4176E+00	5.1641E+00	<b>1.1232E+00</b>	1.1326E+00	1.6077E+01	3.9932E+00	3.3997E+00	1.1455E+00
	Std	9.2000E-01	2.0040E-01	4.2855E+00	1.0178E+01	8.7500E-02	5.2875E+00	5.3649E+00	6.2348E+00	<b>7.7900E-02</b>	8.8800E-02	4.7262E+00	1.1295E+00	1.2300E+00	1.3290E-01
	P	1.9568E-10	3.0199E-11	3.0199E-11	3.3384E-11	2.6243E-03	3.0199E-11	3.0199E-11	2.4157E-02	9.4696E-01	6.7350E-01	3.0199E-11	3.0199E-11	3.0199E-11	—
	Wr	(+)	(+)	(+)	(+)	(+)	(+)	(+)	(+)	(=)	(+)	(+)	(+)	(+)	—
F7	T	5.6667E-02	1.3347E-01	5.2400E-02	1.0253E-01	2.6895E+00	5.7233E-02	3.1277E-01	4.6933E-02	4.7367E-02	5.4900E-02	6.4000E-03	9.0000E-03	2.1467E-02	1.4827E-01
	Mean	2.9019E+00	8.2974E+00	7.9538E+00	4.9360E+00	6.0253E+00	8.0410E+00	5.4160E+00	3.5784E+00	<b>2.7783E+00</b>	4.4354E+00	1.0595E+01	8.5556E+00	7.8516E+00	3.4063E+00
	Std	1.5076E+00	1.6230E+00	1.1307E+00	1.5549E+00	1.6987E+00	1.8808E+00	1.1559E+00	1.6907E+00	<b>1.1713E+00</b>	1.2047E+00	1.0639E+00	1.3850E+00	1.4558E+00	1.1902E+00
	P	7.7272E-02	6.0658E-11	3.0199E-11	2.2539E-04	2.0283E-07	9.9186E-11	2.1959E-07	9.0000E-01	5.1877E-02	1.7666E-03	3.0199E-11	3.3384E-11	3.3384E-11	—
F8	Wr	(=)	(+)	(+)	(+)	(+)	(+)	(+)	(=)	(=)	(+)	(+)	(+)	(+)	—
	T	5.3467E-01	1.2839E+00	5.3370E-01	5.8533E-01	2.9715E+00	5.3033E-01	1.2554E+00	5.2423E-01	5.2060E-01	5.3343E-01	2.3600E-02	2.7367E-02	4.2467E-02	1.1404E+00
	Mean	8.2703E+02	1.2281E+03	1.6493E+03	1.1371E+03	1.2911E+03	1.1317E+03	1.2871E+03	8.1401E+02	7.9413E+02	6.3012E+02	2.1442E+03	1.9738E+03	2.0321E+03	<b>5.2092E+02</b>
	Std	3.7117E+02	3.1987E+02	2.3023E+02	3.7072E+02	3.4768E+02	3.7007E+02	2.9760E+02	2.6267E+02	3.1079E+02	2.6140E+02	2.8551E+02	2.4970E+02	2.8390E+02	<b>2.2513E+02</b>
F9	P	7.6973E-04	4.1997E-10	3.0199E-11	1.4110E-09	4.6159E-10	1.0105E-08	9.9186E-11	1.2477E-04	9.5207E-04	1.1199E-01	3.0199E-11	3.0199E-11	3.0199E-11	—
	Wr	(+)	(+)	(+)	(+)	(+)	(+)	(+)	(+)	(+)	(=)	(+)	(+)	(+)	—
	T	5.7067E-02	1.3447E-01	5.4867E-02	1.0437E-01	2.5391E+00	5.5733E-02	3.0327E-01	4.7967E-02	4.8200E-02	5.5767E-02	6.6667E-03	9.0333E-03	2.8067E-02	1.5370E-01
	Mean	3.7429E+00	4.6758E+00	4.4684E+00	4.1568E+00	4.5824E+00	4.4762E+00	4.4767E+00	3.9215E+00	3.7715E+00	3.9383E+00	5.1269E+00	4.9943E+00	4.9647E+00	<b>3.6153E+00</b>
F10	Std	4.9850E-01	2.8440E-01	3.1920E-01	4.0110E-01	3.1570E-01	3.2870E-01	3.4610E-01	4.0060E-01	<b>4.4480E-01</b>	4.2750E-01	1.4610E-01	2.3850E-01	2.2690E-01	4.7760E-01
	P	3.7108E-01	9.9186E-11	1.0105E-08	5.2650E-05	1.2870E-09	8.4848E-09	4.9980E-09	9.8834E-03	2.7071E-01	6.9724E-03	3.0199E-11	3.0199E-11	3.0199E-11	—
	Wr	(=)	(+)	(+)	(+)	(+)	(+)	(+)	(=)	(=)	(+)	(+)	(+)	(+)	—
	T	5.4933E-02	1.2880E-01	5.3067E-02	1.0763E-01	2.5779E+00	5.3000E-02	3.0403E-01	4.5733E-02	4.4200E-02	5.3000E-02	6.3000E-03	8.9667E-03	2.7633E-02	1.4287E-01
Wilcoxon's rank sum test	Mean	1.2153E+00	1.4152E+00	1.6805E+00	1.3152E+00	1.3538E+00	1.4089E+00	1.3451E+00	1.2382E+00	<b>1.1759E+00</b>	1.3093E+00	2.0830E+00	1.7236E+00	1.5593E+00	1.1949E+00
	Std	9.0500E-02	2.0460E-01	1.7090E-01	1.0860E-01	1.4030E-01	1.4980E-01	9.1300E-02	1.2650E-01	7.9200E-02	1.1030E-01	2.5420E-01	2.1900E-01	1.5830E-01	<b>7.2600E-02</b>
	P	6.3088E-01	2.8790E-06	3.0199E-11	3.3681E-05	5.0912E-06	2.3897E-08	2.6015E-08	3.2553E-01	3.1119E-01	1.1058E-04	3.0199E-11	3.0199E-11	3.0199E-11	—
	Wr	(=)	(+)	(+)	(+)	(+)	(+)	(+)	(=)	(=)	(+)	(+)	(+)	(+)	—
F10	T	4.9667E-02	1.1253E-01	4.6467E-02	1.0100E-01	2.4814E+00	4.6767E-02	2.9600E-01	4.0800E-02	3.9133E-02	4.8000E-02	6.0667E-03	8.3667E-03	1.9167E-02	1.3173E-01
	Mean	2.1471E+01	2.1196E+01	2.1486E+01	2.1491E+01	2.1029E+01	2.1478E+01	2.1392E+01	2.1272E+01	<b>2.0504E+01</b>	2.1468E+01	2.1729E+01	2.1682E+01	2.1741E+01	2.0605E+01
	Std	1.0500E-01	1.1410E-01	9.3500E-02	9.6100E-02	<b>7.8900E-02</b>	8.5800E-02	2.8750E-01	1.7960E-01	3.4673E+00	9.2400E-02	1.5470E-01	1.3580E-01	1.1840E-01	3.3664E+00
	P	2.8389E-04	2.1327E-05	4.0840E-05	3.3681E-05	1.4294E-08	7.6588E-05	5.0842E-03	9.0490E-02	2.3768E-07	2.2539E-04	7.3803E-10	1.8567E-09	8.1527E-11	—
Wilcoxon's rank sum test	T	4.7833E-02	1.0333E-01	4.0467E-02	7.4700E-02	2.2500E+00	4.2433E-02	2.3023E-01	3.8333E-02	4.2667E-02	4.0800E-02	4.9333E-03	6.5667E-03	2.2400E-02	1.1240E-01
	Friedman value	6/4/0	8/1/1	10/0/0	10/0/0	9/0/1	10/0/0	10/0/0	7/3/0	3/6/1	7/3/0	10/0/0	10/0/0	10/0/0	—
	Friedman rank	4	6	11	10	7	9	5	8	2	3	14	12	13	<b>1</b>

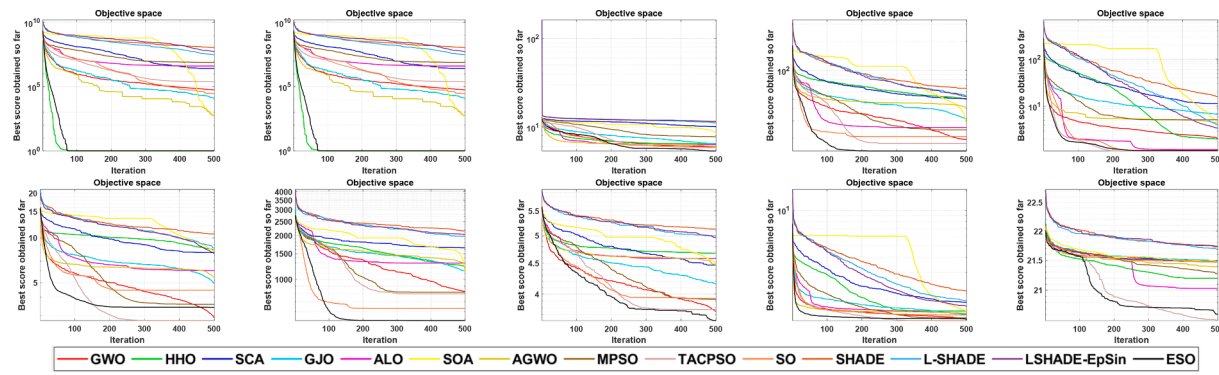


Fig. 9. Convergence curves of 14 algorithms on CEC 2019 functions.

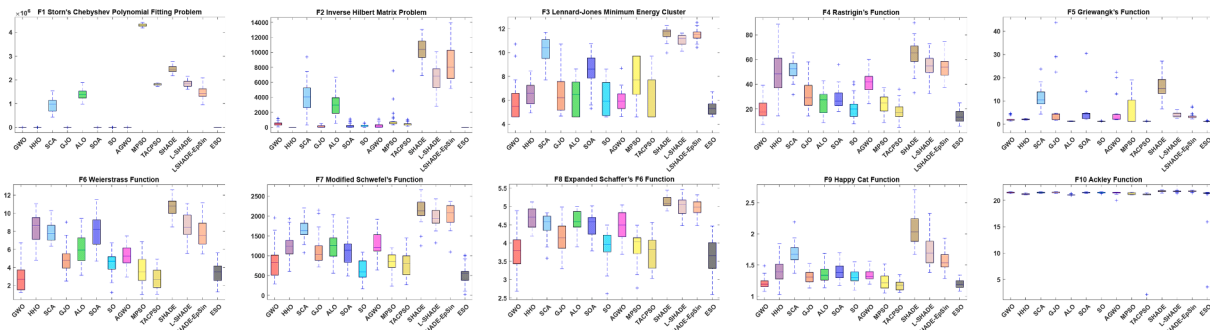


Fig. 10. Boxplot analysis for CEC2019 benchmark functions.

achieves more excellent results than other algorithms in 2000 dimensions. Fig. 7 shows the results of 14 algorithms on 13 functions more comprehensively in the form of box plots, and it can be seen that ESO achieves excellent results.

Table 9 shows the performance of 14 algorithms in fixed-dimension functions. It can be seen that ESO achieves optimal values for 9 of the ten fixed-dimensional functions. In order to show the performances of ESO and other algorithms more objectively, the statistical methods of Wilcoxon's rank sum test and Friedman test are introduced in this paper. The Wilcoxon's rank sum test counts the results of ESO compared with other algorithms, and ESO achieves the result of 101/24/5. The Friedman value shows the overall results achieved by each algorithm in 10 functions. The result of 2.1500 is ranked first in the Friedman rank, which proves that ESO achieves more excellent results than other algorithms in fixed dimensions. Fig. 8 shows the results of 14 algorithms on 13 functions more comprehensively in the form of box plots, and it can be seen that ESO achieves excellent results.

All functions are in fixed dimensions for the second function set, which is the CEC 2019 function set. The value of fixed dimensions is listed in Table 2. In the previous experiment, the non-fixed dimensional function used five different dimensions. Therefore, CEC 2019 can be considered as a supplement to the fixed dimensional functions, and the design of the CEC 2019 is more complex, which can be used to demonstrate the robustness and universality of the proposed ESO. Table 10 shows the results of CEC 2019, including Mean, Std, p-value, Wilcoxon's rank sum test, Friedman test, and run time per iteration of 14 algorithms. Evaluate the algorithm from multiple perspectives. Fig. 9 shows the curve plot of 14 algorithms iterating 500 times on each CEC 2019 function because CEC 2019 functions are more complex, the iterative curve is shown, and Fig. 10 is the box plot of 14 algorithms after solving ten functions with fixed dimensions. The iterative curve and box plot can be an excellent supplement to the data in Table 10 to compare the results of all algorithms better and more comprehensively.

Table 10 shows the performance of 14 algorithms in CEC 2019. ESO

achieved optimal values for 9 of the ten functions, the most significant number among all 14 algorithms. The function that failed to obtain the optimal value ranked second. In order to show the performances of ESO and other algorithms more objectively, the statistical methods of Wilcoxon's rank sum test and Friedman test are introduced in this paper. The Wilcoxon's rank sum test counts the results of ESO compared with other algorithms, and ESO achieves the result of 110/17/3. The Friedman value shows the overall results achieved by each algorithm in ten functions. The result of 3.1000 is ranked first in the Friedman rank. Both statistical methods demonstrate that ESO achieves superior results over other algorithms in the CEC 2019, which proves that ESO achieves more excellent results than other algorithms in fixed dimensions. Fig. 10 shows the results of the 14 algorithms on the CEC 2019 functions more comprehensively in the form of box plots, and in aggregate, ESO achieves excellent results.

Four strategies are added in this paper: parameters dynamic update strategy, mirror imaging strategy based on convex lens imaging, sine-cosine composite perturbation factors, and Tent-chaos & Cauchy mutation. To verify the effectiveness of the four strategies, strategy comparison experiments were conducted. The population size was set to 30, and the number of iterations was 500. ESO-1 demonstrates that only the parameters dynamic update strategy is used, ESO-2 demonstrates that only the mirror imaging strategy based on convex lens imaging is used, ESO-3 demonstrates that only the sine-cosine composite perturbation factors strategy is used, and ESO-4 demonstrates that only the Tent-chaos & Cauchy mutation strategy is used. The results are shown in Table 11 and Fig. 11. For ease of comparison, the optimal values for each function are displayed in bold.

The following conclusions can be drawn from Table 11 and Fig. 11. Compared to the basic SO, ESO-1 obtained better results on functions F18, F20, and F23 while obtaining similar results on other functions. This is because the novel parameters dynamic update strategy accelerates the convergence performance of the function and helps the algorithm jump out of the local optimum. ESO-2 achieved optimal results in

**Table 11**

Experimental results of SO, ESO-1, ESO-2, ESO-3, and ESO on 23 benchmark functions.

F(x)		SO	ESO-1	ESO-2	ESO-3	ESO-4	ESO
F1	Mean	7.8290E-93	1.4535E-62	0.0000E+00	2.0495E-93	1.1571E-273	0.0000E+00
	Std	3.5992E-92	6.2875E-62	0.0000E+00	9.7107E-93	3.1155E-290	0.0000E+00
F2	Mean	2.8768E-43	4.4939E-15	0.0000E+00	9.5518E-43	1.3492E-134	0.0000E+00
	Std	5.2752E-43	2.8134E-15	0.0000E+00	2.4810E-42	6.3121E-134	0.0000E+00
F3	Mean	4.2069E-53	9.9824E-39	0.0000E+00	5.6671E-57	5.6391E-234	0.0000E+00
	Std	2.2709E-52	3.9502E-38	0.0000E+00	1.9947E-56	0.0000E+00	0.0000E+00
F4	Mean	2.4516E-40	8.2902E-14	0.0000E+00	1.6737E-40	9.7679E-128	0.0000E+00
	Std	6.0608E-40	9.0143E-14	0.0000E+00	3.9264E-40	4.1302E-127	0.0000E+00
F5	Mean	2.1319E+01	2.1395E+01	1.8156E+01	3.4427E+01	1.6658E+01	8.6942E-01
	Std	1.1067E+01	1.1037E+01	1.1913E+01	5.4293E+01	1.3040E+01	2.5725E+00
F6	Mean	9.4211E-01	6.6676E-01	3.8600E-01	8.6106E-01	1.7548E-01	1.6781E-02
	Std	5.9754E-01	5.0070E-01	2.1470E-01	6.9794E-01	1.7059E-01	3.0664E-02
F7	Mean	2.3118E-04	3.6057E-04	0.00017315	2.4720E-04	1.6348E-04	1.8186E-04
	Std	2.0789E-04	2.7563E-04	1.3875E-04	1.7435E-04	1.3389E-04	1.1748E-04
F8	Mean	-1.2488E+04	-1.2516E+04	-1.2541E+04	-1.2380E+04	-1.2567E+04	-1.2569E+05
	Std	1.2175E+02	7.8503E+01	8.6572E+01	2.7725E+02	3.7100E+00	1.5719E+00
F9	Mean	2.7043E+00	6.4257E+00	0.0000E+00	1.4576E+00	0.0000E+00	0.0000E+00
	Std	6.6149E+00	1.2438E+01	0.0000E+00	5.7635E+00	0.0000E+00	0.0000E+00
F10	Mean	8.0846E-02	1.6144E-01	8.8818E-16	1.6608E-01	8.8818E-16	8.8818E-16
	Std	4.4281E-01	4.9338E-01	0.0000E+00	6.3524E-01	0.0000E+00	0.0000E+00
F11	Mean	4.7890E-02	1.2862E-01	0.0000E+00	1.0317E-01	0.0000E+00	0.0000E+00
	Std	1.5327E-01	2.1089E-01	0.0000E+00	1.6814E-01	0.0000E+00	0.0000E+00
F12	Mean	6.5040E-02	1.0959E-01	1.8121E-02	6.6953E-02	2.3004E-03	3.7785E-04
	Std	1.9078E-01	2.1839E-01	1.6007E-02	1.1528E-01	1.4620E-03	4.2695E-04
F13	Mean	2.5541E-01	6.7999E-01	6.3569E-02	2.6866E-01	3.5075E-02	1.6083E-03
	Std	4.5664E-01	9.8332E-01	7.1529E-02	5.7823E-01	2.4652E-02	2.6224E-03
F14	Mean	9.9805E-01	1.1741E+00	9.9803E-01	1.1293E+00	9.9803E-01	9.9800E-01
	Std	2.6490E-04	8.9981E-01	1.4151E-04	5.6334E-01	1.1940E-04	1.1068E-10
F15	Mean	1.0973E-03	9.5420E-04	5.4350E-04	4.8865E-04	3.2938E-04	3.6649E-04
	Std	3.6410E-03	1.2574E-03	3.0604E-04	2.3504E-04	7.2498E-05	9.0291E-05
F16	Mean	-1.0316E+00	-1.0316E+00	-1.0316E+00	-1.0316E+00	-1.0316E+00	-1.0316E+00
	Std	1.0973E-03	5.6082E-16	5.8312E-16	5.3761E-16	5.7460E-12	5.7460E-12
F17	Mean	3.9789E-01	3.9789E-01	3.9789E-01	3.9789E-01	3.9789E-01	3.9789E-01
	Std	0.0000E+00	0.0000E+00	0.0000E+00	0.0000E+00	0.0000E+00	0.0000E+00
F18	Mean	6.6000E+00	5.7000E+00	3.0000E+00	3.0000E+00	3.0000E+00	3.0000E+00
	Std	9.3351E+00	8.2385E+00	2.8886E-15	2.8886E-15	1.3039E-15	9.8958E-16
F19	Mean	-3.8628E+00	-3.8628E+00	-3.8628E+00	-3.8628E+00	-3.8628E+00	-3.8628E+00
	Std	2.5270E-15	2.4795E-15	2.4491E-15	2.5684E-15	2.5391E-15	2.5829E-15
F20	Mean	-3.3101E+00	-3.3101E+00	-3.3141E+00	-3.3141E+00	-3.3219E+00	-3.3220E+00
	Std	3.6278E-02	3.6278E-02	3.0164E-02	3.0164E-02	1.6940E-04	4.1381E-05
F21	Mean	-1.0108E+01	-1.0129E+01	-1.0152E+01	-1.0071E+01	-1.0153E+01	-1.0153E+01
	Std	1.5362E-01	5.9603E-02	2.8977E-03	3.9651E-01	4.6777E-05	1.8511E-11
F22	Mean	-1.0376E+01	-1.0325E+01	-1.0363E+01	-1.0233E+01	-1.0403E+01	-1.0403E+01
	Std	6.8158E-02	2.9163E-01	1.2007E-01	4.1354E-01	1.3055E-06	3.5570E-06
F23	Mean	-1.0484E+01	-1.0462E+01	-1.0513E+01	-1.0434E+01	-1.0536E+01	-1.0536E+01
	Std	1.5359E-01	3.2002E-01	7.2219E-02	3.3942E-01	1.9172E-11	6.4000E-13

18 functions (such as F1, F2, F3, F4, F6, F7, F9, F10, F11, F12, F13, F14, F16, F17, F20, F21, F22, F23), and obtained similar results in other functions. This is because a nonlinear dynamic scaling factor is used to maintain population diversity in the mirror imaging strategy based on convex lens imaging. The range of scaling factors is [-10, 10]. At the beginning of the iteration, when  $\delta > 0$ , the newly generated individuals have a larger distance from the original individuals, increasing the diversity of the population, greatly enhancing the global search ability of the algorithm. When  $\delta < 0$ , the newly generated individuals are near the original individuals, increasing the local optimum ability of the algorithm. ESO-3 can jump out of local and accelerate convergence on F17, F18, and F23 because sine-cosine composite perturbation factors are used to replace fixed coefficients in the mating part of SO. The perturbation factors have a large fluctuation range in the early stage, which helps the algorithm avoid falling into iteration stagnation. The small fluctuation range tends to be 1 in the late stage of iteration, which can accelerate the convergence speed of the algorithm. ESO-4 greatly improves the speed of optimization and convergence accuracy in 23 functions. The Cauchy mutation strategy focuses on searching a local region near the original individual, so its local search ability is strong. For optimization problems with many local minima, it is conducive to the algorithm to find global minimum points efficiently and accurately while also improving the algorithm's robustness. Tent-Chaos enhances

the ability of the algorithm to jump out of the local optimum and improves the global search ability and optimization accuracy. The effect of a single strategy may be obscure, but the four strategies are significant for improving SO. For almost every function, the performance of the ESO is better than that of the SO.

In this section, the performance of ESO is verified by comparing the non-fixed dimensional and fixed dimensional functions in two different function sets with thirteen SOTA algorithms, demonstrating that the proposed four strategies all affect the improvement of the optimization mechanism in the original SO to obtain a better solution. The proposed ESO algorithm has powerful exploitation capability and efficient space exploration to solve optimization problems effectively.

#### 4.3. Convergence and stability analysis

The convergence performance of ESO is observed by performing 500 iterations for 30-dimension and fixed-dimension functions, and the convergence process is shown in Fig. 12 with five columns. The plot in the first column is the three-dimensional plot of the benchmark function, which can be used to visualize the extreme value points that the function has. The plot in the second column is the convergence curve, where the best values of ESO and SO are shown for the same conditions of iteration in order to better compare with the original SO. It can be seen that ESO

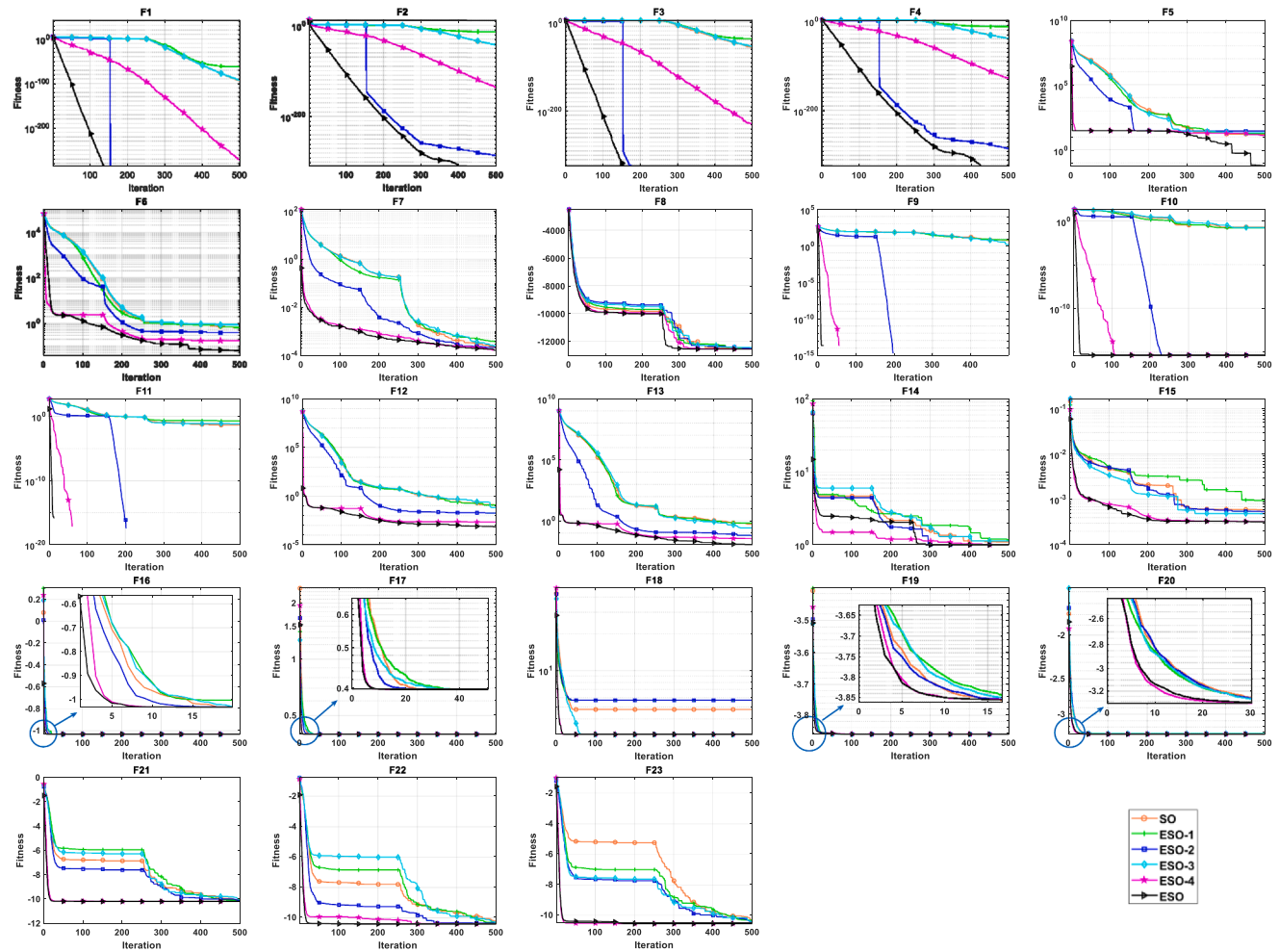


**Fig. 11.** Convergence curves of five algorithms for 23 benchmark functions.

converges fast on the unimodal function, and the ladder declines on the multimodal function, which shows that the improved algorithm has better exploration and development capabilities, and in all functions, ESO not only convergence is higher than SO, but also better than SO in the optimal value. The graph in the third column shows the trajectory of the first individual in the first dimension. The initial significant fluctuations are due to the global optimization early in the iteration. By adding novel opposition-based learning strategy and dynamic update mechanisms, ESO fluctuations converge rapidly compared to the SO and converge to stable values. The plot in the fourth column shows the average fit of the individual, which is used to evaluate the overall performance. In the initial iteration, the curve will be relatively high, and as the number of iterations increases, the average fitness will gradually decrease and stabilize. The fifth column graph shows the individual's historical position during the iterations. It is demonstrated through Fig. 12 that the improvements of the proposed ESO in this paper can balance the exploration and exploitation capabilities of the algorithm. The proposed ESO can achieve higher search accuracy and faster convergence speed with these improvements.

## 5. ESO for real-world engineering problems

Real-world engineering is one of the critical application scenarios for optimization problems (Peng et al., 2022; Yang et al., 2023; Zhao, Fang, Ma, & Liu, 2022; Wang et al., 2022). Solving engineering design

problems can help save materials, improve product quality, and achieve the goals of green design and manufacturing. In this section, ESO will be used to solve the four engineering design problems of Speed reducer design, Pressure vessel design, Corrugated bulkhead design, and Welded beam design. These problems are fundamental practical problems in society. In order to validate the ESO results effectively, the same thirteen algorithms (SO, HHO, SCA, GJO, ALO, SOA, AGWO, MPSO, TACPSO, GWO, SHADE, LSHADE, and LSHADE-EpSin) used here as in the theoretical tests will be used to solve these problems as well and compared with the ESO results.

### 5.1. Speed reducer design

Speed reducer is a mechanical transmission device in many national economy fields. Its applications involve metallurgy, non-ferrous metals, coal, building materials, ships, water conservancy, electric power, construction machinery, and petrochemical industries. In the speed reducer design problem, under the constraints of 11 conditions, the weight of the speed reducer is required to be the smallest. The problem has seven variables: face width  $b(=x_1)$ , module of teeth  $m(=x_2)$ , the number of teeth in the pinion  $z(=x_3)$ , length of the first shaft between bearings  $l_1(=x_4)$ , length of the second shaft between bearings  $l_2(=x_5)$ , the diameter of first shafts  $d_1(=x_6)$ , and the diameter of second shafts  $d_2(=x_7)$ . The mathematical model of the speed reducer design is as follows:

$$\text{Min } f(x) = 0.7854x_1x_2^2(3.333x_3^2 + 14.9334x_3 - 43.0934) - 1.508x_1(x_6^2 + x_7^2) + 7.4777(x_6^3 + x_7^3) + 0.7854(x_4x_6^2 + x_5x_7^2)$$

Subject to

$$\begin{aligned} h_1(x) &= \frac{27}{x_1x_2^2x_3} - 1 \leq 0 & h_2(x) &= \frac{397.5}{x_1x_2^2x_3^2} - 1 \leq 0 \\ h_3(x) &= \frac{1.93y_4^3}{y_2y_6^4y_3} - 1 \leq 0 & h_4(x) &= \frac{1.93x_5^3}{x_2x_7^4x_3} - 1 \leq 0 \\ h_5(x) &= \frac{[(745(x_4/x_2x_3))^2 + 16.9*10^6]}{110y_6^3} - 1 \leq 0 & \\ h_6(x) &= \frac{[(745(x_5/x_2x_3))^2 + 157.5*10^6]}{85x_7^3} - 1 \leq 0 & \\ h_7(x) &= \frac{x_2x_3}{40} - 1 \leq 0 & h_8(x) &= \frac{5x_2}{x_1} - 1 \leq 0 \\ h_9(x) &= \frac{x_1}{12x_2} - 1 \leq 0 & h_{10}(x) &= \frac{1.5x_6 + 1.9}{x_4} - 1 \leq 0 \\ h_{11}(x) &= \frac{1.1x_7 + 1.9}{x_5} - 1 \leq 0 & \end{aligned}$$

where,

$$\begin{aligned} 2.6 \leq x_1 \leq 3.6 & & 0.7 \leq x_2 \leq 0.8 \\ 17 \leq x_3 \leq 28 & & 7.3 \leq x_4 \leq 8.3 \\ 7.3 \leq x_5 \leq 8.3 & & 2.9 \leq x_6 \leq 3.9 \\ 5.0 \leq x_7 \leq 5.5 & & \end{aligned}$$

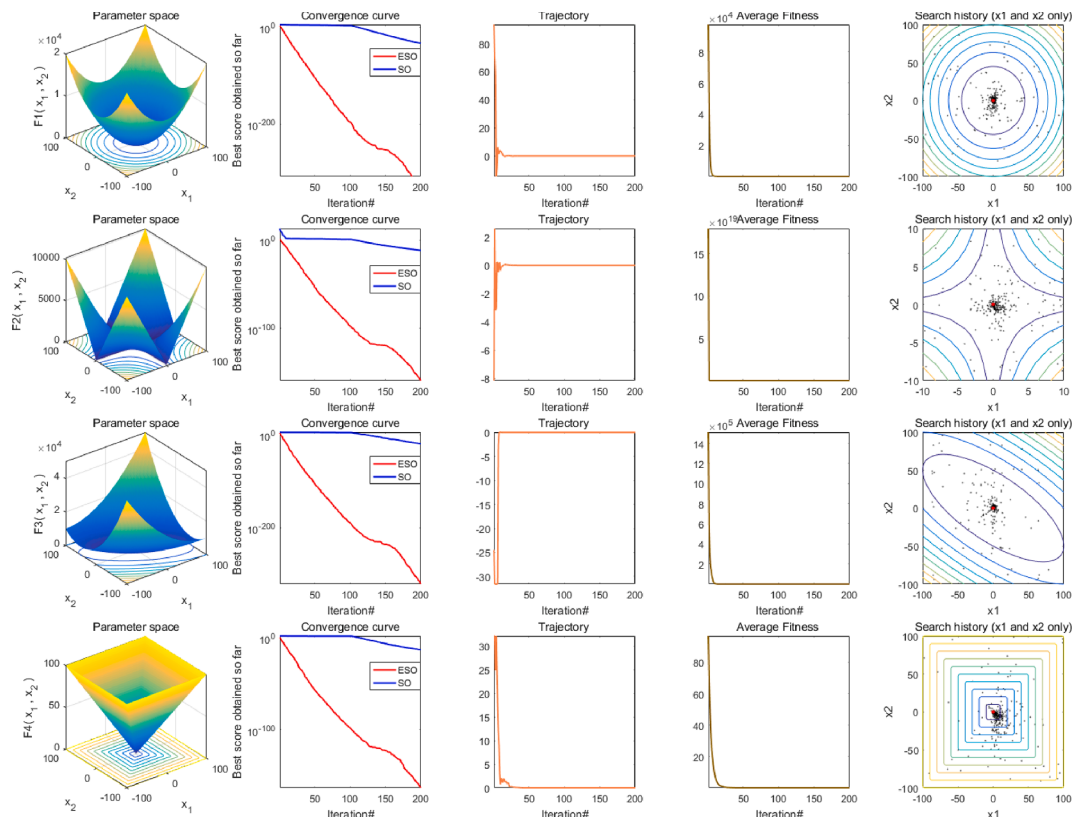


**Fig. 12.** The convergence curve, the trajectories, the average fitness history, and the search history of certain functions.

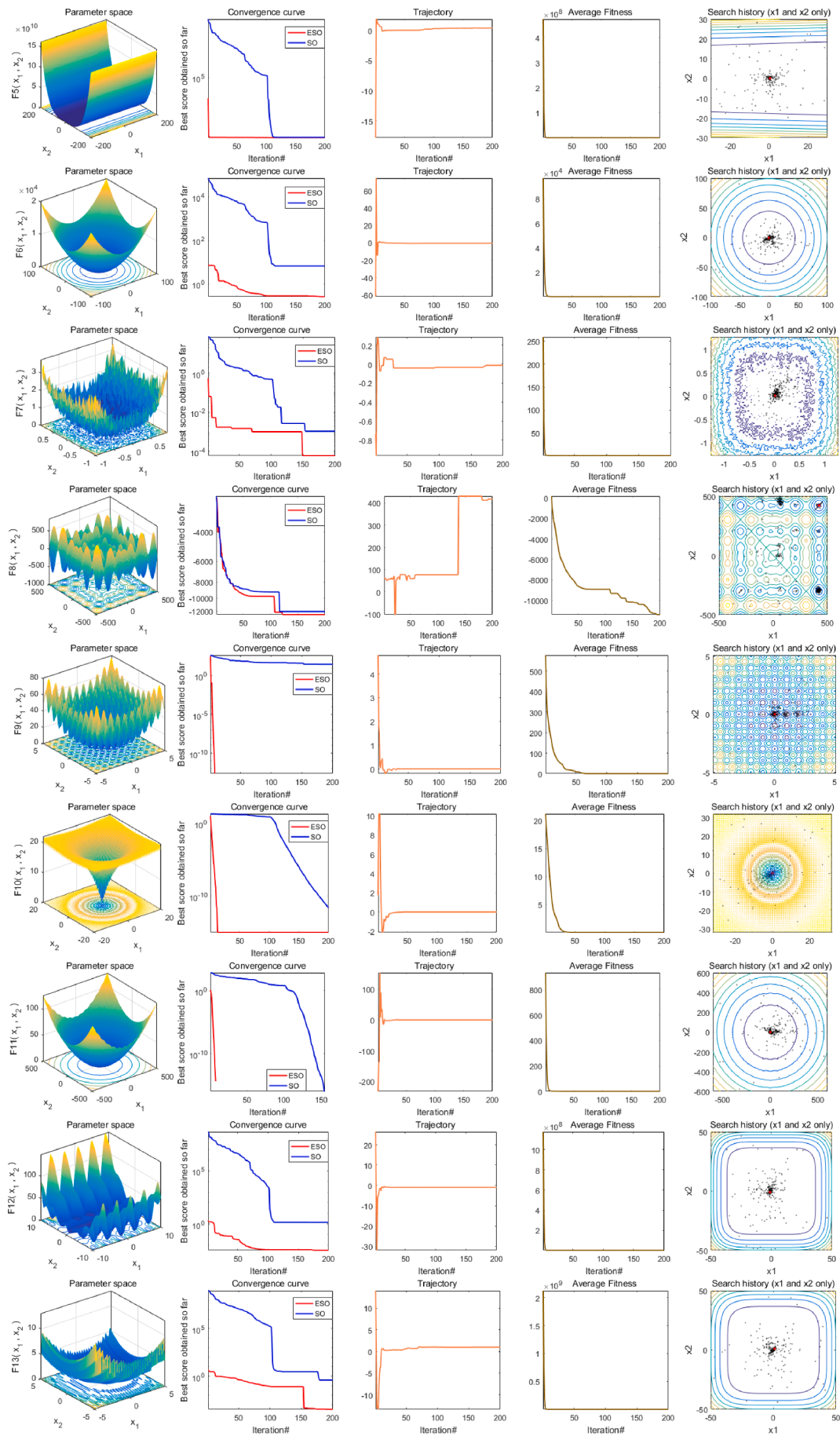


Fig. 12. (continued).

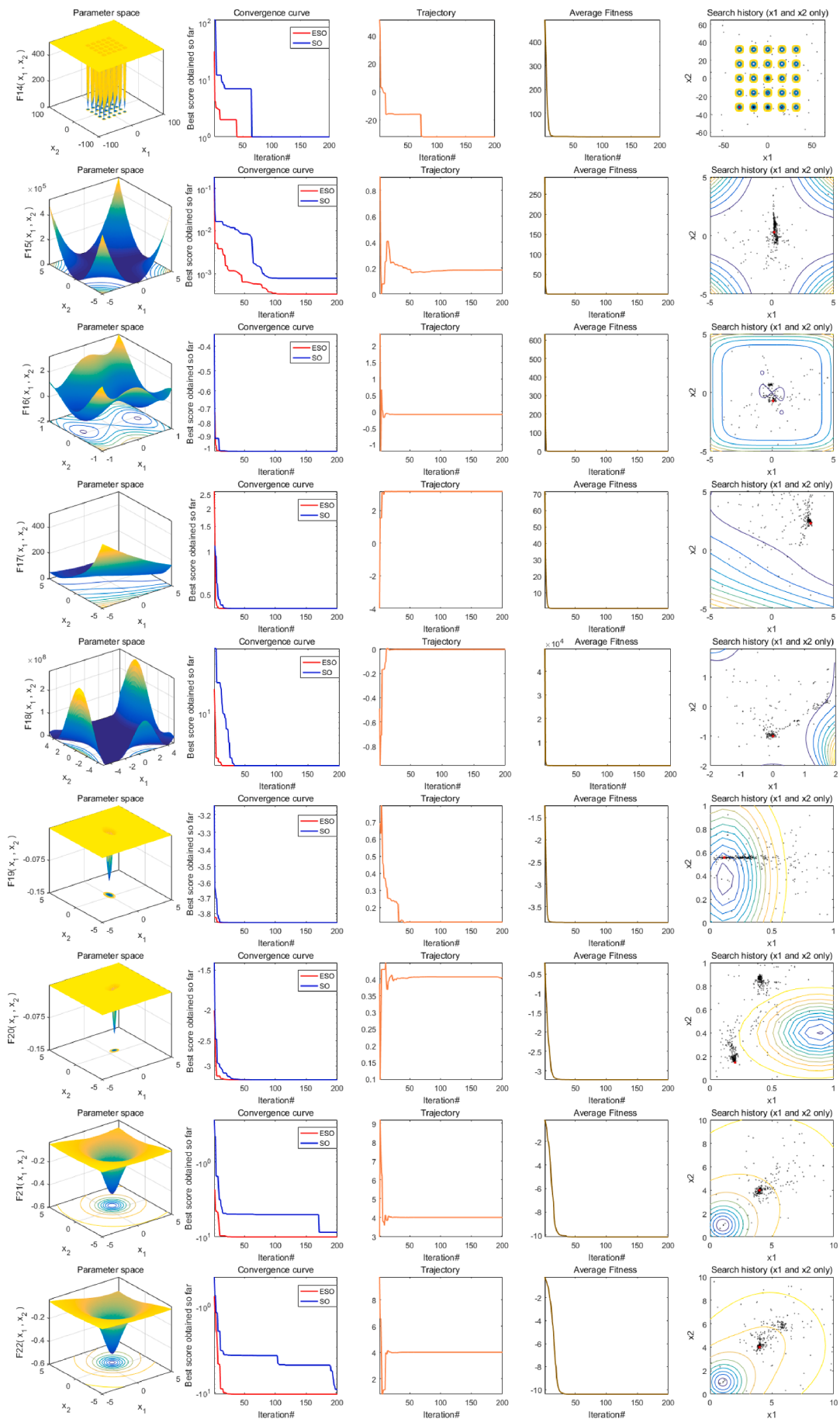


Fig. 12. (continued).

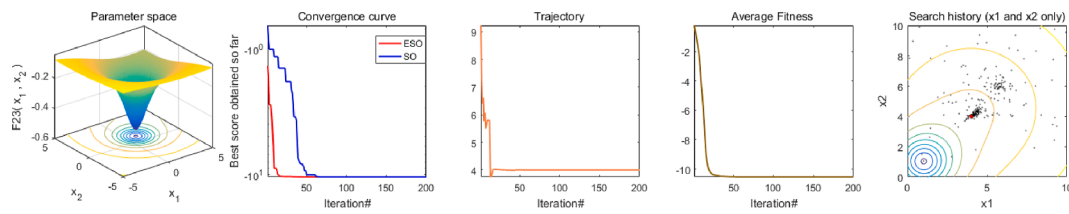


Fig. 12. (continued).

**Table 12** shows the results of ESO and other thirteen algorithms on the speed reducer design problem. The results contain the values of seven variables and the weight values of the reducer corresponding to these values. As seen from the table, the minimum weight of the reducer calculated by the ESO algorithm is  $\text{Min } f(\vec{x}) = 2771.5663103$ , and the corresponding values of the seven variables are  $\vec{x} = \{3.7528760, 0.7000000, 14.7698226, 7.2981353,$

$$7.9506002, 3.4770167, 5.3314598\}$$

. In order to show the performances of ESO and other algorithms more objectively, the statistical methods of Wilcoxon's rank sum test are introduced in this paper. **Table 13** shows the statistical results for the speed reducer design problem. Wilcoxon's rank sum test counts the results of ESO compared with other algorithms, and ESO achieves the result of 12/1/0. After comparing the results with those of the other thirteen algorithms, the SO algorithm achieves good results, but the ESO algorithm achieves optimal results. In order to reflect the performance of the 14 algorithms more intuitively in terms of computation, **Fig. 13** shows the convergence curves of the 14 algorithms, including ESO. It shows each variable's variation curves, reflecting the variation trend among the parameters in the multiparameter design. It can be seen in the figure that ESO has faster convergence and higher accuracy, which proves the rationality and effectiveness of the ESO algorithm.

## 5.2. Pressure vessel design

The pressure vessel is a closed container that can withstand pressure. The use of pressure vessels is pervasive, and it has an important position and role in many sectors, such as industry, civil use, military industry, and many fields of scientific research. In the design of a pressure vessel, under the constraints of four conditions, it is required to meet the production needs while the total cost is the smallest. The problem has four variables: thickness of the shell  $T_s (= x_1)$ , the thickness of the head  $T_h (= x_2)$ , the inner radius  $R (= x_3)$ , and the length of the cylindrical section of the vessel, not including the head  $L (= x_4)$ . The mathematical model of the pressure vessel design is as follows:

$$\text{Min } f(x) = 0.6224x_1x_3x_4 + 1.7781x_2x_3^2 + 3.1661x_1^2x_4 + 19.84x_1^2x_3$$

Subject to

$$g_1(x) = -x_1 + 0.0193x_3 \leq 0$$

$$g_2(x) = -x_2 + 0.00954x_3 \leq 0$$

$$g_3(x) = -\pi x_3^2 x_4 - \frac{4}{3}\pi x_3^2 + 1296000 \leq 0$$

$$g_4(x) = x_4 - 240 \leq 0$$

where,

$$0 \leq x_1 \leq 99$$

$$0 \leq x_2 \leq 99$$

$$10 \leq x_3 \leq 200$$

$$10 \leq x_4 \leq 200$$

**Table 14** shows the results of ESO and thirteen other algorithms on

the pressure vessel design. The results contain the values of four variables and the minimum cost values required for the production of the pressure vessel corresponding to that group of variables. As seen from the table, the minimum cost of the pressure vessel calculated by the ESO algorithm is  $\text{Min } f(\vec{x}) = 5885.3327736$ , and the corresponding values of the four variables are  $\vec{x} = \{0.7781686, 0.3846492, 40.3196187, 200.0000000\}$ . In order to show the performances of ESO and other algorithms more objectively, the statistical methods of Wilcoxon's rank sum test are introduced in this paper. **Table 15** shows the statistical results for the pressure vessel design problem. Wilcoxon's rank sum test counts the results of ESO compared with other algorithms, and ESO achieves the result of 11/2/0. After comparing the results with those of the other thirteen algorithms, the SO algorithm achieves good results, but the ESO algorithm achieves optimal results. In order to reflect the performance of the 14 algorithms more intuitively in terms of computation, **Fig. 14** shows the convergence curves of the 14 algorithms, including ESO. It shows each variable's variation curves, reflecting the variation trend among the parameters in the multiparameter design. It can be seen in the figure that ESO has faster convergence and higher accuracy, which proves the rationality and effectiveness of the ESO algorithm.

## 5.3. Corrugated bulkhead design

The corrugated bulkhead is made of pressed steel plate, and the corrugated bulkhead is bent to replace the function of the stiffener. In the Corrugated bulkhead design problem, the minimum weight is required under the constraints of 6 conditions. The problem has four variables, which are width ( $x_1$ ), depth ( $x_2$ ), length ( $x_3$ ), and plate thickness ( $x_4$ ). The mathematical model of the corrugated bulkhead design is as follows:

$$\text{Min } f(x) = \frac{5.885x_4(x_1 + x_3)}{x_1 + \sqrt{|x_3^2 - x_2^2|}}$$

Subject to

$$g_1(x) = -x_4x_2\left(0.4x_1 + \frac{x_3}{6}\right) + 8.94\left(x_1 + \sqrt{|x_3^2 - x_2^2|}\right) \leq 0$$

$$g_2(x) = -x_4x_2^2\left(0.3x_1 + \frac{x_3}{12}\right) + 2.2\left(8.94\left(x_1 + \sqrt{|x_3^2 - x_2^2|}\right)\right)^{\frac{4}{3}} \leq 0$$

$$g_3(x) = -x_4 + 0.0156x_1 + 0.15 \leq 0$$

$$g_4(x) = -x_4 + 0.0156x_3 + 0.15 \leq 0$$

$$g_5(x) = -x_4 + 1.05 \leq 0$$

$$g_6(x) = -x_3 + x_2 \leq 0$$

where,

$$0 \leq x_1, x_2, x_3 \leq 100$$

$$0 \leq x_4 \leq 5$$

**Table 16** shows the results of ESO and thirteen other algorithms on the corrugated bulkhead design. The results include the values of four variables and the weight of the corrupted bulkhead corresponding to the

**Table 12**

Comparison of the results for the speed reducer design problem.

Algorithms	$x_1$	$x_2$	$x_3$	$x_4$	$x_5$	$x_6$	$x_7$	Optimum Value
SO	3.5000000	0.7000000	7.0000000	7.3000000	7.7153199	3.3502147	5.2866545	2994.4710782
HHO	3.5015140	0.7000000	17.0000000	7.3000000	8.0483486	3.3616037	5.2867694	3005.3613601
SCA	3.6000000	0.7000000	17.0000000	7.3336554	8.3000000	3.3763235	5.3408964	3088.5497688
GJO	3.5078212	0.7000000	17.0000000	7.3253187	7.8816586	3.3679222	5.2874984	3006.4920188
ALO	3.5000000	0.7000000	17.0000000	3.5000000	7.7176983	3.3502476	5.2866557	2994.6837278
SOA	3.5112197	0.7000000	17.0000000	7.5825996	7.8504960	3.3817406	5.2888958	3021.2294862
AGWO	3.5015403	0.7000000	17.0000000	7.3000000	8.1811740	3.3890969	5.3241335	3039.4456951
MPSO	3.5000000	0.7000000	17.0000000	7.3000000	7.7153199	3.3502147	5.2866545	2994.4710661
TACPSO	3.5000000	0.7000000	17.0000000	7.3000000	7.7153199	3.3502147	5.2866545	2994.4710661
GWO	3.5027661	0.7000000	17.0077847	7.3182216	7.9548243	3.3523261	5.2873024	3003.2732481
SHADE	3.5107545	0.7000960	17.0286987	8.0560793	8.1981114	3.3674463	5.3449892	3063.5416088
L SHADE	3.5090418	0.7007936	17.0008414	7.3367919	7.3367919	3.3564656	5.2912854	3012.0879801
L SHADE-EpSin	3.4481988	0.6846573	17.0621642	7.6493835	8.2570094	3.5826117	5.3048426	3007.3427643
ESO	<b>3.7528760</b>	<b>0.7000000</b>	<b>14.7698226</b>	<b>7.2981353</b>	<b>7.9506002</b>	<b>3.4770167</b>	<b>5.3314598</b>	<b>2771.5663103</b>

values of this group of variables. As seen from the table, the minimum weight of the corrupted bulkhead calculated by the ESO algorithm is  $\text{Min } f(\vec{x}) = 6.8429580$ , and the corresponding values of the four variables are  $\vec{x} = \{57.6923077, 34.1476202, 57.6923066, 1.0500000\}$ . In order to show the performances of ESO and other algorithms more objectively, the statistical methods of Wilcoxon's rank sum test are introduced in this paper. Table 17 shows the statistical results for the corrugated bulkhead design problem. Wilcoxon's rank sum test counts the results of ESO compared with other algorithms, and ESO achieves the result of 12/1/0. Compared with the results of the other thirteen advanced algorithms, ESO, SO, MPSO, and TACPSO algorithms achieve optimal results simultaneously. In order to reflect the performance of the 14 algorithms more intuitively in terms of calculation. Fig. 15 shows the convergence curves of the 14 algorithms, such as ESO, and the change curves of each variable, which reflects the changing trend of parameters during multi-parameter design, and proves the rationality and effectiveness of the ESO algorithm.

#### 5.4. Welded beam design problem

The welded beam is a simplified model obtained in the mechanics of materials for ease of computational analysis, where one end of the cantilever beam is a fixed support, and the other is a free end. The problem is a structural engineering design problem related to the weight optimization of a cantilever beam with a square section. Welded beam design is a minimization problem in which optimization algorithms are used to reduce the manufacturing cost of the design. The optimization problem can be described as seeking to satisfy the shearing stress ( $\tau$ ), bending stress ( $\theta$ ), beam bending load ( $P_c$ ). The four design variables constrained by boundary conditions, namely, the length ( $l$ ), height ( $t$ ), thickness ( $b$ ), and weld thickness ( $h$ ) of the beam, minimize the cost of manufacturing a welded beam. The mathematical description of the

welded beam design problem is as follows:

$$\begin{aligned} \text{Min } f(x) &= 1.1047x_1^2x_2 + 0.04811x_3x_4(14.0 + x_2) \\ &\quad \text{Subject to} \\ g_1(x) &= \tau(x) - 13600 \leq 0, \quad g_2(x) = \sigma(x) - 30000 \leq 0, \quad g_3(x) = \delta(x) - 0.25 \leq 0, \\ g_4(x) &= x_1 - x_4 \leq 0, \quad g_5(x) = 6000 - P_c(x) \leq 0, \quad g_6(x) = 0.125 - x_1 \leq 0, \\ g_7(x) &= 1.1047x_1^2 + 0.04811x_3x_4(14.0 + x_2) - 5.0 \leq 0, \\ \tau(x) &= \sqrt{(\tau')^2 + 2\tau'\tau''\frac{x_2}{2R} + (\tau'')^2}, \quad \tau' = \frac{P}{\sqrt{2}x_1x_2}, \quad \tau'' = \frac{MR}{J}, \\ M &= P\left(L + \frac{x_2}{2}\right), \quad R = \sqrt{\frac{x_2^2}{4} + \left(\frac{x_1 + x_3}{2}\right)^2}, \quad J = 2\left\{\sqrt{2}x_1x_2\left[\frac{x_2^2}{4} + \left(\frac{x_1 + x_3}{2}\right)^2\right]\right\}, \\ \sigma(\vec{x}) &= \frac{6PL}{x_4x_3^2}, \quad \delta(\vec{x}) = \frac{6PL^3}{Ex_4x_3^2}, \quad P_c(\vec{x}) = \frac{4.013E\sqrt{x_3^2x_4^6/36}}{L^2} \left(1 - \frac{x_3}{2L}\sqrt{\frac{E}{4G}}\right) \end{aligned}$$

where,

$$0.1 \leq x_1 \leq 2, 0.1 \leq x_2 \leq 10, 0.1 \leq x_3 \leq 10, 0.1 \leq x_4 \leq 2, 0.01 \leq x_1, x_2, x_3, x_4, x_5 \leq 100$$

$$P = 6000 \text{ lb}, L = 14 \text{ in}, E = 30 \times 10^6 \text{ psi}, G = 12 \times 10^6 \text{ psi}$$

Table 18 shows the results of ESO and thirteen other advanced algorithms on the welded beam design. The result contains the values of four variables and the minimum cost value of the welded beam corresponding to this group of variables. As seen from the table, the minimum cost of welded beam calculated by the ESO algorithm is  $\text{Min } f(\vec{x}) = 1.7248523$ , and the corresponding values of the four variables are  $\vec{x} = \{0.2057296, 3.4704887, 9.0366239, 0.2057296\}$ . In order to show the performances of ESO and other algorithms more objectively, the statistical methods of Wilcoxon's rank sum test are introduced in this paper. Table 19 shows the statistical results for the welded beam design problem. Wilcoxon's rank sum test counts the

**Table 13**

Statistical results for the speed reducer design problem.

Algorithms	Best	Mean	Std	Worst	Time	P	Wr
SO	2994.4710782	2994.6789585	0.6902594	2997.4209573	0.1155	4.0350E-01	(=)
HO	3005.3613601	3979.8906075	829.3277098	5337.9497138	0.2687	3.0199E-11	(+)
SCA	3088.5497688	3152.5638756	40.2813945	3201.4248513	0.1084	3.0199E-11	(+)
GJO	3006.4920188	3023.6755178	10.4758413	3053.7036972	0.1598	3.0199E-11	(+)
ALO	2994.6837278	3002.3156802	4.7138717	3012.4436510	1.7890	8.1527E-11	(+)
SOA	3021.2294862	3047.8753051	18.3820676	3099.3576666	0.1093	3.0199E-11	(+)
AGWO	3039.4456951	3068.0923718	26.1140505	3159.0046192	0.5533	3.0199E-11	(+)
MPSO	2994.4710661	3044.8618942	49.7300034	3215.6922931	0.1056	6.3813E-06	(+)
TACPSO	2994.4710661	3038.9800241	41.7076525	3180.0090852	0.1045	6.9146E-07	(+)
GWO	3003.2732481	3010.5337309	4.7456950	3020.3417352	0.1145	3.0199E-11	(+)
SHADE	3063.5416088	3114.7120249	30.4008368	3176.4133536	0.0094	3.0199E-11	(+)
L SHADE	3012.0879801	3030.8898850	11.5055175	3058.5771429	0.0111	3.0199E-11	(+)
L SHADE-EpSin	3007.3427643	3166.8559513	77.7140140	3345.8802971	0.0300	3.0199E-11	(+)
ESO	2771.5663103	2987.2641364	40.7438727	2997.7350589	0.2780	—	—

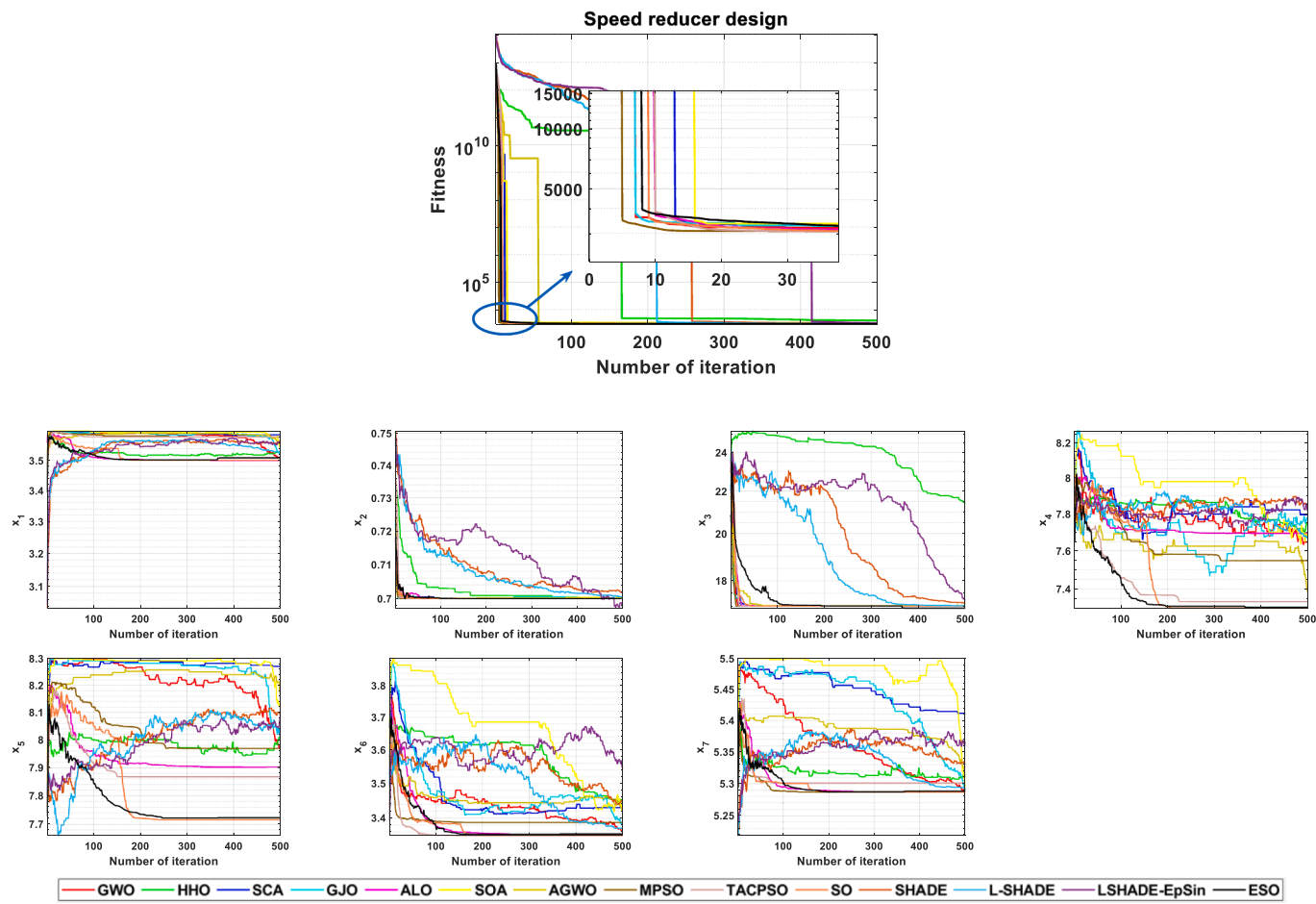


Fig. 13. Convergence curves for the speed reducer design problem.

**Table 14**

Comparison of the results for the pressure vessel design problem.

Algorithms	$x_1$	$x_2$	$x_3$	$x_4$	Optimum Value
SO	0.8011687	0.3960177	41.5112031	184.0561061	5925.9317654
HHO	0.9155315	0.4544300	46.0555237	133.0801287	6325.4825886
SCA	0.8179068	0.4425218	40.9466742	193.8529616	6314.0730693
GJO	0.7808200	0.3933610	40.3950811	198.9616734	5919.8660982
ALO	0.7894060	0.3902078	40.9018318	192.7152992	5919.4990305
SOA	0.7811307	0.3964601	40.4507881	200.0000000	5962.7698986
AGWO	0.7844245	0.4240785	40.5959775	200.0000000	6091.9361286
MPSO	<b>0.7781686</b>	<b>0.3846492</b>	<b>40.3196187</b>	<b>200.0000000</b>	<b>5885.3327736</b>
TACPSO	0.7799658	0.3855375	40.4127348	198.7078044	5888.4117775
GWO	0.7791210	0.3861775	40.3659434	199.4305063	5892.0312476
SHADE	0.8621925	0.5166362	42.3432305	189.1640166	7015.0739119
LSHADE	0.8185935	0.4081713	41.8693095	180.6982137	6066.9819132
LSHADE-EpSin	0.8378080	0.6557268	42.9357217	173.4630026	7016.4690445
ESO	<b>0.7781686</b>	<b>0.3846492</b>	<b>40.3196187</b>	<b>200.0000000</b>	<b>5885.3327736</b>

results of ESO compared with other algorithms, and ESO achieves the result of 12/1/0. Compared with the results of the other thirteen algorithms, ESO and TACPSO have achieved optimal results simultaneously. In order to reflect the performance of the 14 algorithms more intuitively in the calculation, Fig. 16 shows the convergence curves of the 14 algorithms, such as ESO, and the changing curves of each variable, which reflects the change trend of parameters during multi-parameter design.

## 6. Conclusions and future works

In order to enhance the global optimization capability of the SO

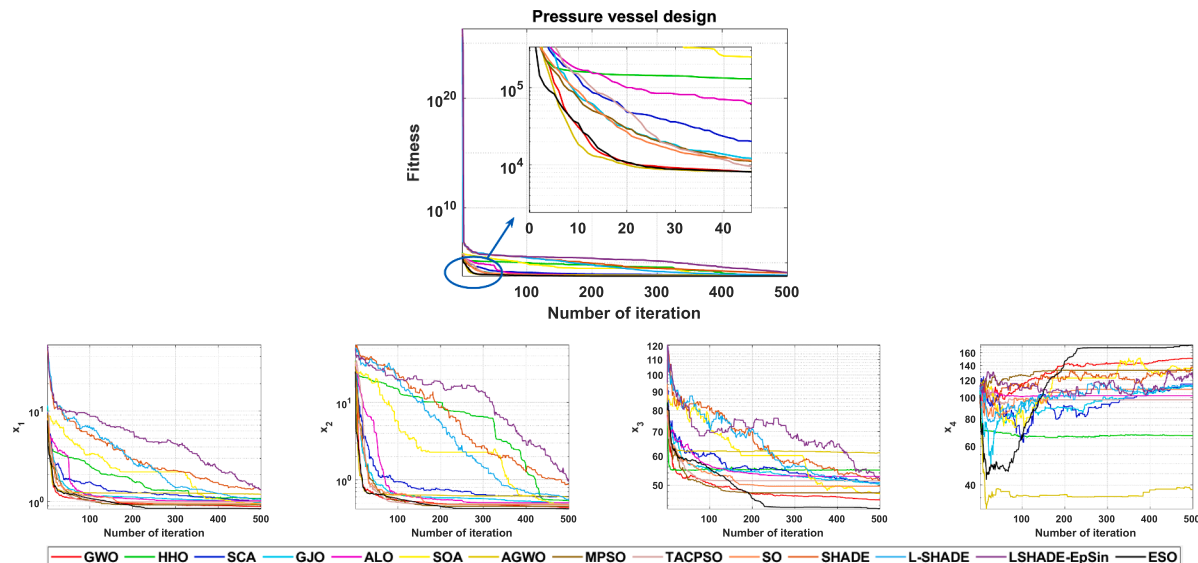
algorithm, in this paper, based on the original SO, four improved strategies are targeted to obtain an enhanced ESO algorithm based on its shortcomings and deficiencies. Furthermore, the effectiveness of the proposed ESO is proved by two function sets, 13 SOTA comparison algorithms, and various statistical validation methods.

New dynamic update mechanisms are proposed in response to the phenomenon that fixed values affect the exploration and exploitation phase in SO. A mirror imaging strategy based on convex lens imaging is proposed at the small solution range in SO. A strategy of adding sine-cosine to conform to the disturbance factor is proposed to aim at the phenomenon that SO optimization depends on the optimal

**Table 15**

Statistical results for the pressure vessel design problem.

Algorithms	Best	Mean	Std	Worst	Time	P	Wr
SO	5925.9317654	6322.4517360	355.1173410	7319.0007117	0.1805	2.5974E-05	(+)
HHO	6325.4825886	6775.8436970	343.8108545	7599.6908326	0.1637	5.4617E-09	(+)
SCA	6314.0730693	7459.5507775	750.4056595	9556.6795582	0.0664	3.1589E-10	(+)
GJO	5919.8660982	6450.4959122	538.5911102	7375.0689337	0.1066	1.4067E-04	(+)
ALO	5919.4990305	7101.3122503	1767.0372586	14178.8734400	1.0062	2.0023E-06	(+)
SOA	5962.7698986	6343.4053223	443.4811626	7505.5076169	0.0660	2.7726E-05	(+)
AGWO	6091.9361286	7331.9679644	528.7542485	7948.4249307	0.3175	2.8716E-10	(+)
MPSO	5885.3327736	6248.6037880	491.3091232	7319.0007020	0.0630	5.0064E-01	(=)
TACPSO	5888.4117775	6418.6634964	436.6135762	7319.0007020	0.0620	6.7634E-05	(+)
GWO	5892.0312476	6162.8906378	436.1392864	7265.1476141	0.0686	1.5798E-01	(=)
SHADE	7015.0739119	12377.1599599	2920.0948282	18786.9088827	0.0064	3.3384E-11	(+)
L SHADE	6066.9819132	7398.0386871	883.5204201	9897.5503588	0.0086	7.3803E-10	(+)
L SHADE-EpSin	7016.4690445	12606.8513760	4739.3581966	27866.6073510	0.0208	3.3384E-11	(+)
ESO	5885.3327736	5974.3815189	144.8303453	6572.8838872	0.2901	—	—

**Fig. 14.** Convergence curves for the pressure vessel design problem.**Table 16**

Comparison of the results for the corrugated bulkhead design problem.

Algorithms	$x_1$	$x_2$	$x_3$	$x_4$	Optimum Value
SO	57.6922529	34.1476199	57.6923099	1.0500001	6.8429586
HHO	54.6026196	34.1031547	57.8139813	1.0500000	6.8773172
SCA	51.7464787	33.8082607	49.0485933	1.0506163	7.1401234
GJO	57.5396949	34.1306269	57.5889035	1.0502363	6.8469525
ALO	57.6921607	34.1475587	57.6919350	1.0500002	6.8429655
SOA	49.7324829	34.0761045	57.5841044	1.0517734	6.9084134
AGWO	56.8247801	34.1642044	57.2652854	1.0516943	6.8701190
MPSO	<b>57.6923077</b>	<b>34.1476203</b>	<b>57.6923077</b>	<b>1.0500000</b>	<b>6.8429580</b>
TACPSO	<b>57.6923077</b>	<b>34.1476203</b>	<b>57.6923077</b>	<b>1.0500000</b>	<b>6.8429580</b>
GWO	57.5007689	34.1496902	57.5595021	1.0500943	6.8478597
SHADE	17.0394334z	35.108535	57.1874581	1.0530964	7.3980195
L SHADE	58.0107652	35.0680499	57.9151839	1.0573440	6.9292211
L SHADE-EpSin	59.2273344	36.7307034	56.5414776	1.0887587	7.2570853
ESO	<b>57.6923077</b>	<b>34.1476202</b>	<b>57.6923066</b>	<b>1.0500000</b>	<b>6.8429580</b>

individual position and is easy to fall into local optimization. In response to the phenomenon that the newly generated offspring replace the original individual in SO, Tent-chaos and Cauchy mutation are introduced to calculate the average fitness to replace the population individual better.

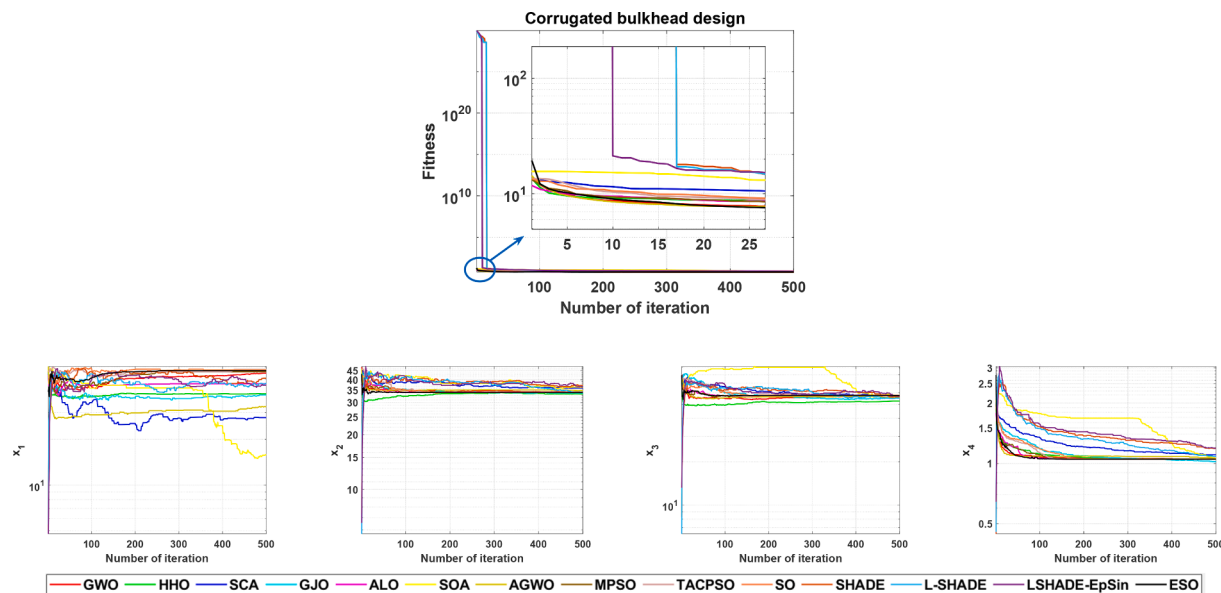
Two function sets to evaluate the adequate performance of the proposed ESO, including non-fixed dimensional and fixed dimensional

functions, are used, where the non-fixed dimensional functions are selected for testing in five different dimensions (30, 100, 500, 1000, and 2000). Experimental and statistical results show that ESO has excellent performance and is validated from theoretical aspects regarding accuracy, convergence speed and stability compared with thirteen state-of-the-art algorithms. Then ESO is applied to solve four real-world engineering optimization problems, and the results and comparisons prove

**Table 17**

Statistical results for the corrugated bulkhead design problem.

Algorithms	Best	Mean	Std	Worst	Time	P	Wr
SO	6.8429586247	6.8550587393	0.0432032633	7.0705958219	0.0218	0.1668E+00	(=)
HHO	6.8773172361	7.1673382530	0.2078888147	7.6190715727	0.0539	6.0658E-11	(+)
SCA	7.1401234299	7.8331455155	0.5538924414	8.6991406593	0.0190	3.0199E-11	(+)
GJO	6.8469525229	7.2178048870	0.5730191271	8.2975865996	0.0625	1.5574E-08	(+)
ALO	6.8429655102	6.9437200555	0.1234273485	7.2171118143	1.0284	4.1178E-06	(+)
SOA	6.9084134048	7.7337445316	0.6121179925	8.3232637265	0.0193	4.9752E-11	(+)
AGWO	6.8701189787	7.3450588585	0.4519750789	8.3849007389	0.2418	4.0772E-11	(+)
MPSO	6.8429580101	6.8901969673	0.2587384207	8.2601267058	0.0160	5.4249E-10	(+)
TACPSO	6.8429580101	6.8526811236	0.0532556616	7.1346512864	0.0164	5.8561E-10	(+)
GWO	6.8478597102	6.9030810760	0.2567625508	8.2619817958	0.0213	1.1674E-05	(+)
SHADE	7.3980194790	8.1439827746	0.4585050477	9.3955933498	0.0057	3.0199E-11	(+)
L SHADE	6.8950268754	7.2665706837	0.2674732410	7.9956050767	0.0083	3.6897E-11	(+)
L SHADE-EpSin	7.1070767047	8.1645102315	0.4817555341	9.3420570526	0.0246	3.0199E-11	(+)
ESO	6.8429580310	6.8523808292	0.0216022170	6.9445897216	0.0839	—	—

**Fig. 15.** Convergence curves for the corrugated bulkhead design problem.**Table 18**

Comparison of the results for the welded beam design problem.

Algorithms	$x_1$	$x_2$	$x_3$	$x_4$	Optimum Value
SO	0.2056072	3.4731455	9.0365721	0.2057320	1.7250300
HHO	0.2037080	3.3988367	9.4404473	0.2037986	1.7662676
SCA	0.1755298	4.1881375	9.3442296	0.2059297	1.8263339
GJO	0.2050042	3.4881740	9.0378487	0.2057338	1.7263568
ALO	0.2021011	3.5369064	9.0706733	0.2055604	1.7327312
SOA	0.2030705	3.5274473	9.0424317	0.2060791	1.7320458
AGWO	0.2012495	3.6462971	9.0515926	0.2062729	1.7482415
MPSO	<b>0.2057296</b>	<b>3.4704887</b>	<b>9.0366239</b>	<b>0.2057296</b>	<b>1.7248523</b>
TACPSO	<b>0.2057296</b>	<b>3.4704887</b>	<b>9.0366239</b>	<b>0.2057296</b>	<b>1.7248523</b>
GWO	0.2054433	3.4763056	9.0378609	0.2057560	1.7256068
SHADE	0.1818669	4.1332658	9.4958433	0.2070808	1.8665017
L SHADE	0.2095041	3.4041447	9.0354924	0.2101340	1.7548366
L SHADE-EpSin	0.1831072	3.7743249	9.7104696	0.2057077	1.8479203
ESO	<b>0.2057296</b>	<b>3.4704889</b>	<b>9.0366239</b>	<b>0.2057296</b>	<b>1.7248523</b>

the algorithm's effectiveness in solving practical problems, which is verified from the practical aspect.

In conclusion, the proposed ESO algorithm has better convergence accuracy, speed, and optimization performance. The test of fixed and non-fixed dimension functions proves that the proposed ESO method can adapt to the optimization problems of fixed, low, and high-

dimension functions, and the algorithm's robustness is verified. In future research, work will focus on the following aspects to apply the method to different domains, such as computer vision (CV) and natural language processing (NLP), for more complex and meaningful work, such as classification and feature extraction.

**Table 19**

Statistical results for the welded beam design problem.

Algorithms	Best	Mean	Std	Worst	Time	P	Wr
SO	1.7250300	1.7395431	0.0219452	1.8149353	0.0899	5.4941E-11	(+)
HHO	1.7662676	2.1186878	0.4328069	3.9852851	6.2700	3.0199E-11	(+)
SCA	1.8263339	1.9170249	0.0510634	2.0229553	2.5370	3.0199E-11	(+)
GJO	1.7263568	1.7349568	0.0061981	1.7528180	3.9010	3.0199E-11	(+)
ALO	1.7327312	1.8256136	0.0768187	1.9867386	32.4320	3.0199E-11	(+)
SOA	1.7320458	1.7555337	0.0212962	1.8098547	2.5560	3.0199E-11	(+)
AGWO	1.7482415	1.7952288	0.0295750	1.8819388	11.0930	3.0199E-11	(+)
MPSO	1.7248523	1.7356467	0.0315120	1.8515418	2.4850	3.5547E+00	(=)
TACPSO	1.7248523	1.7895880	0.1250673	2.2055879	2.4630	5.0842E-03	(+)
GWO	1.7256068	1.7293450	0.0033657	1.7429728	2.6760	3.3384E-11	(+)
SHADE	1.8665017	2.2600444	0.2620343	3.0009105	0.2200	3.0199E-11	(+)
L SHADE	1.7548366	1.9586148	0.1818865	2.5767634	0.3180	3.0199E-11	(+)
L SHADE-EpSin	1.8479203	2.1893283	0.1646962	2.5701736	0.5980	3.0199E-11	(+)
ESO	1.7248523	1.7249378	0.0001950	1.7257070	6.6510	—	—

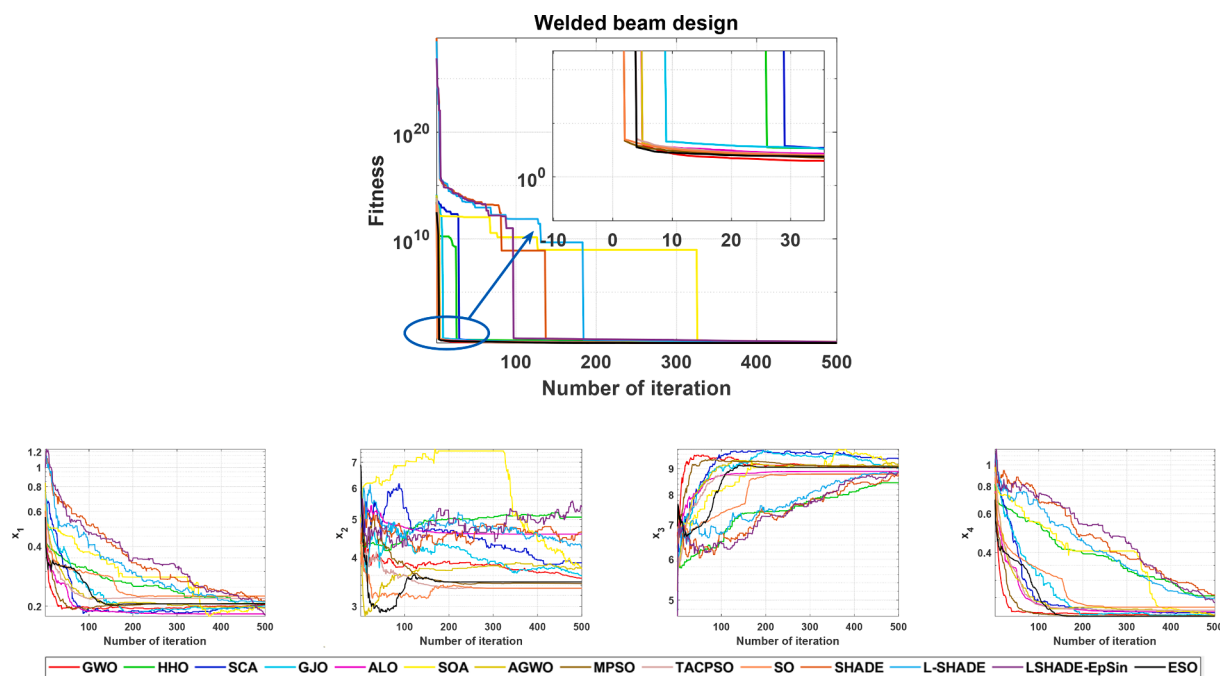


Fig. 16. Convergence curves for the welded beam design problem.

## Declaration of interests

The authors declare that they have no known competing financial interests or personal relationships that could have appeared to influence the work reported in this paper.

## CRediT authorship contribution statement

**Liguo Yao:** Conceptualization, Writing – original draft, Methodology, Formal analysis, Writing – review & editing, Software. **Panliang Yuan:** Software, Visualization. **Chieh-Yuan Tsai:** Supervision, Writing – review & editing. **Taihua Zhang:** Supervision, Conceptualization, Writing – review & editing. **Yao Lu:** Methodology. **Shilin Ding:** Data curation.

## Declaration of Competing Interest

The authors declare that they have no known competing financial interests or personal relationships that could have appeared to influence the work reported in this paper.

## Data availability

Data will be made available on request.

## Acknowledgments

This work was supported by the Guizhou Provincial Science and Technology Projects (Grant No. Qiankehejichu-ZK[2022]General 320), Growth Project for Young Scientific and Technological Talents in General Colleges and Universities of Guizhou Province (Grant No. Qianjiaoho KY[2022]167), National Natural Science Foundation (Grant No.72061006, 71761007) and Academic New Seedling Foundation Project of Guizhou Normal University (Grant No. Qianshixinmiao-[2021]A30).

## References

- Aala Kalananda, V. K. R., & Komanapalli, V. L. N. (2021). A combinatorial social group whale optimization algorithm for numerical and engineering optimization problems. *Applied Soft Computing*, 99.https://doi.org/10.1016/j.asoc.2020.106903.
- Adam, S. P., Alexandropoulos, S.-A. N., Pardalos, P. M., & Vrahatis, M. N. (2019). No Free Lunch Theorem: A Review. In *Approximation and Optimization* (pp. 57-82).

- Alsattar, H. A., Zaidan, A. A., & Zaidan, B. B. (2019). Novel meta-heuristic bald eagle search optimisation algorithm. *Artificial Intelligence Review*, 53, 2237–2264. <https://doi.org/10.1007/s10462-019-09732-5>
- Askari, Q., & Younas, I. (2021). Improved political optimizer for complex landscapes and engineering optimization problems. *Expert Systems with Applications*, 182, 115178. <https://doi.org/10.1016/j.eswa.2021.115178>
- Askari, Q., Younas, I., & Saeed, M. (2020). Political Optimizer: A novel socio-inspired meta-heuristic for global optimization. *Knowledge-Based Systems*, 195, 105709. <https://doi.org/10.1016/j.knosys.2020.105709>
- Awad, N. H., Ali, M. Z., Suganthan, P. N., & Reynolds, R. G. (2016). An ensemble sinusoidal parameter adaptation incorporated with L-SHADE for solving CEC2014 benchmark problems. In *2016 IEEE congress on evolutionary computation (CEC)* (pp. 2958–2965). IEEE.
- Bertsimas, D., & Tsitsiklis, J. (1993). Simulated annealing. *Statistical science*, 8, 10–15. <https://doi.org/DOI: 10.1214/ss/1177011077>.
- Bharti, K. K., & Singh, P. K. (2016). Opposition chaotic fitness mutation based adaptive inertia weight BPSO for feature selection in text clustering. *Applied Soft Computing*, 43, 20–34. <https://doi.org/10.1016/j.asoc.2016.01.019>.
- Bouchekara, H. R. E. H. (2019). Electrostatic discharge algorithm: a novel nature-inspired optimisation algorithm and its application to worst-case tolerance analysis of an EMC filter. *IET Science, Measurement & Technology*, 13, 491–499. <https://doi.org/10.1049/iet-smt.2018.5194>.
- Chopra, N., & Mohsin Ansari, M. (2022). Golden jackal optimization: A novel nature-inspired optimizer for engineering applications. *Expert Systems with Applications*, 198. <https://doi.org/10.1016/j.eswa.2022.116924>
- Cil, Z. A., Mete, S., & Serin, F. (2020). Robotic disassembly line balancing problem: A mathematical model and ant colony optimization approach. *Applied Mathematical Modelling*, 86, 335–348. <https://doi.org/10.1016/j.apm.2020.05.006>.
- Dabiri, N., J. Tarokh, M., & Alinaghian, M. (2017). New mathematical model for the bi-objective inventory routing problem with a step cost function: A multi-objective particle swarm optimization solution approach. *Applied Mathematical Modelling*, 49, 302–318. <https://doi.org/10.1016/j.apm.2017.03.022>.
- Das, B., Mukherjee, V., & Das, D. (2020). Student psychology based optimization algorithm: A new population based optimization algorithm for solving optimization problems. *Advances in Engineering Software*, 146. <https://doi.org/10.1016/j.advengsoft.2020.102804>.
- Dehghani, M., Montazeri, Z., Trojovská, E., & Trojovský, P. (2022). Coati Optimization Algorithm: A new bio-inspired metaheuristic algorithm for solving optimization problems. *Knowledge-Based System*. <https://doi.org/10.1016/j.knosys.2022.110011>
- Dhiman, G., & Kumar, V. (2019). Seagull optimization algorithm: Theory and its applications for large-scale industrial engineering problems. *Knowledge-Based Systems*, 165, 169–196. <https://doi.org/10.1016/j.knosys.2018.11.024>
- Dorigo, M., Birattari, M., & Stutzle, T. (2006). Ant colony optimization. *IEEE computational intelligence magazine*, 1, 28–39.
- Esmaelian, M., Tavana, M., Santos-Arteaga, F. J., & Vali, M. (2018). A novel genetic algorithm based method for solving continuous nonlinear optimization problems through subdividing and labeling. *Measurement*, 115, 27–38. <https://doi.org/10.1016/j.measurement.2017.09.034>
- Fan, Q., Huang, H., Li, Y., Han, Z., Hu, Y., & Huang, D. (2021). Beetle antenna strategy based grey wolf optimization. *Expert Systems with Applications*, 165. <https://doi.org/10.1016/j.eswa.2020.113882>
- Fan, S.-K.-S., Lin, W.-K., & Jen, C.-H. (2022). Data-driven optimization of accessory combinations for final testing processes in semiconductor manufacturing. *Journal of Manufacturing Systems*, 63, 275–287. <https://doi.org/10.1016/j.jmsy.2022.03.014>
- Faramarzi, A., Heidarinejad, M., Mirjalili, S., & Gandomi, A. H. (2020). Marine Predators Algorithm: A nature-inspired metaheuristic. *Expert Systems with Applications*, 152. <https://doi.org/10.1016/j.eswa.2020.113377>
- Farshchin, M., Maniat, M., Camp, C. V., & Pezeshk, S. (2018). School based optimization algorithm for design of steel frames. *Engineering Structures*, 171, 326–335. <https://doi.org/10.1016/j.engstruct.2018.05.085>
- Gaidhane, P. J., & Nigam, M. J. (2018). A hybrid grey wolf optimizer and artificial bee colony algorithm for enhancing the performance of complex systems. *Journal of Computational Science*, 27, 284–302. <https://doi.org/10.1016/j.jocs.2018.06.008>
- Gbadega, P. A., & Sun, Y. (2022). A hybrid constrained Particle Swarm Optimization-Model Predictive Control (CPSO-MPC) algorithm for storage energy management optimization problem in micro-grid. *Energy Reports*, 8, 692–708. <https://doi.org/10.1016/j.ejvr.2022.10.035>
- Hashim, F. A., Hussain, K., Houssein, E. H., Mabrouk, M. S., & Al-Atabany, W. (2020). Archimedes optimization algorithm: A new metaheuristic algorithm for solving optimization problems. *Applied Intelligence*, 51, 1531–1551. <https://doi.org/10.1007/s10489-020-01893-z>
- Hashim, F. A., & Hussien, A. G. (2022). Snake Optimizer: A novel meta-heuristic optimization algorithm. *Knowledge-Based Systems*, 242. <https://doi.org/10.1016/j.knosys.2022.108320>
- Hayyolalam, V., & Pourhaji Kazem, A. A. (2020). Black Widow Optimization Algorithm: A novel meta-heuristic approach for solving engineering optimization problems. *Engineering Applications of Artificial Intelligence*, 87. <https://doi.org/10.1016/j.engappai.2019.103249>.
- Heidari, A. A., Mirjalili, S., Faris, H., Aljarah, I., Mafarja, M., & Chen, H. (2019). Harris hawks optimization: Algorithm and applications. *Future Generation Computer Systems*, 97, 849–872. <https://doi.org/10.1016/j.future.2019.02.028>
- Ho, Y.-C., & Pepyne, D. L. (2002). Simple explanation of the no-free-lunch theorem and its implications. *Journal of optimization theory and applications*, 115, 549–570. <https://doi.org/10.1023/A:1021251113462>
- Holland, J. H. (1992). *Adaptation in natural and artificial systems: an introductory analysis with applications to biology, control, and artificial intelligence*: MIT press.
- Houssein, E. H., Çelik, E., Mahdy, M. A., & Ghoniem, R. M. (2022). Self-adaptive Equilibrium Optimizer for solving global, combinatorial, engineering, and Multi-Objective problems. *Expert Systems with Applications*, 195. <https://doi.org/10.1016/j.eswa.2022.116552>
- Huang, Y.-Y., Pan, Q.-K., Huang, J.-P., Suganthan, P. N., & Gao, L. (2021). An improved iterated greedy algorithm for the distributed assembly permutation flowshop scheduling problem. *Computers & Industrial Engineering*, 152. <https://doi.org/10.1016/j.cie.2020.107021>.
- Ibrahim, R. A., Elaziz, M. A., & Lu, S. (2018). Chaotic opposition-based grey-wolf optimization algorithm based on differential evolution and disruption operator for global optimization. *Expert Systems with Applications*, 108, 1–27. <https://doi.org/10.1016/j.eswa.2018.04.028>
- Jafari, M. R., Arefi, M. M., & Panahi, M. (2022). Convex reformulations for self-optimizing control optimization problem: Linear Matrix Inequality approach. *Journal of Process Control*, 116, 172–184. <https://doi.org/10.1016/j.jprocont.2022.06.003>
- Khishe, M., & Mosavi, M. R. (2020). Chimp optimization algorithm. *Expert Systems with Applications*, 149. <https://doi.org/10.1016/j.eswa.2020.113338>
- Kumar, S., Jangir, P., Tejani, G. G., & Premkumar, M. (2022). MOTEQ: A novel physics-based multiobjective thermal exchange optimization algorithm to design truss structures. *Knowledge-Based Systems*, 242. <https://doi.org/10.1016/j.knosys.2022.108422>
- Li, C., Zhang, N., Lai, X., Zhou, J., & Xu, Y. (2017). Design of a fractional-order PID controller for a pumped storage unit using a gravitational search algorithm based on the Cauchy and Gaussian mutation. *Information Sciences*, 396, 162–181. <https://doi.org/10.1016/j.ins.2017.02.026>
- Li, Y., Yu, X., & Liu, J. (2023). An opposition-based butterfly optimization algorithm with adaptive elite mutation in solving complex high-dimensional optimization problems. *Mathematics and Computers in Simulation*, 204, 498–528. <https://doi.org/10.1016/j.matcom.2022.08.020>
- Liang, Y.-C., Hsiao, Y.-M., & Tien, C.-Y. (2013). Metaheuristics for drilling operation scheduling in Taiwan PCB industries. *International Journal of Production Economics*, 141, 189–198. <https://doi.org/10.1016/j.ijpe.2012.04.014>
- Liu, Q., Liu, M., Wang, F., & Xiao, W. (2022). A dynamic stochastic search algorithm for high-dimensional optimization problems and its application to feature selection. *Knowledge-Based Systems*, 244. <https://doi.org/10.1016/j.knosys.2022.108517>
- Long, W., Jiao, J., Xu, M., Tang, M., Wu, T., & Cai, S. (2022). Lens-imaging learning Harris hawks optimizer for global optimization and its application to feature selection. *Expert Systems with Applications*, 202. <https://doi.org/10.1016/j.eswa.2022.117255>
- López-Vázquez, C., & Hochsztain, E. (2017). Extended and updated tables for the Friedman rank test. *Communications in Statistics - Theory and Methods*, 48, 268–281. <https://doi.org/10.1080/03610926.2017.1408829>
- Luiz Junho Pereira, J., Antônio Oliver, G., Brendon Francisco, M., Simões Cunha Jr, S., & Ferreira Gomes, G. (2022). Multi-objective lichtenberg algorithm: A hybrid physics-based meta-heuristic for solving engineering problems. *Expert Systems with Applications*, 187, 115939. <https://doi.org/10.1016/j.eswa.2021.115939>
- Ma, C., Huang, H., Fan, Q., Wei, J., Du, Y., & Gao, W. (2022). Grey wolf optimizer based on Aquila exploration method. *Expert Systems with Applications*, 205. <https://doi.org/10.1016/j.eswa.2022.117629>
- Mirjalili, S. (2015). The Ant Lion Optimizer. *Advances in Engineering Software*, 83, 80–98. <https://doi.org/10.1016/j.advengsoft.2015.01.010>
- Mirjalili, S. (2016). SCA: A Sine Cosine Algorithm for solving optimization problems. *Knowledge-Based Systems*, 96, 120–133. <https://doi.org/10.1016/j.knosys.2015.12.022>
- Mirjalili, S., Gandomi, A. H., Mirjalili, S. Z., Saremi, S., Faris, H., & Mirjalili, S. M. (2017). Salp Swarm Algorithm: A bio-inspired optimizer for engineering design problems. *Advances in Engineering Software*, 114, 163–191. <https://doi.org/10.1016/j.advengsoft.2017.07.002>
- Mirjalili, S., & Lewis, A. (2016). The Whale Optimization Algorithm. *Advances in Engineering Software*, 95, 51–67. <https://doi.org/10.1016/j.advengsoft.2016.01.008>
- Mirjalili, S., Mirjalili, S. M., & Lewis, A. (2014). Grey Wolf Optimizer. *Advances in Engineering Software*, 69, 46–61. <https://doi.org/10.1016/j.advengsoft.2013.12.007>
- Mollajan, A., Memarian, H., & Quintal, B. (2018). Nonlinear rock-physics inversion using artificial neural network optimized by imperialist competitive algorithm. *Journal of Applied Geophysics*, 155, 138–148. <https://doi.org/10.1016/j.jappgeo.2018.06.002>
- Moraes, A. O. S., Mitre, J. F., Lage, P. L. C., & Secchi, A. R. (2015). A robust parallel algorithm of the particle swarm optimization method for large dimensional engineering problems. *Applied Mathematical Modelling*, 39, 4223–4241. <https://doi.org/10.1016/j.apm.2014.12.034>
- Mortazavi, A. (2021). Bayesian Interactive Search Algorithm: A New Probabilistic Swarm Intelligence Tested on Mathematical and Structural Optimization Problems. *Advances in Engineering Software*, 155. <https://doi.org/10.1016/j.advengsoft.2021.102994>
- Mousavi-Aval, S. H., Rafiee, S., Sharifi, M., Hosseinpour, S., Notarnicola, B., Tassielli, G., & Renzulli, P. A. (2017). Application of multi-objective genetic algorithms for optimization of energy, economics and environmental life cycle assessment in oilseed production. *Journal of Cleaner Production*, 140, 804–815. <https://doi.org/10.1016/j.jclepro.2016.03.075>
- Omran, M. G. H., & Al-Sharhan, S. (2019). Improved continuous Ant Colony Optimization algorithms for real-world engineering optimization problems. *Engineering Applications of Artificial Intelligence*, 85, 818–829. <https://doi.org/10.1016/j.engappai.2019.08.009>

- Peng, H., Xiao, W., Han, Y., Jiang, A., Xu, Z., Li, M., & Wu, Z. (2022). Multi-strategy firefly algorithm with selective ensemble for complex engineering optimization problems. *Applied Soft Computing*, 120. <https://doi.org/10.1016/j.asoc.2022.108634>
- Poli, R., Kennedy, J., & Blackwell, T. (2007). Particle swarm optimization. *Swarm Intelligence*, 1, 33–57.
- Qin, C., Ming, F., Gong, W., & Gu, Q. (2022). Constrained multi-objective optimization via two archives assisted push-pull evolutionary algorithm. *Swarm and Evolutionary Computation*, 75. <https://doi.org/10.1016/j.swevo.2022.101178>.
- Rao, R. V., Savsani, V. J., & Vakharia, D. P. (2011). Teaching-learning-based optimization: A novel method for constrained mechanical design optimization problems. *Computer-Aided Design*, 43, 303315. <https://doi.org/10.1016/j.cad.2010.12.015>
- Rosner, B., Glynn, R. J., & Lee, M. L. (2003). Incorporation of clustering effects for the Wilcoxon rank sum test: A large-sample approach. *Biometrics*, 59, 1089–1098. <https://www.ncbi.nlm.nih.gov/pmc/articles/PMC1496948/>. <https://doi.org/10.1111/j.0006-341x.2003.00125.x>
- Satapathy, S., & Naik, A. (2016). Social group optimization (SGO): a new population evolutionary optimization technique. *Complex & Intelligent Systems*, 2, 173–203. <https://doi.org/10.1007/s40747-016-0022-8>.
- Segura-Domínguez, I., Herrera-Guzmán, R., Serrano-Rubio, J. P., & Hernández-Aguirre, A. (2020). Geometric probabilistic evolutionary algorithm. *Expert Systems with Applications*, 144. <https://doi.org/10.1016/j.eswa.2019.113080>
- Shokri-Ghaleh, H., Alfi, A., Ebadollahi, S., Mohammad Shahri, A., & Ranjbaran, S. (2020). Unequal limit cuckoo optimization algorithm applied for optimal design of nonlinear field calibration problem of a triaxial accelerometer. *Measurement*, 164. <https://doi.org/10.1016/j.measurement.2020.107963>.
- Si, T., Miranda, P. B. C., & Bhattacharya, D. (2022). Novel enhanced Salp Swarm Algorithms using opposition-based learning schemes for global optimization problems. *Expert Systems with Applications*, 207. <https://doi.org/10.1016/j.eswa.2022.117961>
- Simon, D. (2008). Biogeography-Based Optimization. *IEEE Transactions on Evolutionary Computation*, 12, 702–713. <https://doi.org/10.1109/tevc.2008.919004>
- Talatahari, S., & Azizi, M. (2020). Optimization of constrained mathematical and engineering design problems using chaos game optimization. *Computers & Industrial Engineering*, 145. <https://doi.org/10.1016/j.cie.2020.106560>.
- Tanabe, R., & Fukunaga, A. (2013). Success-history based parameter adaptation for differential evolution. In *2013 IEEE congress on evolutionary computation* (pp. 71–78). IEEE.
- Tanabe, R., & Fukunaga, A. S. (2014). Improving the search performance of SHADE using linear population size reduction. In *2014 IEEE congress on evolutionary computation (CEC)* (pp. 1658–1665). IEEE.
- Tang, Z., & Zhang, D. (2009). A Modified Particle Swarm Optimization with an Adaptive Acceleration Coefficients. 2009 Asia-Pacific Conference on Information Processing. 330–332. <https://doi.org/10.1109/apcip.2009.217>.
- Tanyildizi, E., & Demir, G. (2017). Golden sine algorithm: A novel math-inspired algorithm. *Advances in Electrical and Computer Engineering*, 17, 71–78. <https://doi.org/10.4316/AECE.2017.02010>
- Tawhid, M. A., & Ibrahim, A. M. (2021). Solving nonlinear systems and unconstrained optimization problems by hybridizing whale optimization algorithm and flower pollination algorithm. *Mathematics and Computers in Simulation*, 190, 1342–1369. <https://doi.org/10.1016/j.matcom.2021.07.010>.
- Tay, T., & Osorio, C. (2022). Bayesian optimization techniques for high-dimensional simulation-based transportation problems. *Transportation Research Part B: Methodological*, 164, 210–243. <https://doi.org/10.1016/j.trb.2022.08.009>
- Tian, D., & Shi, Z. (2018). MPSO: Modified particle swarm optimization and its applications. *Swarm and Evolutionary Computation*, 41, 49–68. <https://doi.org/10.1016/j.swevo.2018.01.011>
- Tinkle, D. W., Wilbur, H. M., & Tilley, S. G. (1970). Evolutionary strategies in lizard reproduction. *Evolution*, 24, 55–74. <https://doi.org/10.1111/j.1558-5646.1970.tb01740.x>.
- Tizhoosh, H. R. (2005). *Opposition-based learning: a new scheme for machine intelligence*. International conference on computational intelligence for modelling, control and automation and international conference on intelligent agents, web technologies and internet commerce (CIMCA-IAWTIC'06). 695–701. <https://doi.org/10.1109/cimca.2005.1631345>.
- Tsai, C.-Y., Chang, H.-T., & Kuo, R. J. (2017). An ant colony based optimization for RFID reader deployment in theme parks under service level consideration. *Tourism Management*, 58, 1–14. <https://doi.org/10.1016/j.tourman.2016.10.003>.
- Vieira, R. S. S., & Mosna, R. A. (2022). Homoclinic chaos in the Hamiltonian dynamics of extended test bodies. *Chaos, Solitons & Fractals*, 163. <https://doi.org/10.1016/j.chaos.2022.112541>.
- Wang, K., Guo, M., Dai, C., & Li, Z. (2022). Information-decision searching algorithm: Theory and applications for solving engineering optimization problems. *Information Sciences*, 607, 1465–1531. <https://doi.org/10.1016/j.ins.2022.06.008>.
- Wang, W.-c., Xu, L., Chau, K.-w., & Xu, D.-m. (2020). Yin-Yang firefly algorithm based on dimensionally Cauchy mutation. *Expert Systems with Applications*, 150. <https://doi.org/10.1016/j.eswa.2020.113216>.
- Wang, Y., Yu, J., Yang, S., Jiang, S., & Zhao, S. (2019). Evolutionary dynamic constrained optimization: Test suite construction and algorithm comparisons. *Swarm and Evolutionary Computation*, 50. <https://doi.org/10.1016/j.swevo.2019.100559>.
- Wardhana, S. G., & Pranowo, W. (2022). Rock-physics modeling by using particle swarm optimization algorithm. *Journal of Applied Geophysics*, 202. <https://doi.org/10.1016/j.jappgeo.2022.104683>.
- Wu, C., Yang, X., & Zhu, Y. (2021). On the design of potential turbine positions for physics-informed optimization of wind farm layout. *Renewable Energy*, 164, 1108–1120. <https://doi.org/10.1016/j.renene.2020.10.060>
- Xia, M., & Dong, M. (2022). A novel two-archive evolutionary algorithm for constrained multi-objective optimization with small feasible regions. *Knowledge-Based Systems*, 237. <https://doi.org/10.1016/j.knosys.2021.107693>.
- Xiao, J., Liu, S., Liu, H., Wang, M., Li, G., & Wang, Y. (2022). A jerk-limited heuristic feedrate scheduling method based on particle swarm optimization for a 5-DOF hybrid robot. *Robotics and Computer-Integrated Manufacturing*, 78. <https://doi.org/10.1016/j.rcim.2022.102396>
- Xu, Y., Li, X., Yang, J., & Zhang, D. (2014). Integrate the original face image and its mirror image for face recognition. *Neurocomputing*, 131, 191–199. <https://doi.org/10.1016/j.neucom.2013.10.025>
- Yang, X., Wang, R., Zhao, D., Yu, F., Huang, C., Heidari, A. A., ... Chen, H. (2023). An adaptive quadratic interpolation and rounding mechanism sine cosine algorithm with application to constrained engineering optimization problems. *Expert Systems with Applications*, 213. <https://doi.org/10.1016/j.eswa.2022.119041>
- Yang, Y., Gao, Y., Tan, S., Zhao, S., Wu, J., Gao, S., Zhang, T., Tian, Y.-C., & Wang, Y.-G. (2022). An opposition learning and spiral modelling based arithmetic optimization algorithm for global continuous optimization problems. *Engineering Applications of Artificial Intelligence*, 113. <https://doi.org/10.1016/j.engappai.2022.104981>.
- Zhao, W., Wang, L., & Zhang, Z. (2019). A novel atom search optimization for dispersion coefficient estimation in groundwater. *Future Generation Computer Systems*, 91, 601–610. <https://doi.org/10.1016/j.future.2018.05.037>
- Zhao, X., Fang, Y., Liu, L., Xu, M., & Li, Q. (2022). A covariance-based Moth-flame optimization algorithm with Cauchy mutation for solving numerical optimization problems. *Applied Soft Computing*, 119. <https://doi.org/10.1016/j.asoc.2022.108538>.
- Zhao, X., Fang, Y., Ma, S., & Liu, Z. (2022). Multi-swarm improved moth-flame optimization algorithm with chaotic grouping and Gaussian mutation for solving engineering optimization problems. *Expert Systems with Applications*, 204. <https://doi.org/10.1016/j.eswa.2022.117562>